Self-organizing Dynamic Spectrum Management: Novel Scheme for Cognitive Radio Networks.

Self-organizing Dynamic Spectrum Management: Novel Scheme for Cognitive Radio Networks.

By

FARHAD KHOZEIMEH, B.Sc, M.A.Sc.

A Thesis

Submitted to the School of Graduate Studies

in Partial Fulfilment of the Requirements

for the Degree

Doctor of Philosophy

McMaster University

Farhad Khozeimeh. Ph.D. thesis.
Dept. of Electrical and Computer Engineering,
McMaster Univ., Hamilton, Canada, 2012.

DOCTOR OF PHILOSOPHY (2012) McMaster University
Hamilton, Ontario

TITLE: Self-Organizing Dynamic Spectrum Management: Novel Scheme For Cognitive Radio Networks

AUTHOR: Farhad Khozeimeh, B.Sc, M.A.Sc. (McMaster Univ.)

SUPERVISOR: Dr. S. Haykin

NUMBER OF PAGES: xxvi, 207

In loving memory of my parents, Dr. S. R. Yazdi and Dr. B. Khozeimeh,

and to Golnar

Farhad Khozeimeh. Ph.D. thesis.
Dept. of Electrical and Computer Engineering,
McMaster Univ., Hamilton, Canada, 2012.

Abstract

A cognitive radio network is a multi-user system, in which different radio units compete for limited resources in an opportunistic manner, interacting with each other for access to the available resources. The fact that both users and spectrum holes (i.e., under-utilized spectrum sub-bands) can come and go in a stochastic manner, makes a cognitive radio network a highly non-stationary, dynamic and challenging wireless environment. Finding robust decentralized resource-allocation algorithms, which are capable of achieving reasonably good solutions fast enough in order to guarantee an acceptable level of performance, is crucial in such an environment. In this thesis, a novel dynamic spectrum management (DSM) scheme for cognitive radio networks, termed the self-organizing dynamic spectrum management (SO-DSM), is described and its practical validity is demonstrated using computer simulations.

In this scheme, CRs try to exploit the primary networks' unused bands and establish link with neighbouring CRs using those bands. Inspired by human brain, the CRs extract and memorize primary network's and other CRs' activity patterns and create temporal channel assignments on sub-bands with no recent primary user activities using self-organizing maps (SOM) technique. The proposed scheme is decentralized and employs a simple learning rule with low complexity and minimal memory requirements. A software testbed was

developed to simulate and study the proposed scheme. This testbed is capable of simulating CR network alongside of a cellular legacy network. In addition to SO-DSM, two other DSM schemes, namely centralized DSM and no-learning decentralized DSM, can be used for CR networks in this software testbed. The software testbed was deployed on parallel high capacity computing clusters from Sharcnet to perform large scale simulations of CR network. The simulation results show, comparing to centralized DSM and minority game DSM (MG-DSM), the SO-DSM decreases the probability of collision with primary users and also probability of CR link interruption significantly with a moderate decrease in CR network spectrum utilization.

Acknowlegements

During my graduate studies at McMaster, I have learned and benefited from the support, guidance and friendship of many people. I would like to express my deep appreciation to my adviser, Professor Simon Haykin, for his guidance and valuable advice all through this work and for being a wonderful source of scientific insight. It was a privilege for me to work closely with him and have the opportunity to observe a unique personality, who has helped to shape and influence various scientific fields for the past fifty years. Many thanks to Dr. D. Down and Dr. T. Kirubarajan for sitting on my supervisory committee and their helpful comments on the thesis.

I also wish to thank many friends and relatives who were always there for me, especially my brother Kamyar, my sister Mahta and her husband Ramin. Finishing this work would not have been possible without their infinite love and support. I also owe many thanks to all my friends in the McMaster Univerity, specially Hosein Yarmand, Kaveh Elizeh and Peyman Setoodeh, for their kindness, friendship and valuable help.

Sincere thanks go to Mrs. Cheryl Gies, Mrs. Lola Brooks, Mr. Terry Greenlay, and Mrs. Helen Jachna, who were always welcoming, supportive,

and helpful.

My parents provided me with everything I needed, endless love and care throughout my life. Words cannot express my gratitude to them. Although they are not present anymore, the inspiration and encouragement they gave me will be with me for the rest of my life, and their love and memory will forever remain in my heart.

Glossary of Symbols

AR	AutoRegressive
CAPL	Channel Allocation Priority
CDS	Cognitive Dynamic Systems
CDSM	Centralized Dynamic Spectrum Management
CR	Cognitive Radio
DSM	Dynamic Spectrum Management
EMA	Exponential Moving Average
FFT	Fast Fourier Transform
FFTW	Fastest Fourier Transform in the West
GCP	Graph Colouring Problem
GSM	Global System for Mobile Communications
HD	High Definition
HMM	Hidden Markov Model
IWFC	Iterative Waterfilling Controller
LCP	List-Colouring Problem
LDO	Largest Degree Ordering
MG	Minority Game
MG-DSM	Minority Game Dynamic Spectrum Management
MMB	Max-Min Bandwidth
MSB	Max-Sum Bandwidth
MTM	Multi-Taper Method

NP-Hard	Non-deterministic Polynomial-time hard
PDA	Personal Digital Assistant
PU	Primary User
RF	Radio Frequency
RGC	Retinal Ganglion Cell
RSA	Radio Scene Analysis
RX	Receiver
SC	Superior Colliculus
SINR	Signal to Interference and Noise Ratio
SLS	Stochastic Local Search
SO-DSM	Self-Organizing Dynamic Spectrum Management
SOM	Self-Organizing Map
TK	Tsigankov-Koulakov
TPC	Transmit-Power Control
TX	Transmitter
γ_{CR}	Spectrum utilization efficiency for CRs
γ_{PU}	Spectrum utilization efficiency for PUs
η_1	learning rate of the first stage of SO-DSM
η_2	learning rate of second stage of SO-DSM
β_1	Quality level signal for free sub-bands
β_2	Quality level signal for sub-bands used by other CRs
P_{col}	Probability of collision with CRs for PUs

P_{intr}	Probability of CR link interruption
$\mathcal{I}_{TX}$	Average received interference during TX by PUs
$\mathcal{I}_{RX}$	Average received interference during RX by PUs
$\mathcal{M}_s$	Mean of CR sub-band assignment distribution
$\mathcal{V}_s$	Variance of CR sub-band assignment distribution
D_{RSA}	Time delay of spectrum analyzer

Contents

Contents xiii

List of Figures xvi

List of Tables xxv

1 Introduction 1

1.1 Motivation 1
1.2 Cognitive Radio 6
1.3 Perception-Action cycle of cognitive radio 7
1.4 Self-Organizing Maps in the Human Brain 15
1.5 Contributions of Thesis 20
1.6 Thesis Organization 21

2 Dynamic Spectrum Management 25

2.1 Spectrum Sharing 27
2.2 The DSM problem 30
2.3 The DSM graph-colouring 36
2.4 Centralized versus decentralized approaches to the DSM . . . 41
2.5 Summary 46

3 Tsigankov-Koulakov Model for Self-Organizing Maps **47**

3.1 Mathematical Model of Hebbian Learning 51

3.2 Maximum Eigenfilter 54

3.3 The Tsigankov-Koulakov Model 56

3.4 Summary 59

4 Self-Organizing Dynamic Spectrum Management **61**

4.1 SO-DSM 66

4.2 Complexity Analysis 74

4.3 Degrees of freedom 76

4.4 Summary 83

5 Simulation Results **85**

5.1 Simulations Setup 85

5.2 Results 89

5.3 SO-DSM vs MG-DSM 89

5.4 SO-DSM vs CDSM 101

5.5 SO-DSM parameters 115

5.6 Quality Level Signal Parameters 127

5.7 Summary 139

6 Robustness **141**

6.1 Robustness 141

6.2 Robustness of SO-DSM 143

6.3 Simulation Results 143

6.4 Summary 161

7 Contributions to the Literature **163**

7.1 Future Directions 166

Appendices **171**

A Minority Game DSM **173**

B Robust Transmit Power Control **175**

B.1 Iterative Waterfilling Controller (IWFC) 176

B.2 Dominant Sources of Uncertainty 178

B.3 Dealing with Uncertainty 179

C Autoregressive Model (AR) **183**

D Proof of Theorem 1 **185**

Bibliography **191**

List of Figures

1.1 (a) Directed-information flow in cognitive radio. DSM: dynamic spectrum manager; TPC: transmit-power controller; RSA: radio-scene analyzer; RX: receiver; TX: transmitter; TX CR: transmitter unit in the transceiver of cognitive radio; RX CR: receiver unit in the transceiver of cognitive radio. (b) Perceptionaction cycle of cognitive radio unit. 8

1.2 Von der Malsburg model (reproduced from [1]). 16

1.3 Structure of a neuron (Reproduced from [2]). 18

1.4 The model of a neuron. 20

2.1 An example of spectrum set up at two time instants. The spectrum holes are shown with white colour, spectrum bands used by CR, with grey colour and unavailable spectrum bands are shown with black colour. 26

2.2 Markov model for traffic. 35

2.3 (a) An invalid graph-colouring. (b) A valid graph-colouring. . . . 36

2.4 (a) A DSM problem scene with 11 CR units; the solid lines represent data links between CR units and dot lines represent interference between two CR unit. (b) The graph representation of (a). . 38
2.5 A list-colouring problem. 39
2.6 LDO algorithm for solving GCP. 40
2.7 The cognitive radio network set up using centralized DSM. 42
2.8 The cognitive radio network set up using decentralized DSM. . . . 44

3.1 Diagram of a neural network governed by maximum eigenfilter learning rule. The weights are adaptively adjusted according to Eqn. 3.3 and based on input and output. 56
3.2 A self-organizing map (a)initial state. (b) organized state. 57

4.1 Normalized load of three different cell sectors over three weeks. We plot the moving average of each cell over 1 s. The cells show high load (top), varying load (middle), and low load (bottom). (reproduced from [3]) 63
4.2 (a) Distribution of system-wide average call arrival rates during four different days. The arrival rates are averaged over 5-min slots. (b) Distribution of average call duration over 5-min periods during four different days. The large spikes during the mornings are due to small gaps in collection. (reproduced from [3]) 64
4.3 An example of SO-DSM weight dynamics for one CR unit. b_1 and b_2 are used by neighbouring CRs and b_3 by the CR unit from $n = 20$ until $n = 70$. Simulation parameters used are: (μ_1, μ_2)=(0.1,0.1), β_1=0.7, β_2=0.1 and η_2=0.05 75

4.4 Example of SO-DSM weight dynamics of Fig. 4.3, reproduced with $\eta_2 = 0.005$. The rate of weight changes is slower than Fig. 4.3 and the effect of using the channel b_3 is not completely cleared in this case. 79

4.5 An example of SO-DSM weight dynamics showing the effect of β_1. Sub-bands b_1 and b_2 were used by neighbouring CRs from $n = 1$ to $n = 70$. Sub-band b_3 was used by the CR unit from $n = 20$ to $n = 70$ and all sub-bands were free after $n = 70$ (a)$\beta_1 = 0.5$ (b) $\beta_1 = 0.8$. 81

4.6 An example of SO-DSM weight dynamics showing the effect of β_2. Sub-bands b_1 and b_2 were used by neighbouring CRs from $n = 1$ to $n = 70$. Sub-band b_3 was used by the CR unit from $n = 20$ to $n = 70$ and all sub-bands were used by neighbouring CRs after $n = 70$ (a)$\beta_2 = 0.1$ (b) $\beta_2 = 0.5$. 82

5.1 The simulated area with four base stations. 88

5.2 Legacy network spectrum utilization. (a) numerical results (b) graphical plot. As the number of PUs increase, the spectrum utilization of legacy network increases. The legacy network is independent of CR network, thus, the results are approximately equal for all simulations. 90

5.3 The CR network spectrum utilization. (a) N_{CR}=50 (b) N_{CR}=300. γ_{CR} at worst case is about 50% lower for SO-DSM. As the number of PUs increases, γ_{CR} decreases for both schemes due to vanishing of spectrum holes. 91

5.4 Probability of collision for PUs. (a) N_{CR}=50 (b) N_{CR}=300. $P_{\text{col}}$is significantly lower for SO-DSM. SO-DSM imposes about 33 times less collisions on PUs for $N_{\text{CR}} = 300$ and $N_{\text{PU}} = 30$; and at $N_{\text{PU}} = 180$ there is no collisions for SO-DSM with $N_{\text{CR}} = 300$. 93

5.5 Probability of CR link interruption. (a) N_{CR}=50 (b) N_{CR}=300. The CR links experienced significantly fewer interruptions using SO-DSM. For $N_{\text{PU}} = 30$ $P_{\text{intr}}$is about 10 times lower for SO-DSM while for $N_{\text{PU}} = 180$ the difference is even higher 94

5.6 Average received interference by TX PUs. (a) N_{CR}=50 (b) N_{CR}=300. For $N_{\text{PU}} = 30$, $\mathcal{I}_{TX}$is about 10 times lower for SO-DSM. However, for $N_{\text{PU}} = 180$ $\mathcal{I}_{TX}$is slightly higher for SO-DSM. This is due to slightly higher $\gamma_{\text{CR}}$and much lower P_{col} of SO-DSM in this case. . 96

5.7 Average received interference by RX PUs. (a) N_{CR}=50 (b) N_{CR}=300. For $N_{\text{PU}} = 30$, $\mathcal{I}_{RX}$is about 10 times lower for SO-DSM. However, for $N_{\text{PU}} = 180$ $\mathcal{I}_{RX}$is slightly higher for SO-DSM. This is due to slightly higher $\gamma_{\text{CR}}$and much lower P_{col} of SO-DSM in this case. . 97

5.8 Mean of CR sub-band utilization distribution. (a) N_{CR}=50 (b) N_{CR}=300. The CRs have used lower number of sub-bands for SO-DSM which is an indication of map formation in SO-DSM. 99

5.9 Variance of CR sub-band utilization distribution. (a) N_{CR}=50 (b) N_{CR}=300. $\mathcal{V}_s$is higher for SO-DSM which demonstrates CRs have successfully built temporal organization. 100

5.10 The simulation results for centralized DSM and SO-DSM. Legacy network spectrum utilization. As the number of PUs increase, the spectrum utilization of legacy network increases. The legacy network is independent of CR network, thus, the results are approximately equal for all simulations. 103

5.11 The CR network spectrum utilization. (a) N_{CR}=50 (b) N_{CR}=300. γ_{CR}at worst case is about 80% lower for SO-DSM. As the number of PUs increases, γ_{CR}decreases for both schemes due to vanishing of spectrum holes. 104

5.12 Probability of collision for PUs. (a) N_{CR}=50 (b) N_{CR}=300. $P_{\text{col}}$is significantly lower for SO-DSM. SO-DSM imposes about 33 times less collisions on PUs for $N_{\text{CR}} = 300$ and $N_{\text{PU}} = 30$; and at $N_{\text{PU}} = 180$ there is no collisions for SO-DSM. 106

5.13 Probability of CR link interruption. (a) N_{CR}=50 (b) N_{CR}=300. The CR links experienced significantly fewer interruptions using SO-DSM. For $N_{\text{PU}} = 30$ $P_{\text{intr}}$is about 10 times lower for SO-DSM while for $N_{\text{PU}} = 180$ the difference is even higher, as high as 500 times for $N_{\text{CR}} = 300$. 107

5.14 Average received interference by TX PUs. (a) N_{CR}=50 (b) N_{CR}=300. For $N_{\text{PU}} = 30$, $\mathcal{I}_{TX}$is about 10 times lower for SO-DSM. However, for $N_{\text{PU}} = 180$ $\mathcal{I}_{TX}$is slightly higher for SO-DSM. This is due to slightly higher $\gamma_{\text{CR}}$and much lower $P_{\text{col}}$of SO-DSM scheme for this case. 109

5.15 Average received interference by RX PUs. (a) N_{CR}=50 (b) N_{CR}=300. Similar to $\mathcal{I}_{TX}$, for $N_{\text{PU}} = 30$, $\mathcal{I}_{RX}$is about 10 times lower for SO-DSM. However, for $N_{\text{PU}} = 180$ $\mathcal{I}_{RX}$is slightly higher for SO-DSM. This is due to slightly higher $\gamma_{\text{CR}}$and much lower $P_{\text{col}}$of SO-DSM scheme for this case. 110

5.16 Mean of CR sub-band utilization distribution. (a) N_{CR}=50 (b) N_{CR}=300. The CRs have used lower number of sub-bands for SO-DSM which is an indication of map formation in SO-DSM. 112

5.17 Variance of CR sub-band utilization distribution. (a) N_{CR}=50 (b) N_{CR}=300. $\mathcal{V}_s$is higher for SO-DSM which demonstrates CRs have successfully built temporal organization. 113

5.18 The simulation results for SO-DSM using different values of η_1. CR network spectrum utilization. 116

5.19 The simulation results for SO-DSM using different values of η_1. Probability of collision for PUs. 117

5.20 Probability of CR link interruption for SO-DSM using different values of η_1. Probability of CR link interruption. 118

5.21 The simulation results for SO-DSM using different values of η_1. Average number of sub-bands used by CRs. 119

5.22 The simulation results for SO-DSM using different values of η_1. Average variance of CR sub-band utilization distribution. 120

5.23 The simulation results for SO-DSM using different values of η_2. CR network spectrum utilization. 122

5.24 The simulation results for SO-DSM using different values of η_2. Probability of collision for PUs. 123

5.25 Probability of CR link interruption for SO-DSM for different values of η_2. Probability of CR link interruption. 124
5.26 The simulation results for SO-DSM using different values of η_2. Average number of sub-bands used by CRs. 125
5.27 The simulation results for SO-DSM using different values of η_2. Average variance of CR sub-band utilization distribution. 126
5.28 The simulation results for SO-DSM using different values of β_1. The CR network spectrum utilization. 128
5.29 The simulation results for SO-DSM using different values of β_1. Probability of collision for PUs. 129
5.30 Probability of CR link interruption for SO-DSM using different values of β_1. 130
5.31 The simulation results for SO-DSM using different values of β_1. Average number of sub-bands used by CRs. 131
5.32 The simulation results for SO-DSM using different values of β_1. Average variance of CR sub-band utilization distribution. 132
5.33 The simulation results for SO-DSM using different values of β_2. The CR network spectrum utilization. 134
5.34 The simulation results for SO-DSM using different values of β_2. Probability of collision for PUs. 135
5.35 Probability of CR link interruption for SO-DSM using different values of β_2. 136
5.36 The simulation results for SO-DSM using different values of β_1. Average number of sub-bands used by CRs. 137

5.37 The simulation results for SO-DSM using different values of β_2. Average variance of CR sub-band utilization distribution. 138

6.1 The simulation results for random initial state. The CR network spectrum utilization. 146

6.2 The simulation results for random initial state. The Probability of collision for PUs. 147

6.3 The simulation results for random initial state. Probability of CR link interruption. 148

6.4 The simulation results for random initial state. Average received interference by TX PUs. 149

6.5 The simulation results for random initial state. Average received interference by RX PUs. 150

6.6 The simulation results for random initial state. Average number of sub-bands used by CRs. 151

6.7 The simulation results for random initial state. Average variance of CR sub-band utilization distribution. 152

6.8 The simulation results for noisy PUs' parameters. The CR network spectrum utilization. 154

6.9 The simulation results for noisy PUs' parameters. The Probability of collision for PUs. 155

6.10 The simulation results for noisy PUs' parameters. Probability of CR link interruption. 156

6.11 The simulation results for noisy PUs' parameters. Average received interference by TX PUs. 157

6.12 The simulation results for noisy PUs' parameters. Average received interference by RX PUs. 158

6.13 The simulation results for noisy PUs' parameters. Average number of sub-bands used by CRs. 159

6.14 The simulation results for noisy PUs' parameters. Average variance of CR sub-band utilization distribution. 160

List of Tables

5.1 SO-DSM parameters used in simulations. 88

5.2 The simulation results for SO-DSM and MG-DSM: The numerical results for the average CR network spectrum utilization. 92

5.3 Numerical simulation results for SO-DSM and MG-DSM: Average probability of collision for PUs. 95

5.4 Numerical simulation results for SO-DSM and MG-DSM: Average probability of CR link interruption. 95

5.5 Numerical simulation results for SO-DSM and MG-DSM: Average received interference by TX PUs. 98

5.6 Numerical simulation results for SO-DSM and MG-DSM: Average received interference by RX PUs. 98

5.7 Numerical simulation results for SO-DSM and MG-DSM: Mean of CR sub-band utilization distribution. 101

5.8 Numerical simulation results for SO-DSM and MG-DSM: Variance of CR sub-band utilization distribution. 101

5.9 Numerical simulation results for centralized DSM and SO-DSM. Legacy network spectrum utilization. 102

5.10 Numerical simulation results for centralized DSM and SO-DSM: The CR network spectrum utilization. 105
5.11 The simulation results for centralized DSM and SO-DSM: Probability of collision for PUs. 108
5.12 The simulation results for centralized DSM and SO-DSM: Probability of CR link interruption. 108
5.13 Numerical simulation results for centralized DSM and SO-DSM: Average received interference by TX PUs. 111
5.14 Numerical simulation results for centralized DSM and SO-DSM: Average received interference by RX PUs. 111
5.15 Numerical simulation results for centralized DSM and SO-DSM: Mean of CR sub-band utilization distribution. 114
5.16 Numerical simulation results for centralized DSM and SO-DSM: Variance of CR sub-band utilization distribution. 114
5.17 SO-DSM parameters used in $\eta_1$simulations. 115
5.18 SO-DSM parameters used in η_2 simulations. 121
5.19 SO-DSM parameters used in β_1 simulations. 127
5.20 SO-DSM parameters used in β_2 simulations. 133

6.1 SO-DSM parameters used in random initial state simulations. . . 145
6.2 SO-DSM parameters used in noisy PUs' parameters simulations. . 154

1

Introduction

1.1 Motivation

The world of wireless communication has changed dramatically in recent years. Around a decade or two ago, wireless communications had fewer users and its applications were mostly limited to low-bandwidth voice and text. The emergence of cheap low-power processors and other electronic devices has allowed the new generation of wireless devices to have very high multimedia and processing capabilities. Nowadays, people can watch high definition (HD) videos on their iphones and browse the internet and listen to online music from their Blackberries. Furthermore, the internet has changed our life style; we now do many things online such as buying tickets, finding directions or ordering a pizza. The new generation of wireless devices such as smartphones, personal digital assistants (PDA) and netbooks enables us to access internet everywhere and use our time more efficiently.

When we are using a wireless device, in fact we are establishing a link through the *electromagnetic radio spectrum*, a valuable and limited resource. The electromagnetic radio spectrum is a natural resource which is licensed and carefully managed by governments to ensure secure and reliable wireless communication. With wireless communications becoming increasingly pervasive all over the world, people are more frequently using wireless devices and services, and there is a growing demand for high-speed wireless communications. A key question that arises then, is how do we cater to this continuing growth of wireless devices and services, given that the radio spectrum is of limited extent?

In the current approach to spectrum management, a wireless service provider buys the license of one or some spectrum bands in a certain geographic area (e.g. a country) and only its users, which we term *legacy* or *primary* users, are allowed to operate in these bands in that geographic area. Thus, radio units are designed to operate only on those specific bands and are sure that no other radio will interfere with them. For example, the GSM-900 network uses 890-915 MHz 935-960 MHz bands, and the 108-138 MHz band is reserved for air traffic control [4]. Spectrum management using this *static* policy is simple, optimal, secure and easy to implement; however, it needs to be reviewed and modified for two reasons:

1. The operable spectrum band is limited due to system design and implementation issues. The operational spectrum band for current commercial wireless systems ranges from 0.4 GHz to 6 GHz and most of this band is

already reserved in many countries. Therefore, in the near future there may well be no room left for fast-developing new applications.

2. The efficiency of the current static spectrum management policies is low, resulting in the under-utilization of this limited and highly valuable resource [5]. Several recent studies conducted in North America [6–8] and elsewhere [9–11] have shown that this precious resource is very much underutilized by legacy users. For example, the measurements performed in [6] have shown that from January 2004 to August 2005 on average only 5.2% of the radio spectrum was actually in use in the United States.

Although the operational band is getting slowly wider as new technologies have increased the operational bandwidth of new devices, we need to increase the spectrum utilization efficiency in order to serve the fast-growing demand for broadband wireless communications. According to predictions made by the International Telecommunications Union and the Organization for Economic Cooperation and Development, if serious actions are not taken towards smart, efficient, and dynamic management of the electromagnetic spectrum, the worldwide mobile communication network will collapse by the year 2050 [12].

Cognitive science provides the tools for building a new generation of devices with dynamic applications. These cognitive machines will be able to build up their rules of behaviour over time through learning from experiential interactions with the environment. The fundamental elements of cognition in these systems are:

- Perception-action cycle,

- Memory (encompassing learning)
- Attention
- Intelligence
- Language

Although intelligence is considered to be a computational problem, accurate study of biological systems in general and especially the structure of the brain provides a reliable guide for building cognitive machines. Therefore, we may say that computer science, biology and other related disciplines will play key roles in the newly emerged field of *cognitive dynamic systems (CDS)* [13].

Cognitive radio (CR) [5,14] is a special class of cognitive dynamic systems and offers a novel way of solving the spectrum utilization problem. Spectrum utilization can be improved significantly by making it possible for a *secondary* (cognitive radio) user (who is not being serviced) to access a spectrum hole unoccupied by the primary (legacy) user. Cognitive radio solves the problem by, continuously monitoring the environment, identifying those sub-bands of the electromagnetic spectrum that are underutilized, and providing the means for making those sub-bands available for employment by secondary users. Typically, the sub-bands allocated for wireless communications are the property of legally licensed owners, which, in turn, make them available only to their own customers: the primary users. From the perspective of cognitive radio, underutilized sub-bands are referred to as *spectrum holes*. A spectrum hole is a band or sub-band of frequencies assigned to a primary user, but at a particular time and specific geographic location, it is not being utilized by that user, partially or fully [5].

The entire operation of cognitive radio hinges on the availability of spectrum holes. The identification and exploitation of spectrum holes poses technical challenges rooted in computer software and hardware, signal processing, communication theory, control, optimization, and game theory, just to name a few disciplines. Moreover, the operation of cognitive radio is compounded further by the fact that the spectrum holes come and go in a rather stochastic manner.

The large number of heterogeneous elements in a cognitive radio network that interact with each other indirectly for limited resources makes the cognitive radio network a complex dynamic system [5,15] or a system of systems [16]. In such an environment, each element is a decision-maker. Different degrees of coupling between different decision-makers of one tier or between decision-makers from different tiers influence their chosen policies. Change of policies affects the interaction between the decision makers and alters the degrees of coupling between them. In other words, both upward and downward causations [17] play key roles in a cognitive radio network and lead to positive or negative emergent behaviour, which is not explicitly programmed in different elements. Since the global behaviour of the network cannot be reduced to the local behaviour of different elements and mathematical analysis of such super complex systems are impossible, clearly, large scale computer simulations need to be performed to study their emergent behaviour.

1.2 Cognitive Radio

Cognitive radio (CR) is fast emerging as a way of responding to under-utilization of the radio spectrum. For a working definition of cognitive radio, we offer the following [5, 15]:

> The cognitive radio network is an intelligent multiuser wireless communication system that embodies the following list of primary tasks:
>
> - to perceive the radio environment (i.e., outside world) by empowering each user's receiver to sense the environment on a continuous time basis;
> - to learn from the environment and adapt the performance of each transceiver to statistical variations in the incoming RF stimuli;
> - to facilitate communication between multiple users through cooperation in a self-organized manner;
> - to control the communication processes among competing users through the proper allocation of available resources;
> - to create the experience of intentions and self-awareness.
>
> The primary objective of all these tasks, performed in real-time, is two-fold:
>
> - to provide highly reliable communication for all the users wherever and whenever needed;

- to facilitate efficient utilization of the radio spectrum in a fair-minded way.

1.3 Perception-Action cycle of cognitive radio

Cognitive radio units perform their tasks through a *cognition cycle*, called the *perception-action cycle*, shown in Fig. 1.1. This cycle is depicted in Fig. 1.1 (b), representing a subset of Fig. 1.1 (a) with a minor difference: the functional block labelled nonparametric spectrum estimation in the receiver has been used in Fig. 1.1 (b) so as to add more specificity to the notion of radio scene analysis. As shown in the Fig. 1.1 (a), this cycle has four fundamental elements:

1. *Radio scene analysis (RSA)*, which encompasses

   - estimation of interference temperature of the radio environment localized around a user's receiver;
   - detection of spectrum holes;

   Radio-scene analysis is an essential functional block of cognitive radio. In fact, the performance of the dynamic spectrum management and transmit-power control is dependent on how reliable and accurate the RSA is. The RSA continuously monitors the surrounding environment of the CR unit, analyzes the received signals, and sends the results to the transmitter for dynamic spectrum management and transmit-power con-

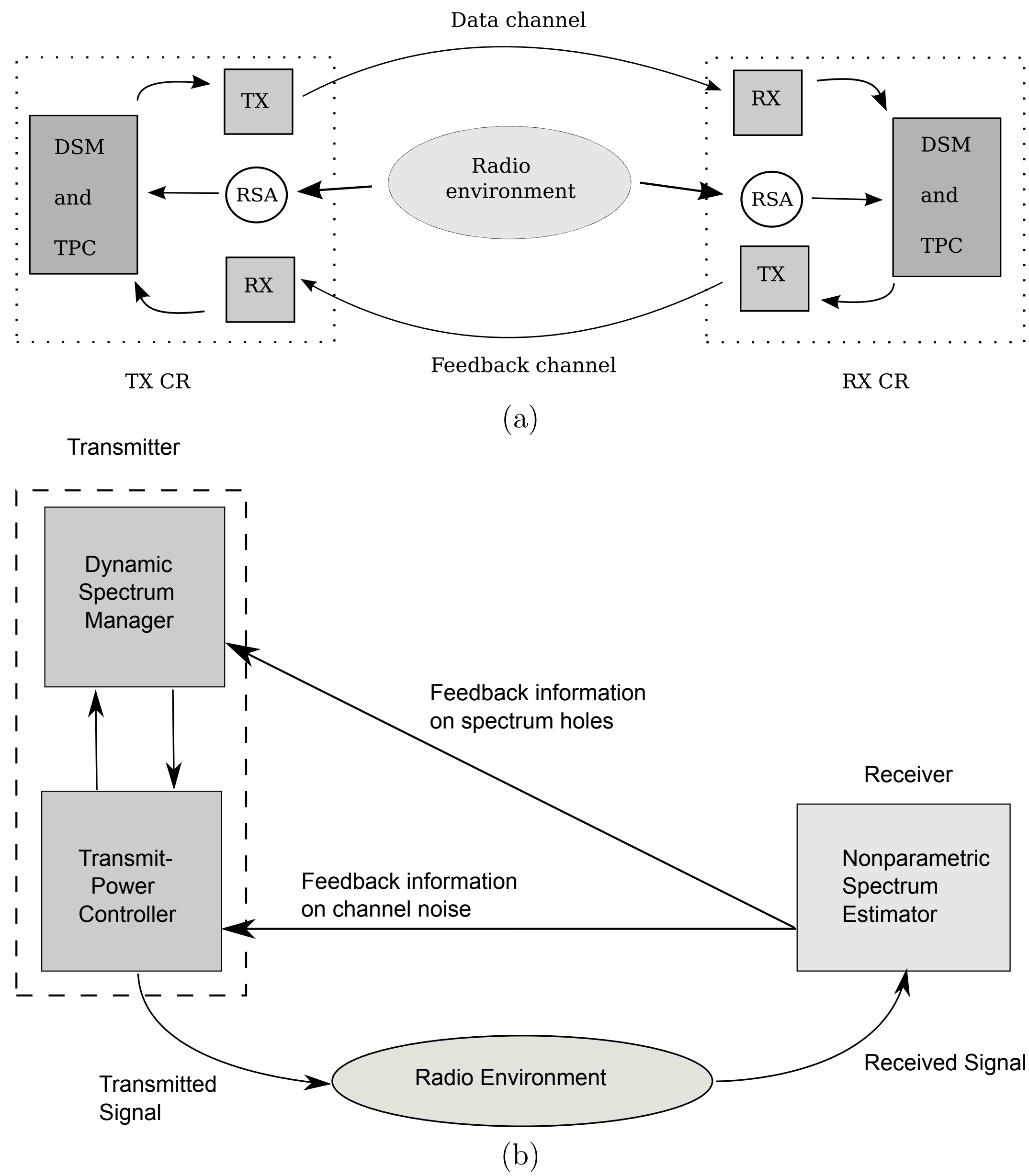

Figure 1.1: (a) Directed-information flow in cognitive radio. DSM: dynamic spectrum manager; TPC: transmit-power controller; RSA: radio-scene analyzer; RX: receiver; TX: transmitter; TX CR: transmitter unit in the transceiver of cognitive radio; RX CR: receiver unit in the transceiver of cognitive radio. (b) Perceptionaction cycle of cognitive radio unit.

trol. The dynamic spectrum management and transmit-power control subsystem decides on an appropriate action based on the information it receives from the RSA subsystem. In this context, there has been an extensive amount of research devoted to spectrum sensing in cognitive radio [4, 18, 19]. There are several techniques proposed for the RSA in the literature such as energy detection [20–22], feature detection with emphasis on cyclostationarity [23–27], and the mutitaper spectrum estimation [5, 28]. However, as it is discussed in [5, 15], the multitaper method (MTM) has several desirable attributes which makes it the method of choice for cognitive radio [29]:

- Accuracy with which the spectrum holes are detected, and which is highly desirable recognizing the need for efficient spectrum utilization.
- Substitution of resolution versus variance in place of bias versus variance
- Intrinsic regularization due to model-independence
- Flexibility to accommodate other desirable features, namely space-time processing for direction finding of interferers, and the provision of cyclstationarity for detection of legacy users' modulations.
- Robustness.
- Last but by no means least, fast computational processing capability by using the FFTW algorithm, with provision made a prescribed library of Slepian sequences.

It is not the computational complexity of the MTM that is responsible for lack of attention in the signal processing literature; rather, this issue can be attributed to the complicated way in which the MTM was first described in the 1982 paper by Thomson [28]. This matter has been rectified by Farhang [30] through the way in which the MTM is derived using filter-bank theory, well-known in the signal processing literature.

Furthermore, spectrum sensing is improved when cognitive radios cooperate with each other and share their radio scene analysis information [31–33]. In actual fact, cooperative sensing not only improves the spectrum sensing in normal conditions of CR units, but also can significantly mitigate *fading* and *shadowing*, two phenomena which can make spectrum sensing a very challenging task.

2. *Transmit-power control (TPC)*, the purpose of which is to determine the transmit-power levels of CR units, given

    - a set of spectrum holes;
    - measurements of the variance of interference plus noise at the receiver input of every user.

    so as to jointly maximize their data transmission rates and subject to the constraint that the permissible interference power level limits in the idle sub-bands (i.e. spectrum holes) are not violated. For the cognitive function of transmit-power control in the transmitter, the issue of prime interest is robustness versus optimality. Moreover, for choosing an algorithm several characteristics are of critical importance such as low complexity, fast convergence, distributed nature, and convexity. Due to different uncertainty sources in a cognitive radio network such as supply-side risks and demand-side risks, adjusting the transmit power of a cognitive radio requires solving an optimization problem under uncertainty. Stochastic and robust optimization can be used to address the uncertainty issue. In [34, 35], a receiver-centric design was described, based on flexible local constraints on transmit power dictated by interference-temperature limit. There is no need for information exchange between different users in the proposed approach and it is well suited for an open spectrum-sharing regime. In this algorithm, optimality in performance is, in effect, traded in favour of robustness and a robust version of the transmit-power controller was proposed, which improves the network robustness against malicious users [36–39] as well as changes in the number of users, network topology, and available unused sub-bands.

3. *Dynamic spectrum management* (DSM), assigns the available unused spectrum among the CR units according to the environmental constraints and is one of the main challenges in cognitive radio. There are two approaches for solving this problem: centralized and decentralized. Although, centralized approaches may achieve a global optimum solution, they are not suitable for CR networks. The DSM problem is equivalent to *graph colouring* problem and practically impossible to solve in a centralized manner [40]. Furthermore, centralized approaches are not scalable and require additional infrastructure. In decentralized

approaches, on the other hand, CR units perform DSM based on what they have learned from their environment and solve the problem locally. These schemes may not achieve global optimization in the network but are scalable and practical.

4. *Feedback*: Global feedback embodies the entire radio unit and the wireless channel and is a facilitator of intelligence, without which the CR loses its cognitive capability. Information on unused sub-bands and the forward channel's condition, extracted by the spectrum sensor at the receiver, is sent to the transmitter via the feedback channel. Having this information enables the transmitter to adaptively adjust the transmitted signal and update its transmit power over desired channels. Specifically, the discovery of unused sub-bands prompts the need to establish the feedback channel from the receiver to the transmitter of a cognitive radio.

The perception-action cycle, as shown in Fig. 1.1 (b), happens between two CR units, the combination of which we term a *link*. Each cognitive radio unit involves a transceiver which includes a transmitter and a receiver. At each time instance, one CR unit, termed transmitter CR (TX CR), is transmitting and the other CR unit, termed receiver CR (RX CR), is receiving through the data channel. Through the cognition cycle, the transmitter CR takes actions, which involve transmitting on a specific sub-band of the spectrum that is decided by the DSM unit, and with the power level chosen by the TPC subsystem. The receiver CR sends back the results of those actions to the transmitter CR. The key element that completes this cycle is the *feedback* channel connecting the two CR units. Through this channel, the receiver sends two forms of information to the transmitter:

- information on the performance of the data channel for adaptive modulation, dynamic spectrum management and transmit-power control;
- information on the radio scene on the receiver's side.

Accordingly, the feedback channel plays a critical role in the cognition cycle and can be established in three ways:

1. **A dedicated universal channel for cognitive radio** [41]: A specific spectrum band is licensed and reserved for cognitive radio feedback channel. This solution has the advantage of simple system design and reliability; however, it is expensive (due to spectrum licensing) and also it is hard to find a worldwide common free channel for this purpose due to different spectrum utilization policies in different countries. Furthermore, the cognitive radio can be easily interrupted by jamming the feedback channel. Finally, dedicating such a spectrum band to cognitive radio contradicts one of the main goals of cognitive radio, which is increasing the radio spectrum utilization, and such dedicated spectrum band would be wasted whenever cognitive radio units are not in use.

2. **Using available spectrum holes**: Cognitive radios can use spectrum holes both for data transmission and feedback channel. Using spectrum holes is more flexible and efficient in terms of spectrum utilization than using a dedicated channel. However, the cognitive radio network cannot always be established because sometimes it is possible that there is no

spectrum hole available in the environment. When there are no spectrum holes available, there is no feedback channel and CR units lose communication and synchronization. Thus, the moment some spectrum holes become available, CR units can not immediately start data transmission and must wait until the necessary synchronization and negotiations are finished. Furthermore, the radio spectrum is a highly dynamic environment and the spectrum holes may change in time. Therefore, every time the feedback channel becomes unavailable, CR units lose synchronization and need to stop data transmission until feedback channel is established again.

3. **Using unlicensed bands**: Cognitive radio units can also establish their feedback channel using unlicensed bands. In this case, the feedback channel is always available and CR units never lose synchronization. The CR network can always be established even when there is no spectrum hole available in the environment. However, using the unlicensed band, the CR units may need to combat a high level of noise and interference due to the other radios working in these bands.

Using the unlicensed bands for establishing the feedback channel is the best choice for the following reasons:

- The CR network is always established and CR units never lose synchronization. Furthermore, even when there is no spectrum hole available in the environment, CR units may use the unlicensed bands to transmit data. Thus, CR units can always provide communication and achieve one of the their primary goals, which is providing reliable communication whenever and wherever needed [5].

- Cognitive radio units can always, even when there is no spectrum hole, cooperate and share their radio-scene analysis information which results in better and faster detection of spectrum holes [31–33].

- When a spectrum hole used by a link becomes unavailable, CR units can negotiate through the feedback channel to find another common spectrum hole and change their data channel momentarily.

As radio-scene analysis and transmit-power control are well understood and well covered in the literature [34, 35], in this work, we focus on the dynamic spectrum management (DSM) problem and propose a novel DSM scheme based on self-organizing maps.

1.4 Self-Organizing Maps in the Human Brain

Self-organizing maps (SOM)s are a special class of artificial neural networks that is inspired by a distinct feature of the cortex in the human brain. Several parts of the human brain are organized in a way that different sensory inputs are represented by *topologically ordered computational maps.* In particular, sensory inputs such as visual [42, 43], tactile [44] and acoustic [45] inputs are mapped in a topologically ordered manner onto different areas of cerebral cor-

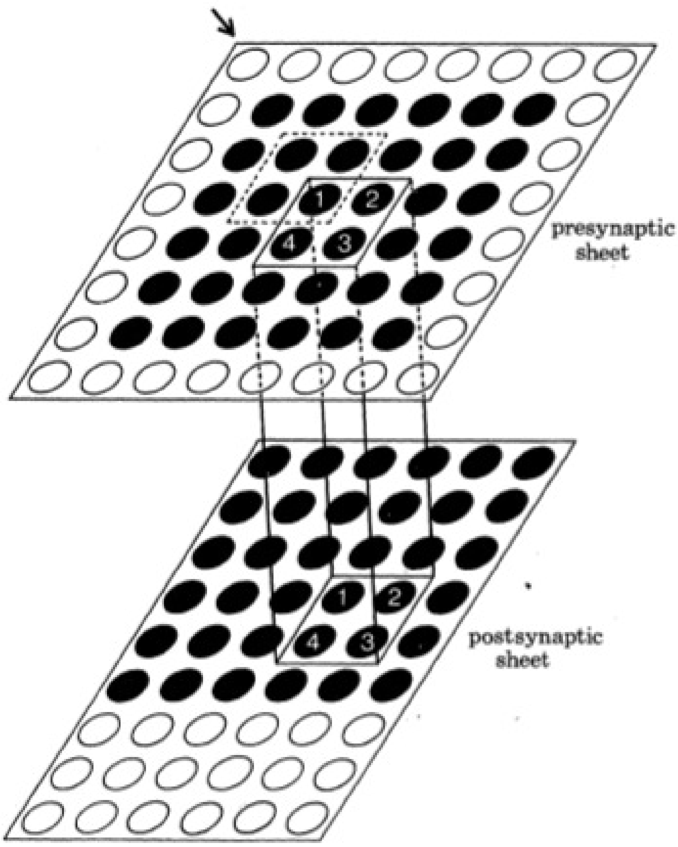

Figure 1.2: Von der Malsburg model (reproduced from [1]).

tex. The SOM have become a popular tool for vector quantization, clustering analysis, feature extraction and data visualization [46].

1.4.1 Historical Notes on SOM

All stages of brain organization more or less involve an element of self-organization. The genes can not contain the tremendous amount of information necessary to describe the brain. For example, celebral cortex, only by itself, contains on the order of 10^{14} synapses [47] and it is impossible for genes to carry the correct wiring of such complex system. Therefore, ontogeny employs mechanisms of self-organization to correctly connect neurons to their targets . Many researches became fascinated with this property of human brain and tried to come up with mathematical model for it. The first model of map formation, introduced by von der Malsburg [48], was for a small patch of retina stimulated with bars of different orientation. This model, illustrated in Fig. 1.2, has two layers of neurons. The goal of the SOM algorithm is to modify the connections between input and output layer so that each neuron in output layer is connected to its spatially corresponding neuron in the input layer.

Another SOM model that has gained attention in the literature is the Kohonen model [49, 50] which is not meant to explain neurobiological details. Rather, this model captures the essential features of the map formation in the brain while remains computationally tractable. The Kohonen model is capable of data compression (i.e. reduction of input dimensionality) [51, 52].

Recent models of SOM [53] have formulated the mapping algorithm in terms of an objective function E_C, termed *energy function*, that must be optimized. However, not all SOM models can be derived using an optimization of energy function dynamics [54] and several models of SOM that can be derived using energy function optimization dynamics are reviewed in [53]. Tsigankov and Koulakov have proposed a energy function based SOM model for the map formation in the superior colliculus [55] which was later validated by Stryker [56].

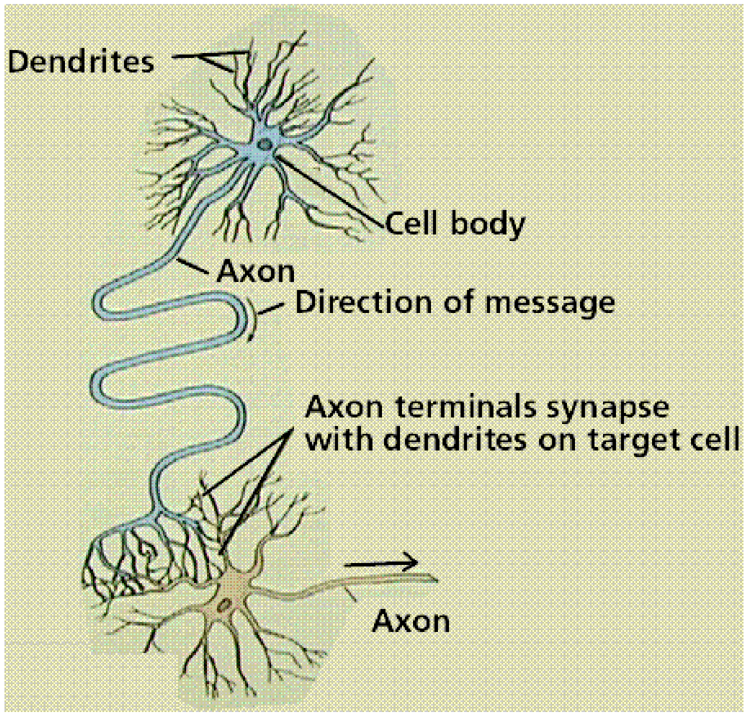

Figure 1.3: Structure of a neuron (Reproduced from [2]).

1.4.2 Neural Networks

The brain is an amazing information-processing system which performs computation differently from conventional digital computers. It is a highly *complex*, *nonlinear* and *parallel* computer that can organize its structural constituents, called neuron and shown in Fig. 1.3, to perform certain computational tasks such as pattern recognition, perception and motor control much faster than current digital computers. A neural network, in its most general form, is a machine that is designed to model the way the brain performs a particular task or function of interest. Haykin offers the following definition for a neural network viewed as an adaptive machine [52]:

A neural network is a massively parallel distributed processor made up of simple processing units that has a natural propensity for storing experiential knowledge and making it available for use. It resembles the brain in two ways:

1. Knowledge is acquired by network from its environment through a learning process.
2. Interneuron connection strengths, known as synaptic weights, are used to store the acquired knowledge.

The building block of neural network is a neuron. Figure 1.4 illustrates a general model of a nonlinear neuron. The relation between an input signal vector

$$\mathbf{x}(n) = [x_1(n)\ x_2(n)\ \ \ldots x_m(n)]$$

and the resulting output signal of neuron $y(n)$ is described by:

$$y(n) = \varphi\left(\sum_{i=1}^{m} w_i(n)x_i(n) + b\right) = \varphi\left(\mathbf{w}(n)\mathbf{x}(n)^T + b\right) \tag{1.1}$$

where b is the bias, $\varphi()$ is the activation function and $\mathbf{w}(n) = [w_1\ w_2\ \ \ldots w_m]$ are the *synaptic weights*.

In a self-organizing map, the neurons are nodes of a usually one- or two-dimensional lattice and become selectively tuned to various input patterns or classes of input patterns [1, 52]. In SOM, neurons act in parallel and process pieces of information that originate from different regions in the input space but are similar in nature. Each neuron gets tuned to the pattern in the input signals it receives, therefore, the whole network becomes tuned to the patterns

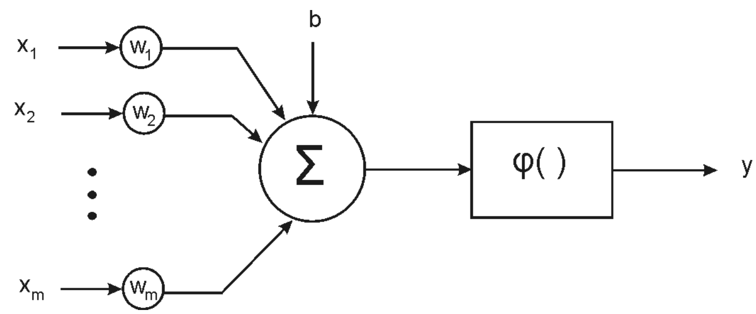

Figure 1.4: The model of a neuron.

in the entire input space. There are three fundamental elements for formation of SOMs:

- self-amplification,
- competition,
- correlation (redundancy) in input signals.

A fundamental and very important property of SOMs is the fact that in SOMs *global* order arises from *local* interactions.

1.5 Contributions of Thesis

This research focuses on resource allocation in cognitive radio networks in which users access the available spectrum in an opportunistic manner. The thesis introduces a novel decentralized dynamic spectrum management scheme for cognitive radios termed *self-organizing dynamic spectrum management (SO-DSM)* which for the first time, employs SOM technique to solve the DSM problem in CR. Inspired by the human brain, this scheme learns the spectrum utilization patterns in the environment using the self-organizing maps technique proposed by Tsigankov and Koulakov [55] and establish CR links according to the obtained knowledge. The SO-DSM adopts the SOM model for a problem that is entirely different from how the brain does it. Furthermore, a multi-agent software testbed is developed to study the emergent behaviour of CR network using the proposed DSM scheme through large-scale computer simulations.

The SO-DSM is a novel decentralized DSM scheme that solves the DSM problem locally for CR units with low complexity. In SO-DSM, each CR unit establishes a feedback channel on unlicensed bands with its neighbouring CR units. Using this channel, CR units are always exchanging information and coordinating for using available spectrum holes in an efficient manner. A form of Hebbian learning rule [57] is employed which is essential for formation of self-organizing map. The complexity of this learning rule is linear in the number of neighbours and therefore, the average complexity of SO-DSM depends on the average density of radio network, not the total number of units. Consequently, the network size is scalable.

1.6 Thesis Organization

This thesis is organized as follows:

- Chapter 2 discusses dynamic spectrum management in cognitive radio networks. Two possible ways of spectrum sharing are explained and discussed. The mathematical equivalent of DSM problem in graph theory is explained and the mathematical optimization problem of DSM is proposed. Two approaches, namely centralized and decentralized approaches, are presented along with advantages and disadvantages of each approach.

- Chapter 3 studies Tsigankov-Koulakov (TK) model for self-organizing maps. The theory of self-organizing maps is presented and TK SOM model which in the basis for the proposed algorithm in this work is explained. Hebbian learning, a learning rule essential to formation of SOMs, is also presented and reviewed.

- Chapter 4 introduces self-organizing dynamic spectrum management (SO-DSM) scheme for CR networks. The assumptions and system requirements for the proposed architecture are explained. Furthermore, the system architecture and design is proposed and system parameters are studied and discussed.

- Simulation results are presented in Chapter 5. In this chapter, the software testbed developed and used for simulations and the network model of simulations are explained and large-scale network computer simulation results are presented. In the simulations, three DSM schemes, namely SO-DSM, a centralized DSM and a decentralized DSM based on minority game, were used and the results are presented and analyzed. Moreover, simulation results for various SO-DSM system parameters were presented.

- Chapter 6 discusses the robustness of the SO-DSM scheme. The concept of robustness is reviewed and its importance for designs concerning complex and large-scale systems such as cognitive radio networks is emphasized. Simulation results are presented to validate the robustness of SO-DSM under perturbation of system parameters and initial state.

- The thesis concludes in Chapter 7 by reviewing the contributions of the thesis to the literature.

- The Appendix provides the proof of the maximum eigenfilter theorem along with explanation of minority game DSM and robust transmit-power controller used in simulations.

2

Dynamic Spectrum Management

Dynamic spectrum management is one of the main challenges in cognitive radio [5, 15]. The goal of DSM is to distribute the spectrum holes among CR units to use them as long as they are not being used by any primary user. When two CR units need to communicate and establish a link, the DSM subsystem chooses one of the common spectrum holes between them and they operate on that band as long as it is available. If during communication, a primary user is detected on that band, the transmitter CR unit must stop transmission *immediately* and they should find another common spectrum hole to use. For example, Fig. 2.1 illustrates a simple example of the DSM at two time instants. In the first time instant shown in Fig. 2.1(a), two spectrum holes, CH2 and CH5, are available where CH2 is being used by a CR unit. At the other time instant shown in Fig. 2.1(b), a primary user has started operating on CH2; thus, the CR unit has stopped using CH2 and has moved to the other spectrum hole CH5. Note that in the second time instant, CH1

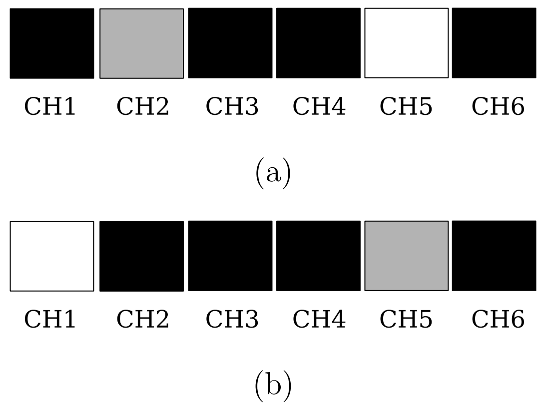

Figure 2.1: An example of spectrum set up at two time instants. The spectrum holes are shown with white colour, spectrum bands used by CR, with grey colour and unavailable spectrum bands are shown with black colour.

has changed to a spectrum hole assumed to be available.

There are several issues which make the DSM problem hard to solve:

1. The DSM problem is a highly dynamic problem because radio units move, stop or start transmitting and change their spectrum utilization pattern over time. Therefore, the problem constraints and parameters change in time and providing robust and reliable communication becomes very challenging.

2. One of the main motivations behind CR is increasing the spectrum utilization efficiency. Desirably the DSM of each link in the network must result in an optimal channel assignment over the entire CR network. Finding such optimal channel assignment is not easy due to large size and dynamic nature of the problem.

3. One of the main constraints in CR problem is ideally avoiding collision

with PUs or at least keeping the probability of collision with PUs below an acceptable threshold. In practice, satisfying this constraint without sacrificing too much efficiency is challenging because the RSA unit discovers PUs after a time delay D_{RSA}.

2.1 Spectrum Sharing

In order to increase the spectrum utilization efficiency, cognitive radio tries to share the spectrum band with legacy users, naturally giving the legacy users the highest priority to use the spectrum. There are two ways for sharing the spectrum with primary users:

1. **Price-based sharing of spectrum:** [58–61] In this approach, primary networks' owners temporary sell their spectrum to CR units whenever it is not used by their own users and CR units compete for buying these spectrum holes. Thus, in this method, there is no need for performing dynamic spectrum management in cognitive radios because it is performed by the primary network.

2. **Opportunistic sharing of spectrum** [5, 15, 62, 63]: In this alternative approach, the CR units utilize spectrum holes whenever they are available in an opportunistic manner and without primary network's permission.

In the first method of spectrum-sharing, cognitive radios communicate with the primary networks in the environment and lease the spectrum holes [64]. This method of spectrum-sharing has several advantages:

- System design is simple because there is no need for spectrum sensing and dynamic spectrum management. These challenging tasks are performed by the primary network, and cognitive radios just negotiate with the primary network to lease spectrum holes.

- The probability of collision between CR units and primary users is zero, because dynamic spectrum management is performed by the primary network and spectrum bands are offered to the CR units only when they are not used by any primary user.

Implementation of price-based spectrum-sharing is easy, in actual fact, this method is being used by cell phone networks currently and is termed *roaming*. In roaming, a cell phone uses a wireless network other than its own service provider's network and pays some fees for using the spectrum. However, for several reasons, the price-based method of spectrum-sharing is not suitable for cognitive radio and can not always be used by CR units :

- Cognitive radios are required to be able to provide reliable communication wherever it is needed, but performing the price-based spectrum-sharing requires the presence of a primary network which is *willing* to sell its spectrum holes to CR units. Thus, using this method, CR units cannot operate in locations where there is no such primary network present.

- Using price-based method, there is no need for radio scene analysis, therefore, radios lack one of the essential elements of cognition which is *awareness* of the surrounding environment.

- Learning and adaptation are different from what is defined for cognitive radio. In price-based spectrum sharing, the CR units should learn the behaviour of other CR units around, which are their competitors, and adapt to their behaviour by changing their own pricing strategy; while cognitive radios are supposed to learn from the surrounding radio environment and adapt to statistical variations in the incoming RF stimuli [15].

Although, price-based spectrum-sharing can not be used solely in cognitive radio, it can be used as a complement to the opportunistic spectrum-sharing; that is, when the primary network is willing to cooperate with the CR units, and the CR units are willing to pay the price for using the spectrum. Cognitive radios can use the price-based method to save battery and processing power and decreasing the probability of collision with primary users to zero.

Opportunistic sharing of the spectrum is the other method for spectrum-sharing, suggested for cognitive radios in the literature [5, 15, 62, 63]. In this alternative method, the CR units try to use the spectrum holes in an opportunistic manner without any cooperation or communication with the primary users. Therefore, CR units need to continuously monitor the environment to detect the primary users and avoid collision with them. Using opportunistic method, there is no need for any infrastructure and CR units can operate everywhere. Furthermore, they do not pay any access fee to spectrum owner, however:

- they have to perform dynamic spectrum management and radio-scene analysis by themselves;

- the probability of collision is not zero because RSA has a time delay in discovering PUs and they have to make sure to decrease the probability of collisions as much as possible.

In this work, a DSM scheme for opportunistic sharing of spectrum for CR networks is proposed.

2.2 The DSM problem

Dynamic spectrum management is a time-varying and location-dependent optimization problem. The spectrum holes come and go in time and also they change from one location to another. In a sense, the DSM problem is an optimization problem that is equivalent to the *graph-colouring* problem in graph theory [62]. Graph-colouring is a well-known optimization problem and is known to be NP-hard and computationally challenging to solve [65, 66]. Therefore, finding the exact solution for the DSM optimization problem is not practical most of the time.

Before proceeding to state the DSM problem in mathematical terms and explain the equivalent graph-colouring representation of the DSM, we first define some necessary mathematical terms. Note that although in the DSM problem, all the problem variables, parameters and constraints are time-dependent, we have omitted t from them for the sake of formulation simplicity, in recognition of the assumption that the environment does not change during the time it takes to solve the DSM problem.

2.2.1 Definitions

We divide the operational radio spectrum into N_{ch} orthogonal sub-bands, which may have different bandwidths, and assume there are M CR units present in the environment. We refer to the ith spectrum sub-band as

$$b_i : \quad i = 1, 2, \ldots, N_{ch}$$

and the jth cognitive radio as

$$C_j : \quad j = 1, 2, \ldots, M.$$

One of the important constraints in the DSM problem is interference with other neighbouring CR units. If two CR units are in the interference range of each other, they cannot use a common spectrum band at the same time. We define the interference factor between C_n and C_m in spectrum sub-band b_j as

$$f(n,m,j) = \begin{cases} 1, & \text{if } C_n \text{ and } C_m \text{ interfere on } b_j \\ 0, & \text{otherwise.} \end{cases} .$$

We further denote the results of the radio-scene analysis for each CR unit C_j is represented by $h_{i,j}$ where

$$h_{i,j} = \begin{cases} 1, & \text{if } b_j \text{ is available for } C_i \\ 0, & \text{otherwise.} \end{cases} .$$

In the CR network, CR units communicate with each other in pairs; therefore, it is not possible to solve the DSM problem by considering the CR units individually. When two CR units need to communicate, they should find a common spectrum hole and start communication on it, which is a challenging problem. Therefore, the DSM problem is assigning one of spectrum holes to *pairs* of CR units, what we refer to as *links*. Thus, the DSM problem is constrained by the active links in the network and in order to solve the DSM problem, instead of considering CR units solely, we need to look at the active links in the CR network.
Among the M CR units in the environment, we assume K CR units are active at current time, i.e. they transmit or receive, where $M \geq K \geq 0$ and K may change in time. These K radios form N_l links in the network where in ith link represented as $l_i = (C_n, C_m)$, C_n is transmitting and C_m is receiving, and

$$K - 1 \geq N_l \geq \lfloor \frac{K}{2} \rfloor$$

where $\lfloor x \rfloor$ denotes the integer part of x.

A spectrum band is available for a link if it is available for both the transmitter and receiver radios, and l_i and l_j interfere on spectrum band b_n if any CR unit of l_i interferes with one or both CR units of l_j on b_n. We denote available spectrum sub-bands for link $l_i = (C_n, C_m)$ as

$$g_{i,j} = h_{n,j} \otimes h_{m,j}$$

where symbol $\otimes$ is defined as

$$x \otimes y = \begin{cases} 1, & x = y = 1 \\ 0, & \text{otherwise.} \end{cases}.$$

Similarly, the interference factor for $l_i = (C_n, C_m)$ and $l_j = (C_s, C_t)$ on spectrum sub-band b_q is denoted by

$$f_l(i,j,q) = f(n,s,q) \oplus f(n,t,q) \oplus f(m,s,q) \oplus f(m,t,q)$$

where the new symbol $\oplus$ is defined as

$$x \oplus y = \begin{cases} 0, & x = y = 0 \\ 1, & \text{otherwise.} \end{cases}.$$

In order to simplify the mathematical representation of problem constraints, we incorporate the available spectrum bands of each link in the interference constraints by defining

$$f_l(i,i,j) = 1 - g_{i,j}. \tag{2.1}$$

The *reward* that link l_i gains from using spectrum sub-band b_j is denoted by $r_{i,j}$ and the channel assignment in the network by $a_{i,j}$, where

$$a_{i,j} = \begin{cases} 1, & b_j \text{ is assigned to } l_i \\ 0, & \text{otherwise.} \end{cases}.$$

For a channel assignment in the CR network to be valid, it has to satisfy two properties:

1. For each link, a channel from its available channels is assigned.

2. When two links interfere on a sub-band b_i, b_i is not assigned to both of them simultaneously.

In other words, the spectrum bands must be assigned to the CR links so that CR links do not interfere with any primary user or other CR link. In mathematical terms, a valid channel assignment is defined by

$$\begin{aligned}
&U = \{a_{i,j} | \in \{0, 1\}\} \\
&\text{subject to} \\
&\forall i, n < M, j < N_{ch} \quad a_{i,j} \cdot a_{n,j} = 0 \\
&\text{if} \quad f_l(i, n, j) = 1
\end{aligned}$$

Note that the first condition is satisfied implicitly by (2.2.1). We denote the set of all valid channel assignments by Λ.

2.2.2 Traffic Model

As been used in several other works in the literature [67–70], the traffic model used for both CR and primary networks is a Markov model (μ_1, μ_2) [71], illustrated in Fig. 2.2. In this model, each transmitter has two states: idle or active. At each time instance, if it is in the idle state, it goes to the TX state with probability μ_1 and if is in the TX state, it goes to the idle state with probability μ_2.

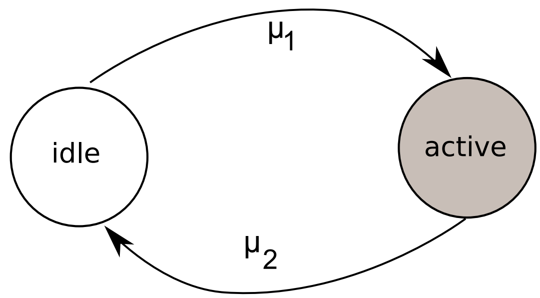

Figure 2.2: Markov model for traffic.

2.2.3 The DSM optimization problem

Now that we have introduced the necessary terminology, we can define the dynamic spectrum management optimization problem. This problem is basically finding one of the optimum channel assignment U^* among all valid channel assignments Λ, which optimizes an objective function. Defining the objective function is an important issue in the DSM problem, because being based on different criteria such as bandwidth, network coverage or fairness, different DSM problems can be defined. Employing each objective function results in a different solution and CR network behaviour. For example, using two different criteria defined in [62], two DSM optimization problems are as follows:

1. *Max-Sum-Bandwidth (MSB)*: The objective here is to maximize the overall spectrum utilization in the network. The optimization problem is expressed by
$$\max_{U\in\Lambda} \sum_{j=1}^{N_{ch}} \sum_{i=1}^{M} a_{i,j}.r_{i,j}$$

2. *Max-Min-Bandwidth (MMB)*: The objective is to maximize the reward (utilization) of the cognitive radio that has the minimum reward (uti-

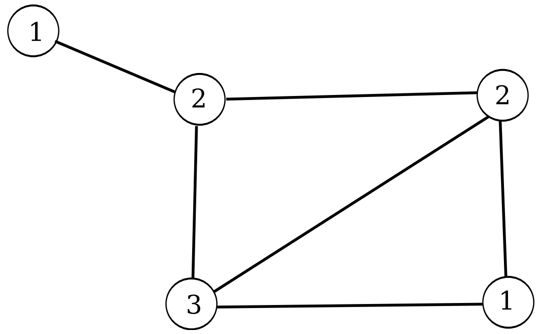

(a)

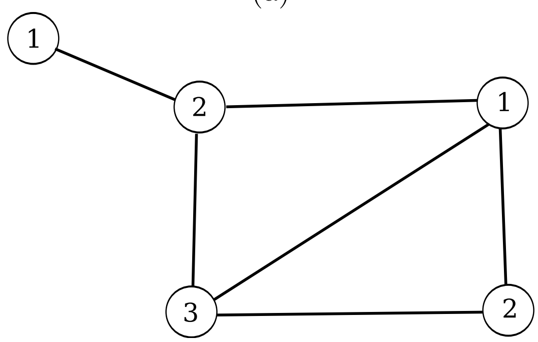

(b)

Figure 2.3: (a) An invalid graph-colouring. (b) A valid graph-colouring.

lization), and it is expressed by

$$\max_{U\in\Lambda}\min_{j<N_{ch}}\sum_{i=1}^{M} a_{i,j}.r_{i,j}$$

2.3 The DSM graph-colouring

Graph-colouring is the problem of colouring the vertices of a graph G with a minimum number of colours. As stated previously, the DSM problem is equivalent to the graph-colouring problem (GCP) in graph theory.

Definition. *Consider the unidirectional graph $G = (V, E)$ with V being the* *set of* $|V| = n$ *vertices and* E *being the set of edges; we call a* $k-colouring$ *of* G*, a mapping* $\phi : V \rightarrow \Gamma$*, where* $\Gamma = \{1, 2, \ldots, k\}$ *is the set of* $|\Gamma| = k$ *integers, each representing one colour. A colouring is valid if*

$$\textit{for all } [u, v] \in E, \quad \phi(v) \neq \phi(u),$$

otherwise, the colouring is called invalid.

In other words, in a valid graph colouring scenario, any two vertices connected by an edge have different colours. For example, Fig. 2.3(a) illustrates an invalid colouring, and Fig. 2.3(b) illustrates a valid graph-colouring. Note that hereafter we represent colours by integer numbers.

Definition. *The chromatic number* $\chi(G)$ *is the minimum number of colours needed for a colouring of graph* G*. A graph* G *is* k*-chromatic, if* $\chi(G) = k$*, and* G *is* k*-colourable, if* $\chi(G) \leq k$*.*

There are two problems in the context of graph colouring:

1. A decision-making problem: Is G k-colourable? which is a NP-complete problem.

2. An optimization problem: Finding the chromatic number of G, which is a NP-hard problem [65, 66, 72].

In order to convert a DSM problem to a graph-colouring problem, we build a graph G by adding a vertex to the graph for each active link in the CR network and connecting those vertices which their corresponding links interfere with each other. For example, in Fig. 2.4 (a), a network of 11 CR units is shown.

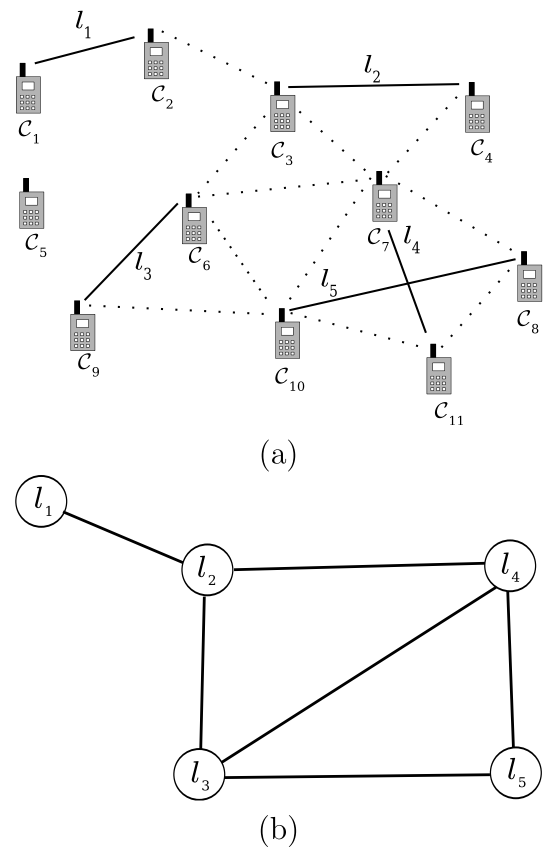

Figure 2.4: (a) A DSM problem scene with 11 CR units; the solid lines represent data links between CR units and dot lines represent interference between two CR unit. (b) The graph representation of (a).

From these 11 units, 10 are active and create 5 links, which are shown by solid lines and the CR units that interfere with each other are connected by dotted lines. The equivalent graph of the network is shown in Fig. 2.4 (b) where we must colour the 5 vertices using minimum number of colours. When graph G is coloured, the corresponding spectrum sub-band to the colour of each vertex is assigned to the corresponding link of that vertex. The equivalent GCP problem of DSM problem is the optimization problem and is NP-hard.

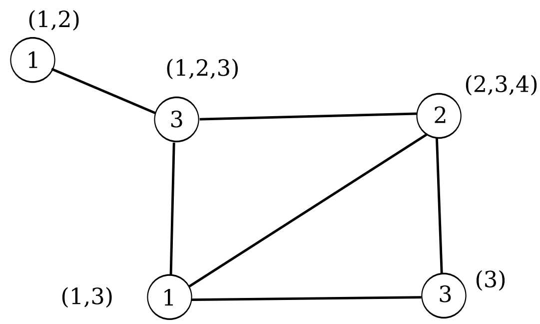

Figure 2.5: A list-colouring problem.

In a general GCP, it is assumed that all the vertices can be coloured from a common list of available colours. However, in the DSM problem, the available channels for each link can be different due to PUs' activities. Thus, by considering the local available channels for links in DSM problem, the exact equivalence of the DSM problem is a GCP with local restrictions on available colours and is called *list colouring*.

Definition. *A list-colouring problem (LCP) is a GCP in which L_i, available colours for each vertex v_i, can be different [65, 73].*

The list-colouring problem is harder to solve than the GCP and is also known to be NP-hard [73]. Figure 2.5 illustrates an example of list-colouring, where the available colour list for each vertex is shown next to it.

2.3.1 The GCP solutions

The graph-colouring problem is a well-known NP-hard problem and there has been extensive research done on this problem. Several exact algorithms such as specialized branch-and-bound algorithms [74, 75] or approaches based on general integer programming formulations of the GCP have been developed to solve the GCP [76–78]. The Brélaz' modification of Randall-Browns colour-

begin
U=V
while $U \neq \emptyset$ **do**
  assign the smallest legal colour to v_i where v_i is the vertex with highest degree in U.
  $U = U - \{v_i\}$
end while
end

Figure 2.6: LDO algorithm for solving GCP.

ing algorithm [74] is known to be one of the best ones to solve the GCP [79]. However, exact algorithms suffer from high complexity, especially for large graphs [78, 80]. Therefore, there have been many approximate algorithms developed to achieve a satisfactory sub-optimum solution such as stochastic local search (SLS) [79] and several heuristics based algorithms [81]. One of the fastest sub-optimum algorithms to solve GCP, which is used in this work as a frame of reference, is called Largest Degree Ordering (LDO).

2.3.2 Largest Degree Ordering Algorithm

Proposed by Welsh and Powel [82], LDO was one of the earliest ordering strategies for solving GCP. In this algorithm, as shown in Fig. 2.6, vertices are first ordered by the descending order of vertex degree. Then starting from the vertex with highest degree, vertices are coloured one after another with smallest legal colour. If there is no colour available for a vertex, it will be left uncoloured.

2.3.2.1 LDO algorithm complexity analysis

This algorithm has two stages

1. Sorting: Vertices has to be sorted in order of largest degree. This can be accomplished by using a sorting algorithm such as *quick sort* which has average complexity of $O(N_l \log(N_l))$ and worst case complexity of $O(N_l^2)$ [83].

2. Colour assignment: Having the sorted list of vertices, the algorithm needs to visit every vertex to colour it, therefore, this stage has complexity of $O(N_l)$.

The average complexity of the LDO algorithm is the larger of $\{O(N_l), O(\log(N_l)N_l)\}$ which is $O(N_l \log(N_l))$ and its worst case complexity is of $O(N_l^2)$.

Due to high complexity of GCP, centralized solutions are simply not practical in some applications. Particularly, in distributed systems, decentralized solutions are more desirable. Therefore, several decentralized algorithms have been proposed to solve GCP [84–87]. As the DSM problem is equivalent to GCP, centralized or decentralized approaches can be used to tackle it.

2.4 Centralized versus decentralized approaches to the DSM

The dynamic spectrum management problem can be solved in either one of two ways:

1. The **centralized** approach, in which the optimization problem is solved globally for the whole network, considering the spectrum set-up data for all the CR units in the network.

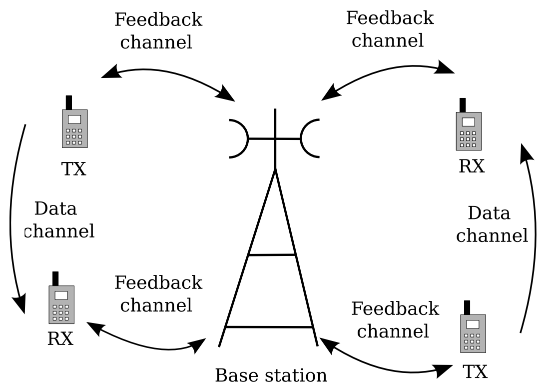

Figure 2.7: The cognitive radio network set up using centralized DSM.

2. The **decentralized** or **distributed** approach, in which the optimization problem is solved locally by each cognitive radio using the local data available for that CR unit.

In the centralized approach, shown in Fig. 2.7, the information of all cognitive radios' spectrum scenes is sent to a *centre* (base station), where an optimization problem is solved having the radio-scene analysis data. The result of solving this optimization problem is an optimum channel assignment for the whole network and once the optimum channel assignment has been computed, it is sent back to all the cognitive radios. This approach may result in a global optimum solution, but it suffers from several disadvantages:

- **High complexity:** Centralized approaches solve an NP-hard optimization problem which is computationally expensive and practically impossible to solve in real time for DSM problem.

- **Wasteful use of resources:** In the centralized approach, data need to be exchanged repeatedly between the base station and all radio units with any change in any part of the network set-up.

- **The system is not scalable:** The centralized approach is feasible only for a small number of radio units and is not scalable due to several reasons:

    1. The complexity of the optimization problem grows very fast; because it is an NP hard problem, it is infeasible to solve it for large number of radio units.

    2. The bandwidth of the base station is limited. As the number of radio units increases, data may need to wait in a queue to get transferred to/from the base station and thus, the system delay increases.

    3. In the centralized approach, the channel assignment for the whole network must be recalculated with *any* change in the network. As the number of radio units grows, the probability and frequency of changes happening in the network increase in a corresponding way. Therefore, as the number of radio units increases, the average frequency of problem-solving increases. Considering the limited processing power and bandwidth of the base station, the total number of cognitive radio units cannot grow to any arbitrary number.

- **Higher Vulnerability:** In a centralized network, all radios are controlled from the base station. Therefore, the whole network can be taken down by attacking the base station. Furthermore, the CR network would not be able to operate if base station stops working for any reason such as power failure or natural disasters.

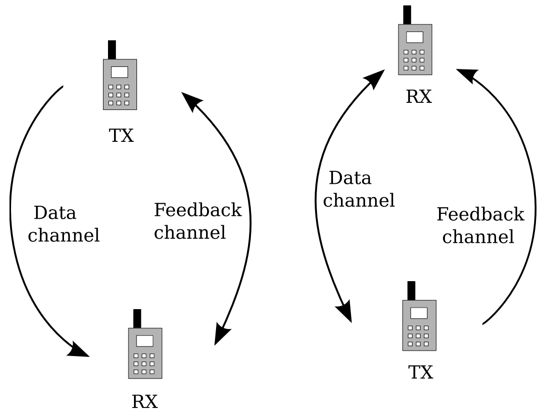

Figure 2.8: The cognitive radio network set up using decentralized DSM.

In the decentralized approach, shown in Fig. 2.8, each two cognitive radios in a link choose the *best* (optimum) channel from the available spectrum holes in the environment, based only on the *local* data available to them.
The decentralized approach is more complicated to design and may not result in a global optimum solution, but it has several advantages over centralized approach that make it attractive and practical for solving the DSM problem:

- **Lower complexity**: A decentralized scheme attempts to solve the DSM problem locally, based on the information available to the CR unit only from its neighbours and aims to find a sub-optimum but satisfactory solution. The decentralized DSM algorithms therefore, have lower complexity than graph-colouring optimization problem in the centralized schemes. Furthermore, the problem is solved only for the CR units in the neighbourhood and thus, the dimensionality and complexity of the problem are lower than the centralized case where the problem is solved for the entire CR network.

- **Robustness**: In the decentralized approach, the CR units need to respond only to environmental changes in their neighbourhood through appropriate changes in their respective channels. Therefore, network changes due to environmental variations happen locally and remain in or close to the neighbourhood in which that change has happened. On the other hand, in centralized schemes, the network changes due to any environmental change can propagate across the whole CR network, and a small change in one location can cause changes in a large portion of the network. Therefore, as the frequency of changes increases, the centralized network may become unstable and therefore, unable to respond to all of the changes in a timely manner.

- **Scalability**: In the decentralized approach, the problem dimension depends only on the number of the neighbours of each CR; thus, approximately the *density* of the CR units in the network. Therefore, as the size of network increases, assuming nearly constant density across the network, the complexity of the problem remains essentially constant for each CR unit and the network can grow to any arbitrary size without increasing the problem complexity.

- **No need for a base station**: In the centralized approach, the processing load is concentrated in a single unit: the base station. Therefore, if the base station stops working or loses the communication with the network, the whole CR network stops operating. Moreover, if there is no infrastructure with a highly capable base station available, a CR unit must handle all the processing and communication load of the base station. This is not practical for mobile radio units with battery and processing-power limitations. On the other hand, in the decentralized approach, the processing and communication loads are distributed over the whole CR network uniformly, and each CR unit needs to handle only a portion of the processing load. Furthermore, the CR network does not depend on any specific radio unit and can continue to work with the failure of any unit.

2.5 Summary

In this chapter, dynamic spectrum management which is one of the challenging problems in cognitive radio was discussed. In order to increase the spectrum efficiency, CR units try to share the licensed spectrum bands with legacy users. Two forms of spectrum sharing, opportunistic or price-based, were explained and discussed. It was shown that, mathematically, the DSM problem is equivalent to list-colouring problem in graph theory. This problem is known to be a NP-hard problem and practically impossible to solve in real time. Therefore, a fast sub-optimum algorithm must be used for solving this problem in CR networks. Two approaches, namely centralized and decentralized, were explained and discussed for solving DSM problem in CR networks. Decentralized schemes were identified as the method of choice for solving the DSM problem in CR networks.

3

Tsigankov-Koulakov Model for Self-Organizing Maps

As explained in Sec. 1.4, in a self-organizing map, the neurons are nodes of a usually one- or two-dimensional lattice and become selectively tuned to various input patterns or classes of input patterns [1, 52]. In SOM, neurons act in parallel and process pieces of information that originate from different regions in the input space but are similar in nature. Each neuron gets tuned to the pattern in the input signals it receives, therefore, the whole network becomes tuned to the patterns in the entire input space. There are three fundamental elements for formation of SOMs:

- Self-amplification
- Competition
- Redundancy (correlation) in input signals

3.0.1 Self-amplification

This principle states the following [52]:

> Modifications in the synaptic weights of a neuron tend to self-amplify in accordance with Hebb's postulate of learning, which is made possible by synaptic plasticity.

Such modifications in a single neuron must be based on presynaptic and postsynaptic signals available at *local* level. In fact, the requirements of self-amplification and locality form a feedback mechanism in the neuron.

Hebb's postulate of learning, named in honour of neuropsychologist Hebb, is the oldest learning rule. It is stated in his book [57] as follows:

> When an axon of cell A is near enough to excite a cell B and repeatedly or persistently takes part in firing it, some growth process or metabolic changes take place in one or both cells such that A's efficiency as one of the cells firing B is increased.

By expanding and rephrasing Hebb's postulate of learning as a two part rule [88, 89], we may define a *Hebbian synapse* as:

1. If two neurons on either side of a synapse (connection) are activated simultaneously (i.e., synchronously), then the strength of that synapse is selectively increased.

2. If two neurons on either side of a synapse are activated asynchronously, then that synapse is selectively weakened or eliminated.

A more precise definition for Hebbian synapse by Haykin [52] states:

> A synapse that uses a time-dependent, highly local, and strongly interactive mechanism to increase synaptic efficiency as a function

of the correlation between the presynaptic and postsynaptic activities.

Hebbian learning is characterized by the following four key mechanisms (properties) [52]:

1. *Time-dependent mechanism:* The modifications in a Hebbian synapse depend on the exact time of occurrence of input and output signals.

2. *Local mechanism:* A synapse, by its nature, is a transmission site where synaptic signals are in *spatiotemporal* contiguity. In a Hebbian synapse, modifications depend on these synaptic signals that represent ongoing activities in the presynaptic and postsynaptic units.

3. *Interactive mechanism:* The modification depends on signals on both sides of the synapse. Therefore, the Hebbian learning process depends on interaction between presynaptic and postsynaptic signals in a sense that learning modifications can not be calculated having only one side's signal.

4. *Correlational or conjunctional mechanism:* If we think of the interactive mechanism of Hebbian learning in statistical terms, we find that the correlation between presynaptic and postsynaptic signals over time is responsible for synaptic changes. Therefore, a Hebbian synapse is sometimes referred to as a *correlational synapse.* Another interpretation of Hebb's postulate of learning is that the conjunction of presynaptic and postsynaptic signals is the condition for a synaptic modification. According to this interpretation, the co-occurrence of presynaptic and

postsynaptic signals over a short time interval is sufficient for producing synaptic modification. Thus, the Hebbian synapse is also referred to as *conjunctional synapse*.

3.0.2 Competition

This principle is made possible by synaptic *plasticity* and states that [52]:

> The limitation of available resources, in one form or another, leads to competition among the synapses of a single neuron or an assembly of neurons, with the result that most vigorously growing (i.e., fittest) synapses, respectively, grow at the expense of the others' decline.

In order for a neuron to stabilize, there must be competition among its synapses for limited resources in a way that any increase in strength of some synapses gets compensated for by a decrease in strength of other synapses.

3.0.3 Correlation or Redundancy

The last principle of self-organization states the following [52]:

> The underlying order and structure that exist in an input signal represent redundant information, which is acquired by a self-organizing system in the form of knowledge.

Correlation is indeed the basis of learning [90] and structural information or correlation in the input data is a prerequisite to self-organized learning. If we remove all the redundant information contained in a signal, what remains is a completely random signal that is unpredictable. Self-organizing or unsupervised learning can not function given such random signal. Note that unlike other principles of self-organization that are carried out within a neuron or neural network, structural information is an inherent characteristic of input signal.

Typically, SOM models use a form of *Hebbian learning rule* to extract patterns or correlation from input data and modify the network organization accordingly.

3.1 Mathematical Model of Hebbian Learning

Hebbian learning is an iterative learning process. In each time step n of the learning process, an appropriate adjustment, $\Delta w_j(n)$, is applied to each synaptic weight $w_j(n)$ and the learning process stores the knowledge gained from the environment in the synaptic weights of the neuron. The general form of the weight adjustment for Hebbian learning process is [52]:

$$\Delta w_j(n) = F(y(n), x_j(n)) \tag{3.1}$$

where $F(y(n), x_j(n))$ is a function of neuron output and jth input signal $x_j(n)$ and satisfies the Hebbian postulate of learning. For example, one of the simplest forms for this function is [52]:

$$F(y(n), x_j(n)) = \eta y(n) x_j(n) \tag{3.2}$$

where η, the learning rate, is a positive constant. Using this learning rule, there is a tendency for weights to grow without bounds which is unacceptable and impractical. Therefore, some form of *normalization* is required to be added to the learning rule. Adding normalization to the learning rule also has the effect of introducing competition among the synapses of the neuron over limited resources. This competition, as stated in the second principle of self-organization, is necessary for stabilization. One possibility to bound weights is to allow the weights grow until each reaches some limit [91] and clip the weights once they passed upper limit w^+ or lower limit w^-. However, if all weights end up in one of the limits, which certainly will happen using Eqn. 3.2, the amount of information that weights can carry becomes very limited [92]. One mathematically convenient normalized form of Eqn. 3.2 is [93]:

$$w_i(n+1) = \frac{w_i(n) + \eta y(n) x_i(n)}{\left(\sum_{j=1}^{m} (w_j(n) + \eta y(n) x_j(n))^2\right)^{1/2}} \tag{3.3}$$

where y, the output signal is defined as:

$$y(n) = \sum_{j=1}^{m} x_i(n) w_i(n) = \mathbf{x}(n)\mathbf{w}^T(n) \tag{3.4}$$

This learning rule keeps the Euclidean norm of weights vector $\mathbf{w}(n)$ equal to unity, i.e.:

$$||\mathbf{w(n+1)}||^2 = 1.$$

Therefore, any increase in some weights would be compensated by proportional reduction in the rest of them. Assuming η is small, we can expand the denominator of Eqn. 3.3 as a power series [52]:

$$\begin{aligned}\left(\sum_{j=1}^{m}(w_j(n)+\eta y(n)x_j(n))^2\right)^{1/2} &= \left(\sum_{j=1}^{m}(wj^2(n)+2\eta w_j(n)y(n)x_j(n))\right)^{1/2}+O(\eta^2)\\ &= \left(\sum_{j=1}^{m}wj^2(n)+2\eta y(n)\sum_{j=1}^{m}w_j(n)x_j(n)\right)^{1/2}+O(\eta^2)\\ &= (1+2\eta y^2(n))^{1/2}+O(\eta^2)\\ &= 1+\eta y^2(n)+O(\eta^2) \qquad (3.5)\end{aligned}$$

In the last line, assuming small η, the following approximation was used:

$$(1+2\eta y^2(n))^{1/2}\approx 1+\eta y^2(n)$$

Now, we replace the denominator of Eqn. 3.3 with Eqn. 3.5 and again assuming small η, we obtain:

$$\begin{aligned}w_i(n+1) &= \frac{w_i(n)+\eta y(n)x_i(n)))}{1+\eta y^2(n)+O(\eta^2)}\\ &= (w_i(n)+\eta y(n)x_i(n))))(1+\eta y^2(n)+O(\eta^2))^{-1}\\ &= (w_i(n)+\eta y(n)x_i(n))(1-\eta y^2(n))+O(\eta^2))^{-1}\\ &= w_i(n)+\eta y(n)x_i(n)-\eta y^2(n)w_i(n)+O(\eta^2)\end{aligned}$$

Ignoring second order terms of η, we finally get:

$$w_i(n+1)=w_i(n)+\eta y(n)(x_i(n)-y(n)w_i(n)) \qquad (3.6)$$

The first term, $y(n)x_i(n)$, on the right-hand side of Eqn. 3.6, is the simple Hebbian modification of Eqn. 3.2 and accounts for the self-amplification which is first principle of self-organization. The second term, $-y^2(n)w_i(n)$, is negative and is responsible for stabilization in accordance with principle 2, which requires competition for limited resources among synapses. We can define *effective input* of ith synapse as:

$$x_i'(n) = x_i(n) - y(n)w_i(n) \tag{3.7}$$

and rewrite Eqn. 3.6 using Eqn. 3.7 as:

$$w_i(n+1) = w_i(n) + \eta y(n)x_i'(n) \tag{3.8}$$

3.2 Maximum Eigenfilter

An interesting property of self-organizing learning is its capability of extracting features or patterns from input data [52]. Let

$$\mathbf{R} = \mathbb{E}\{\mathbf{x}(n)\mathbf{x}^T(n)\}$$

be the correlation matrix of $\mathbf{x}$ which therefore is symmetric and positive-semidefinite. The *eigenvalues* of $\mathbf{R}$ are found by solving the following equation, known as eigenvalue problem:

$$\mathbf{R}\mathbf{q} = \lambda\mathbf{q}$$

where the associated non-zero values of $\mathbf{q}$ are called *eigenvectors*. Assuming distinct eigenvalues, the eigenvectors are unique up to scaling. Here the eigenvectors are tacitly assumed to be of unit length. Let the m eignenvalues of $\mathbf{R}$, arranged in decreasing order, be:

$$\lambda_1 > \lambda_2 > \ldots > \lambda_m$$

and m corresponding eigenvectors be:

$$\mathbf{Q} = [\mathbf{q}_1 \ \mathbf{q}_2 \ \ldots \ \mathbf{q}_m \ ].$$

Then, the correlation matrix $\mathbf{R}$ can be expressed in terms of eigenvalues and eigenvectors as shown by:

$$\mathbf{R} = \sum_{i=1}^{m} \lambda_i \mathbf{q}_i \mathbf{q}_i^T \tag{3.9}$$

which is known as the *spectral theorem*.

Theorem 1. *Using Eqn. 3.3, the weights would approach to the eigenvector corresponding to the largest eigenvalue of input i.e:*

$$\mathbf{w}(n) \rightarrow \mathbf{q}_1 \quad as \quad n \rightarrow \infty$$

Therefore, a neuron governed by Eqn. 3.3 and illustrated in Fig. 3.1, has an interesting property; it adaptively extracts the first principal component of the input data and therefore is called a *maximum eigenfilter*.

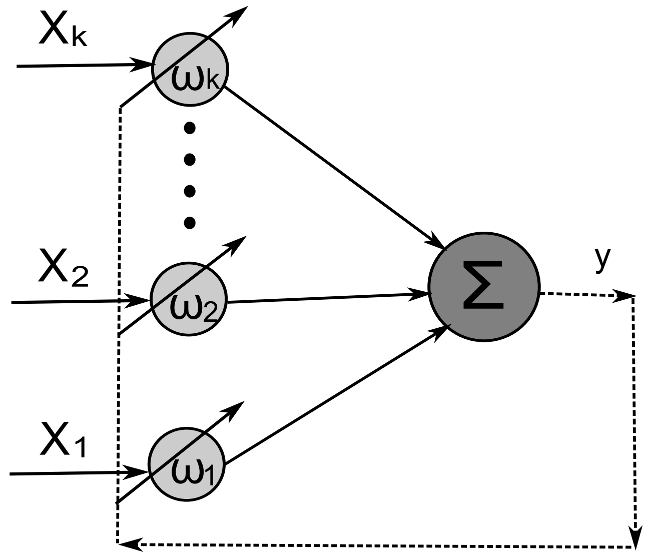

Figure 3.1: Diagram of a neural network governed by maximum eigenfilter learning rule. The weights are adaptively adjusted according to Eqn. 3.3 and based on input and output.

3.3 The Tsigankov-Koulakov Model

The SOM model of map formation in the superior colliculus (SC), explained in [55], uses an energy function minimization approach to achieve map formation. Axons of retinal ganglion cells (RGC) establish orderly projections to the superior colliculus of the midbrain. Axons of neighboring cells terminate proximally in the superior colliculus thus forming a topographically precise representation of the visual world.

In this model, there are two layers of neurons, each consisting of a $N \times N$ lattice of neurons. As illustrated in Fig. 3.2(a), initially the neurons from retina (input) layer are randomly connected to neurons in the collicular (output) layer. The goal of the algorithm is to modify the neuron connections so that, as shown in Fig. 3.2 (b), every neuron in the input layer is connected

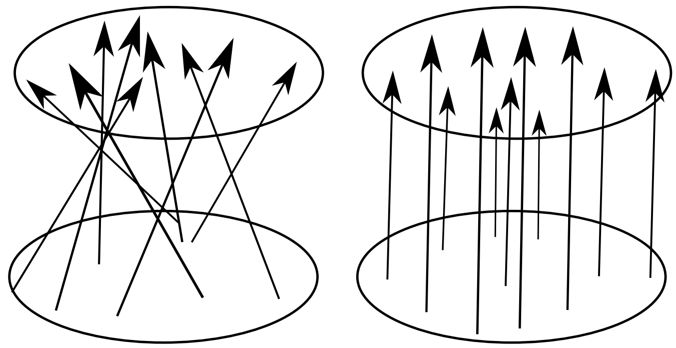

(a) (b)

Figure 3.2: A self-organizing map (a)initial state. (b) organized state.

to its spatially corresponding neuron in the output layer. Total retinal input at point $\vec{r}$ in SC is determined by retino-collicular synaptic weights $w_i(\vec{r})$ and axonal activity a_i through

$$\vec{I}(\vec{r}) = \sum_i w_i(\vec{r})a_i$$

Activity of a collicular cell at point $\vec{r}$ is

$$A(\vec{r}) = \sum_{\vec{r'}} D(\vec{r} - \vec{r'})I(\vec{r'}) = \sum_j v_j(\vec{r})a_j$$

where D is dendritic form-factor and

$$v_j(\vec{r}) = \sum_{\vec{r'}} D(\vec{r} - \vec{r'})w_j(\vec{r'})$$

is the net weight from RGC axon j to the collicular cell at point $\vec{r}$. The weight is modified according to Hebbian rule and the change in this weight is proportional to correlation between activities in this cell and the presynaptic cell:

$$\Delta v_j(\vec{r}) = \eta A(\vec{r}) a_j = -\frac{\partial E_C}{\partial v_j(\vec{r})} \tag{3.10}$$

The last equation interprets the weight adjustment as a gradient descent in E_C.

The map formation occurs through a stochastic minimization of E_C by repeating the following steps:

- Randomly select two not necessarily adjacent cells i, j from output layer.
- Switch the cells of input layer connected to cells i, j with probability

$$P_{\text{switch}} = \frac{1}{1 + \exp(\Delta E_C)}$$

In other words, during the minimization process, if switching two connections decreases the energy of the network, they will be switched with higher probability, leading to stochastic minimization of energy function. According to Eqn. 3.10, the energy function E_C decreases more if the correlation between input and output layer is higher. This happens if the spatial location of input cell in the input layer is close the spatial location of output cell in the output layer.

In the next chapter the self-organized DSM algorithm will be introduced by following a manner similar to the TK model; in so doing, system organization is found by assigning the sub-bands to CR units in the direction of the gradient descent of the objective function defined by Eqn. 3.10.

3.4 Summary

In this chapter Tsigankov-Koulakov model for self-organizing maps was studied and discussed. Three principles of map formation for SOMs, namely self-amplification, competition and correlation, were explained and Hebbian learning rule, the essential learning rule in SOM, was studied and discussed. A form of normalized Hebbian learning rule, termed maximum eigenfilter, was reviewed. This learning rule has several interesting properties and can adaptively extract the maximum eigenvector of input data. Furthermore, The Tsigankov-Koulakov model for self-organizing maps was explained. This model was developed for the self-organization of the geometrically precise sorting of retinal ganglion cell axons in superior colliculus in the brain. The Tsigankov-Koulakov SOM models the SOM problem as an optimization problem which tries to minimize an energy function defined based on Hebbian learning rule. In this model, the map formation process happens through a stochastic minimization process. At each round, the randomly selected neurons' connections are changed in the direction of the gradient descent of energy function.

4

Self-Organizing Dynamic Spectrum Management

The SOM has several interesting attributes that makes it a promising candidate for DSM in CR networks:

- The synaptic weights adapt to locally-generated temporal signals and through performing *local* interactions between neurons and the environment, the network achieves a *global* order. In a similar manner, a decentralized DSM scheme has to achieve a global order by local interactions of CR units.

- The SOM network extracts the pattern in the environment and restructure itself to match this pattern. Similarly, in CR networks, the objective is to find the pattern of spectrum utilization and distribute spectrum holes according to that pattern.

- The DSM is based on the Hebbian learning rule which is computationally simple and suitable for a decentralized DSM scheme where mobile units have limited power and processing capabilities.

The SO-DSM is a decentralized DSM scheme, in which each CR unit extracts the wireless environment spectrum utilization patterns using a form of Hebbian learning rule, and stores the extracted knowledge in an array of weights. These weights act as *short-term memory* and keep recent legacy network's and neighbouring CR units' spectrum utilization patterns. Using the extracted knowledge and a SOM technique similar to the one explained in Sec. 3.3, the CR network reorganizes itself to the latest spectrum configuration of the environment.

As explained in Sec. 1.4.1, the prerequisite of forming a SOM is having correlation or redundancy in the input data. For SO-DSM, this redundancy is caused by the pattern of spectrum utilization of radio units in the environment. The wireless communications depends on humans' activities which are not random and typically follow certain patterns. For example, in an office building, wireless activities increase at office hours during week days and significantly decrease during nights and weekends. Such a pattern for this environment is due to the fact that people are present at that environment mostly during office hours. Similarly, in a home environment, wireless activities increase during times when people are at home and not sleeping i.e. weekday evenings and weekends, and decrease at nights and weekdays during the day when typically people leave home for school or work. Experimental measurements [3], shown in Fig. 4.1 and 4.2, have confirmed this kind of patterns and have shown that these patterns change with a relatively slow pace, in order of hours during the day.

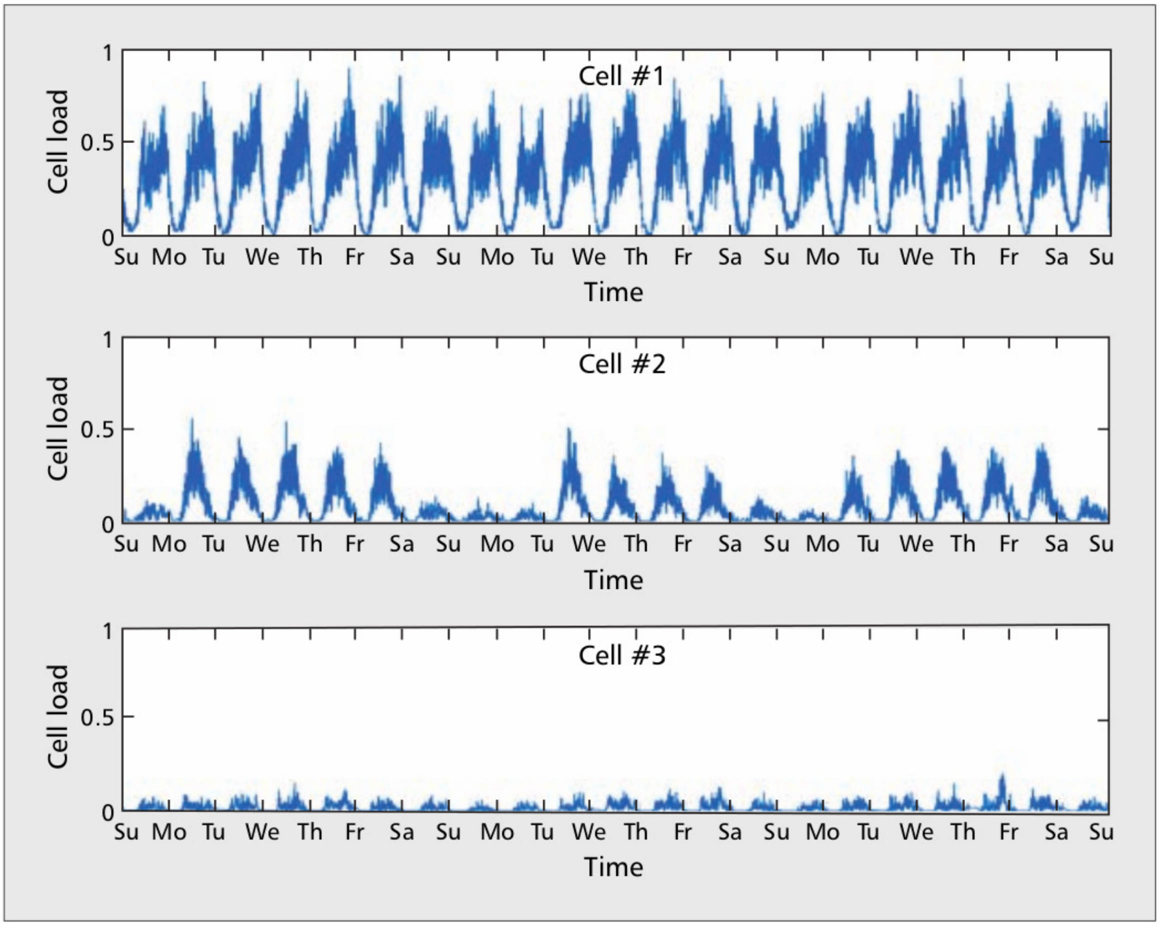

Figure 4.1: Normalized load of three different cell sectors over three weeks. We plot the moving average of each cell over 1 s. The cells show high load (top), varying load (middle), and low load (bottom). (reproduced from [3])

We may therefore infer that wireless spectrum utilization has a pattern that depends on location, and as Fig. 4.2 illustrates, may change slowly during the day. Having a very fast radio scene analyzer, we can consider the environment spectrum pattern to be *pseudo-stationary*, in which case Hebbian learning rule explained in Sec. 3.1 can be applied to extract the inherent pattern of the data. A good candidate for such radio scene analyzer is the MTM method proposed by Haykin *et al.* [94] and discussed in Sec. 1.3. The

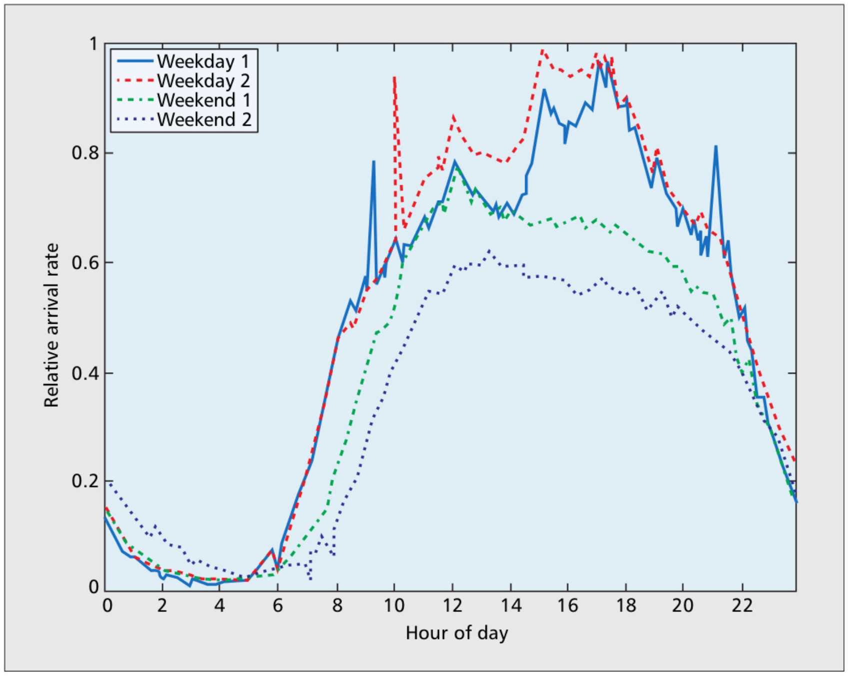

(a)

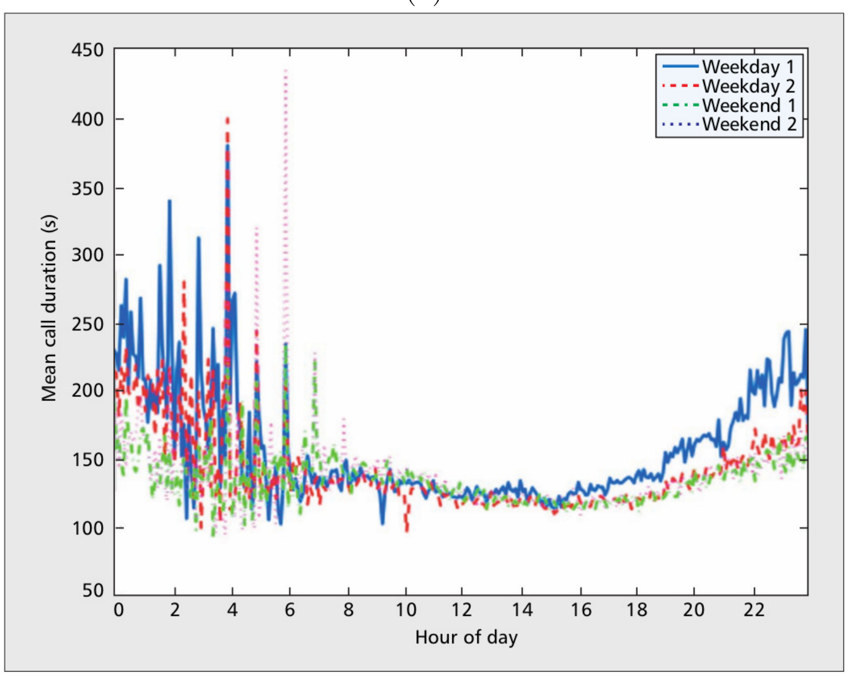

(b)0.7

Figure 4.2: (a) Distribution of system-wide average call arrival rates during four different days. The arrival rates are averaged over 5-min slots. (b) Distribution of average call duration over 5-min periods during four different days. The large spikes during the mornings are due to small gaps in collection. (reproduced from [3])

presented results show that it is able to perform spectrum sensing in about 100 μs, which is relatively fast. Furthermore, by precomputing the Slepian tapers and using the state-of-the-art fast Fourier transform (FFT) algorithm, namely the fastest Fourier transform in the west (FFTW) [95], computation of the MTM for spectrum sensing can be accomplished in a matter of 5 to 20 μs [94]. Even lower sensing time is expected to be achieved in near future as as the speed and computation power of mobile device processors are increasing very fast. Dual-core processors for mobile devices such as NVIDIA Tegra 2 [96] are already commercialized and quad core processor such as NVIDIA Tegra 4 and Qualcomm Snapdragon S4 are coming in the market soon [97]. We may, therefore, assume that having such a fast radio scene analyzer, the spectrum utilization pattern of environment is pseudo-stationary and Hebbian learning rule can extract the patterns from the input data.

We accomplish the other two requirements of SOM, namely self-amplification and competition, by using the Hebbian learning rule explained in Sec. 3.1 and stated in Eqn. 3.3. As discussed in that section, the normalization rule of this learning rule creates a competition among weights that stabilizes the algorithm.

Finally, as SO-DSM is a decentralized CR network, the feedback channel between neighbouring CR units is required to form the network. Clearly, as explained in Sec. 1.3, the feedback channel cannot be established using spectrum holes in the licensed bands because they change fast and sometimes they may not be available at all. Therefore, the low-bandwidth feedback channel must be established in unlicensed bands. For example, the feedback channel can be formed using one of the several available ad hoc wireless network standards operating on unlicensed bands such as Bluetooth or ad hoc 802.11 [98, 99]. Using such a feedback channel, the CR network is always operational and CR units never lose synchronization and control. In this work, a feedback channel between neighbouring CRs is assumed and CR units coordinate, negotiate and share their RSA data through this channel. This information-sharing results in improved primary user detection [31–33] and also improves the learning process in SO-DSM.

4.1 SO-DSM

The proposed SO-DSM technique works as follows:

- Using the feedback channel on unlicensed band, the CR units form an ad hoc network, get synchronized and start sharing RSA information with neighbouring CR units.

- CR units continuously monitor their surrounding environment and save the obtained information in a vector termed *channel allocation priority list (CAPL)*. This vector's size is equal to the total sub-bands N_{ch}, and for each sub-band b_i, CR units keep a weight w_i in CAPL that represents the *quality* of sub-band b_i in the recent past and plays the role of short term memory.

- After receiving each new set of RSA information, the weights are updated using Eqn. 3.3.

- Once two CR units need to establish a new link, sub-bands are allocated to links in the direction of gradient ascent of cost function E_C as described in Sec. 3.3.

The above algorithm forms a SOM, based on spectrum utilization patterns of PUs and CR units. However, it can not meet one important requirement of CR units which is minimizing probability of collision with PUs because using SOM model above, the memory for CR activities and PUs activities are mixed and the weights show the *relative* quality of sub-bands. In other words, they are sorted based on " how better are they compared to each other" and we can not bound probability of collision using such weights. To mitigate this problem, we add an extra stage to the weights to separate the memory of PUs activities from CR units activities. Initially, all the weights are set to 0 so that the CR units do not use any spectrum hole before gaining enough knowledge about the environment and are considered *unavailable* as long as are below 1. An unavailable sub-band will not be used for a CR link even if it is momentarily free i.e. no PU is using it. The memory weights for CR C_m, when they are in the unavailable stage, i.e. $w_{i,m}(n) < 1$, are updated based on the following rule:

$$w_{i,m}(n+1) = \begin{cases} w_{i,m}(n) + \eta_{1,i,m}, & \text{if } b_i \text{ is free} \\ 0, & \text{if PU on } b_i \end{cases} \tag{4.1}$$

where $1 > \eta_{1,i,m} > 0$ is the *forgetting factor* for sub-band b_i and CR unit C_m. When a weight reaches 1, its associated sub-band is considered *available* and will be used for CR communications. Using this rule, at each round the weights for free sub-bands increase by $\eta_{1,i,m}$ and would exceed 1 if no PU uses them for at least $T_G = \lfloor \frac{1}{\eta_{1,i,m}} \rfloor$ consequent time steps where $\lfloor x \rfloor$ denotes the integer part of x. Once a PU is detected on b_i, w_i is set back to zero and b_j will not be used by the CR unit, even if it becomes free, until it has been free for sufficient time to allow w_i grow and reach 1.

After identifying the *available* sub-bands in the environment, the CR units use Eqn. 3.3 to extract the spectrum utilization pattern of neighbouring CR units and create temporal organization based on the obtained knowledge. Therefore, Eqn. 3.3, is applied to the second stage of memory for updating the weights of available sub-bands ($w_{i,m}(n) \geq 1$):

$$w'_{i,m}(n+1) = \frac{w'_i(n) + \eta_{2,m} y(n) x_i(n)}{\left(\sum_j (w'_j(n) + \eta_{2,m} y(n) x_j(n))^2\right)^{1/2}} \tag{4.2}$$

where $1 > \eta_{2,m} > 0$ is the learning rate, and

$$w'(n) = w(n) - 1$$

and $x_{i,m}(n)$ is the quality signal of sub-band b_i received from RSA unit at time n and is defined as:

$$x_{i,m}(n) = \begin{cases} 1, \text{ if } b_i \text{ is used by } C_m \\ \beta_1, \text{ if } b_i \text{ is free} \\ \beta_2, \text{ if } b_i \text{ is used by } C_{k,k\neq m} \end{cases} \tag{4.3}$$

where $\beta_1 > \beta_2 > 0$ are quality levels for free sub-bands and sub-bands used by neighbouring CRs.

Using the Hebbian learning rule of Eqn. 3.3, the cost function E_C exists [53] and similar to the Tsigankov-Koulakov SOM model used in Stryker's work [55, 56], we will follow the gradient ascent of the cost function ∇E_C, when assigning sub-bands to CR links. The gradient ascent of cost function E_C can be derived from [53]:

$$\frac{\partial E_C}{\partial w'_{i,m}} = \Delta w'_{i,m} \tag{4.4}$$

and sub-bands are allocated to links in the direction of gradient ascent of cost function E_C. Define

$$\mathcal{U}_a(k,m) = \{b_j \mid b_j \text{ available for } C_k \text{ and } C_m\} = \{b_j \mid w_{j,m}, w_{j,k} \geq 1\}$$

When a link between C_m and C_k is required, $b_j^* \in U_a(k,m)$ is selected that maximizes gradient ascent of the cost function E_C defined as:

$$\nabla E_C(k,m,j) = \sum_{i=1}^{N_{ch}} \left(\frac{\partial E_C}{\partial w'_{i,m|j}} + \frac{\partial E_C}{\partial w'_{i,k|j}} \right)$$

where $w'_{i,m|j}$ is the next value of $w'_{i,m}$ if b_j gets assigned to the link between C_m and C_k. Using Eqn. 4.4, we obtain:

$$\nabla E_C(k,m,j) = \sum_{i=1}^{N_{ch}} \left(\Delta w'_{i,m|j} + \Delta w'_{i,k|j} \right) \tag{4.5}$$

In order to calculate $w'_{i,k|j}$ for CR unit C_k, we use Eqn. 3.3. By choosing b_j for the link, as Eqn. 4.3 shows, only $x_{j,k}$ changes from β_1 to 1 and the rest of input signals remain the same as before, i.e.

$$x_{i,k|j} = \begin{cases} x_{i,k}, & \text{if} \quad i \neq j \\ b' + x_{i,k}, & \text{if} \quad i = j \end{cases} \tag{4.6}$$

where $b' = 1 - \beta_1$. Substituting $x_{j,k}$ in Eqn. 3.4, $y_{k|j}$ is calculated as

$$y_{k|j} = \sum_{i=1}^{N_{ch}} x_{i,k|j}\, w'_{i,k} = b'\, w'_{j,k} + \sum_{i=1}^{N_{ch}} x_{i,k}\, w'_{i,k} = b'\, w'_{j,k} + y_k \tag{4.7}$$

Now, we can calculate $w'_{i,k|j}$ using Eqn. 3.3:

$$w'_{i,k|j} = \frac{w'_{i,k} + \eta_{2,k}\, y_{k|j}\, x_{i,k|j}}{\left(\sum_l (w'_{l,k} + \eta_{2,k}\, y_{k|j}\, x_{l,k|j})^2\right)^{1/2}} \tag{4.8}$$

we can expand the denominator of Eqn. 4.8 using Eqns. 4.7 and 4.6 as

$$\begin{aligned}
& \sum_l (w'_{l,k} + \eta_{2,k}\, y_{k|j}\, x_{l,k|j})^2 = \sum_l (w'_{l,k} + \eta_{2,k}\, (y_k + w'_{j,k}\, b')\, x_{l,k|j})^2 \\
= \quad & \sum_l ((w'_{l,k} + \eta_{2,k}\, y_k\, x_{l,k|j}) + \eta_{2,k}\, w'_{j,k}\, b'\, x_{l,k|j})^2 \\
= \quad & \sum_l (w'_{l,k} + \eta_{2,k}\, y_k\, x_{l,k|j})^2 + 2\eta_{2,k}\, w'_{j,k}\, b'\, x_{l,k|j}\, (w'_{l,k} + \eta_{2,k}\, y_k\, x_{l,k|j}) \\
+ \quad & (\eta_{2,k}\, w'_{j,k} b'\, x_{l,k|j})^2 = \sum_l (w'_{l,k} + \eta_{2,k}\, y_k\, x_{l,k|j})^2 + 2\, \eta_{2,k}\, w'_{j,k}\, b'\, x_{l,k|j}\, w'_{l,k} \\
+ \quad & 2\eta_{2,k}^2\, w'_{j,k}\, b'\, x_{l,k|j}^2\, y_k + \eta_{2,k}^2\, w'^2_{j,k}\, b'^2\, x_{l,k|j}^2
\end{aligned}$$

having $\eta_{2,k} << 1$, $b' << 1$ and $w'_{j,k}$, $x_{l,k|j}$, $w'_{l,k} < 1$, we neglect last three terms and obtain:

$$\sum_l (w'_{l,k} + \eta_{2,k}\, y_{k|j}\, x_{l,k|j})^2 \approx \sum_l (w'_{l,k} + \eta_{2,k}\, y_k\, x_{l,k|j})^2 = \mathcal{D}^2 \tag{4.9}$$

Therefore, we can rewrite Eqn. 4.8 as:

$$w'_{i,k|j} = \frac{w'_{i,k} + \eta_{2,k}\,(y_k + w'_{j,k}\, b')\, x_{i,k|j}}{\mathcal{D}} = \frac{w'_{i,k} + \eta_{2,k}\, y_k\, x_{i,k|j} + \eta_{2,k}\, w'_{j,k}\, b'\, x_{i,k|j}}{\mathcal{D}} \tag{4.10}$$

and

$$\Delta w'_{i,k|j} = \frac{w'_{i,k} + \eta_{2,k}\, y_k\, x_{i,k|j} + \eta_{2,k}\, w'_{j,k}\, b'\, x_{i,k|j}}{\mathcal{D}} - w'_{i,k} = \mathcal{C}_{i,k|j} + \frac{\eta_{2,k}\, b'\, x_{i,k|j}}{\mathcal{D}} w'_{j,k} \tag{4.11}$$

where

$$\mathcal{C}_{i,k|j} = \frac{w'_{i,k} + \eta_{2,k}\, y_k\, x_{i,k|j}}{\mathcal{D}} - w'_{i,k}$$

is the sum of terms in Eqn. 4.11 that do not depend on $w'_{j,k}$. Using Eqn. 4.6, we get

$$\begin{aligned}
\mathcal{C}_{i,k|j} &= \begin{cases} \dfrac{w'_{i,k} + \eta_{2,k}\, y_k\, x_{i,k}}{\mathcal{D}} - w'_{i,k}, & \text{if} \quad i \neq j \\ \dfrac{w'_{i,k} + \eta_{2,k}\, y_k\, (x_{i,k} + b')}{\mathcal{D}} - w'_{i,k}, & \text{if} \quad i = j \end{cases} \\
&= \begin{cases} \mathcal{C}_{i,k}, & \text{if} \quad i \neq j \\ \mathcal{C}_{i,k} + \dfrac{\eta_{2,k}\, y_k\, b'}{\mathcal{D}}, & \text{if} \quad i = j \end{cases}
\end{aligned}$$

Now we can calculate $\nabla E_C(k,m,j)$ using Eqn. 4.5 and 4.11:

$$\begin{aligned}
\nabla E_C(k,m,j) &= \sum_{i=1}^{N_{ch}} \left(\Delta w'_{i,m|j} + \Delta w'_{i,k|j}\right) \\
&= \sum_{i=1}^{N_{ch}} \left(\mathcal{C}_{i,k|j} + \frac{\eta_{2,k}\, b'\, x_{i,k|j}}{\mathcal{D}} w'_{j,k} + \mathcal{C}_{i,m|j} + \frac{\eta_{2,m}\, b'\, x_{i,m|j}}{\mathcal{D}} w'_{j,m}\right) \\
&= \sum_{i=1,\neq j}^{N_{ch}} \left(\mathcal{C}_{i,k} + \frac{\eta_{2,k}\, b'\, x_{i,k}}{\mathcal{D}} w'_{j,k} + \mathcal{C}_{i,m} + \frac{\eta_{2,m}\, b'\, x_{i,m}}{\mathcal{D}} w'_{j,m}\right) + \mathcal{C}_{j,k} + \frac{\eta_{2,k}\, y_k\, b'}{\mathcal{D}} \\
&+ \frac{\eta_{2,k}\, b'\, (x_{j,k} + b')}{\mathcal{D}} w'_{j,k} + \mathcal{C}_{j,m} + \frac{\eta_{2,m}\, y_m\, b'}{\mathcal{D}} + \frac{\eta_{2,m}\, b'\, (x_{j,m} + b')}{\mathcal{D}} w'_{j,m} \\
&= \sum_{i=1}^{N_{ch}} \left(\mathcal{C}_{i,k} + \frac{\eta_{2,k}\, b'\, x_{i,k}}{\mathcal{D}} w'_{j,k} + \mathcal{C}_{i,m} + \frac{\eta_{2,m}\, b'\, x_{i,m}}{\mathcal{D}} w'_{j,m}\right) \\
&+ \frac{\eta_{2,k}\, y_k\, b'}{\mathcal{D}} + \frac{\eta_{2,k}\, b'^2}{\mathcal{D}} w'_{j,k} + \frac{\eta_{2,m}\, y_m\, b'}{\mathcal{D}} + \frac{\eta_{2,m}\, b'^2}{\mathcal{D}} w'_{j,m} \\
&= \sum_{i=1}^{N_{ch}} (\mathcal{C}_{i,k} + \mathcal{C}_{i,m}) + \frac{\eta_{2,k}\, y_k\, b'}{\mathcal{D}} + \frac{\eta_{2,m}\, y_m\, b'}{\mathcal{D}} \\
&+ \frac{\eta_{2,k}\, b'}{\mathcal{D}} (b' + \sum_{i=1}^{N_{ch}} x_{i,k}) w'_{j,k} + \frac{\eta_{2,m}\, b'}{\mathcal{D}} (b' + \sum_{i=1}^{N_{ch}} x_{i,m}) w'_{j,m} \qquad (4.12)
\end{aligned}$$

Defining

$$\mathcal{S}_{x,k} = \sum_{i=1}^{N_{ch}} x_{i,k}$$

and

$$\mathcal{T}_k = \sum_{i=1}^{N_{ch}} \mathcal{C}_{i,k} + \frac{\eta_{2,k}\, y_k\, b'}{\mathcal{D}}$$

we rewrite Eqn 4.12 as:

$$\nabla E_C(k,m,j) = \mathcal{T}_k + \mathcal{T}_m + \eta_{2,k}\, b'\, \frac{\mathcal{S}_{x,k} + b'}{\mathcal{D}} w'_{j,k} + \eta_{2,m}\, b'\, \frac{\mathcal{S}_{x,m} + b'}{\mathcal{D}} w'_{j,m} \qquad (4.13)$$

Using Eqn. 4.13, the criteria to select b_j^* as the sub-band for CR units C_m and C_k is:

$$b_j^* = \underset{j}{\operatorname{argmax}}(\nabla E_C(k, m, j)) \tag{4.14}$$

Equivalently, b_j^* must satisfy the following equation:

$$\begin{aligned} &\forall \quad b_i \in \mathcal{U}_a(k,m)\ ,\ i \neq j : \\ &\nabla E_C(k,m,j) - \nabla E_C(k,m,i) \geq 0 \end{aligned}$$

or

$$\begin{aligned} &\forall \quad b_i \in \mathcal{U}_a(k,m)\ ,\ i \neq j : \\ &\frac{b'}{\mathcal{D}} \left[\eta_{2,k} \left(\mathcal{S}_{x,k} + b'\right)(w'_{j,k} - w'_{i,k}) + \eta_{2,m} \left(\mathcal{S}_{x,m} + b'\right)(w'_{j,m} - w'_{i,m}) \right] \geq 0 \end{aligned}$$

Assuming $\eta_{2,m} = \eta_{2,k} = \eta_2$ and eliminating positive variables $\eta_2, \mathcal{D}, b'$ we obtain:

$$\begin{aligned} &\forall \quad b_i \in \mathcal{U}_a(k,m)\ ,\ i \neq j : \\ &(\mathcal{S}_{x,k} + b')(w'_{j,k} - w'_{i,k}) + (\mathcal{S}_{x,m} + b')(w'_{j,m} - w'_{i,m}) \geq 0 \end{aligned} \tag{4.15}$$

Using Eqn. 4.2, the weights approach the principal component of quality signals of sub-bands in the recent past. At each step, if a sub-band is used by the CR unit, its weight increases more than other sub-bands' weights and goes higher in CAPL. Therefore, it is more likely that it will be used by that CR in the future. Similarly, weights of sub-bands that are being used by other CRs would decrease; thus, they will go down in CAPL and therefore, less likely to be used. Figure 4.3 illustrates an example of weight dynamics of a particular CR unit C_j with 4 sub-bands. Sub-bands b_1 and b_2 are being used by neighbouring CRs and as can be seen in the figure, their weights have decreased compared to b_3 and b_4. This CR unit has used b_3 for its link time to time during the simulation, consequently, its weight has increased and has become the highest. The other sub-band, b_4, has been free all the time and its weight level is less than b_3 and higher than b_1 and b_2. For this example, when C_j requires to establish a new link, its first preference is b_3, then b_4 and then b_1 or b_2, based on their momentary weight value. However, as Eqn. 4.15 shows, the link is selected based on the value of weights of both CR units of the link, therefore, it is possible that the selected sub-band is not on the top of the CAPL of one of the CR units.

4.2 Complexity Analysis

The SO-DSM algorithm has two parts:

- ***Learning*:** The learning part occurs after each round of performing radio scene analysis by applying Eqn. 4.2 to the available sub-bands and Eqn. 4.1 to the unavailable sub-bands. Therefore, in general the complexity of learning stage is of $O(N_{ch})$. Furthermore, information sharing among neighbouring CR units has complexity of $O(N_{\text{neighbour}})$ where $N_{\text{neighbour}}$ is number of neighbouring CR units. Thus, the complexity of learning stage is $\max\{O(N_{\text{neighbour}}), O(N_{ch})\}$. When the density (i.e. number of CR units per unit area) of CR network is low compared to the number of sub-bands, the complexity of learning part is $O(N_{ch})$.

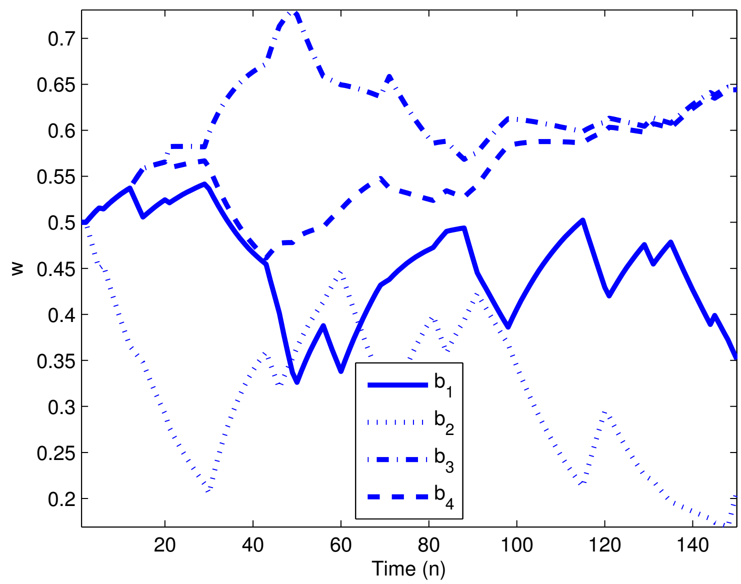

Figure 4.3: An example of SO-DSM weight dynamics for one CR unit. b_1 and b_2 are used by neighbouring CRs and b_3 by the CR unit from $n = 20$ until $n = 70$. Simulation parameters used are: (μ_1, μ_2)=(0.1,0.1), β_1=0.7, β_2=0.1 and η_2=0.05

However, if density of CR network increases, $O(N_{\text{neighbour}})$ becomes the dominant term in the complexity of learning stage.

- ***Channel assignment*:** The second part occurs when a sub-band must be assigned to a link between two CR units and requires searching among all common available sub-bands between two CR units to find b_j^* that maximizes $\nabla E_C(k, m, j)$. Thus, in the worst case, when all the sub-bands are available for both CR units, the complexity of this channel assignment part is $O(N_{ch})$.

Unlike centralized approaches in which complexity depends on the total number of CR links, and consequently total number of CR units, the SO-DSM algorithm is a decentralized DSM scheme and its algorithmic complexity does not increase by expanding the network (as long density of the network does not change or remain negligible compared to N_{ch}).

4.3 Degrees of freedom

The SO-DSM algorithm have several parameters that affect performance and emergent behaviour of the CR network.

4.3.1 Learning-rate Parameter η_1

The learning rate η_1 defines the CR network behaviour in its interaction with legacy networks. A larger η_1 results in faster forgetting PU activities, thus, a more *aggressive* behaviour, while a smaller η_1 results in remembering PU activities for a longer time and therefore a more *conservative* behaviour. By aggressive we mean they wait for a shorter time after a PU has stopped using a sub-band to use that sub-band. A larger η_1 would increase spectrum utilization of CR network while increasing the probability of collision with PUs. CR units should adjust the forgetting factor to maintain the probability of collision at an acceptable level based on legacy network traffic. Let $P_{s,i}(n)$ denote the probability that a PU starts using b_i exactly at time n:

$$P_{s,i}(n) = (1 - \mu_1)^{n-1}\mu_1.$$

Then if a neighbouring CR unit C_j starts using b_i at time T_G for k time steps, then the probability of collision $P_{\mathrm{col},i,j}$ is:

$$P_{\mathrm{col},i,j} = D_{RSA} \times \sum_{T_G}^{T_G+k} P_{s,i}(n)$$

where D_{RSA} is the RSA time delay in discovering PUs. Note that $P_{s,i}(n)$ is a strictly decreasing function because:

$$\frac{dP_{s,i}(n)}{dn} = \frac{\mu_1 \ln(1-\mu_1)}{(1-\mu_1)}$$

which is always negative for $1 \geq \mu_1 > 0$. Therefore, it is possible to decrease the probability of collision by decreasing η_1, i.e. increasing T_G. However, decreasing η_1 also decreases the spectrum utilization of CR network. In order to use the spectrum holes efficiently, CRs need to have a good estimate of μ_1. They can obtain this information in two ways:

- *Using a stored look-up table of forgetting-factor profiles based on time and location and finding the best match for their current condition* For example: (university, daytime) or (home, night). As it was discussed earlier, the wireless traffic is caused by human activities and has patterns that can be predicted to some extend having the time and location.

- *Adaptively refining the learning rate based on recent observations of the environment.* The traffic pattern of PU changes slowly, in order of hours, during the day [3]. Therefore, a moving-average technique, such as Exponential moving average (EMA) algorithm, can be used to adaptively estimate the $\mu_{1,i}$ from average observed idle time intervals $\bar{\tau}_i$ on each sub-band. The EMA algorithm updates the estimate using the following equations:

$$\begin{aligned}\bar{\tau}_i(0) &= \tau_{i,0}\\ \bar{\tau}_i(n) &= \alpha\tau_i(n) + (1-\alpha)\bar{\tau}_i(n)\\ \bar{\mu}_1(n) &= \frac{1}{\bar{\tau}_i(n)}\end{aligned}$$

where $1 > \alpha > 0$ is the *smoothing factor* and $\tau_{i,0}$ is the initial estimate. The EMA algorithm has been suggested for finding traffic parameters in the literature [100–102] and is suitable for estimating time-variant numerical series because in this algorithm, the weights decrease exponentially, and therefore, recent observations have more effect in the average than the older ones. Furthermore, it does not need extra memory to store any old values. There have been also other methods suggested for learning PUs traffic parameters such as autoregressive models [103] which is discussed in appendix C[1].

From a practical prospective, we suggest combining these two methods to achieve a more precise estimation in a shorter time. First using a look-up table, the CR units can obtain a rough estimation and then, they can refine their estimation adaptively using the second method.

[1] we can make it even more refined through the use of hidden Markov model (HMM) [104] but the complexity becomes unmanageable and it could very well be out of practical scope.

4.3.2 Learning-rate Parameter η_2

The second learning rate η_2 controls the sensitivity of the SOM algorithm to CR network changes. A higher η_2 would result in a more rapid response to a similar input than a lower η_2. If η_2 is too small, on the other hand, barely any learning or organization would happen and SO-DSM would basically assign sub-bands in a random manner. For example, Fig. 4.4 shows the same weights

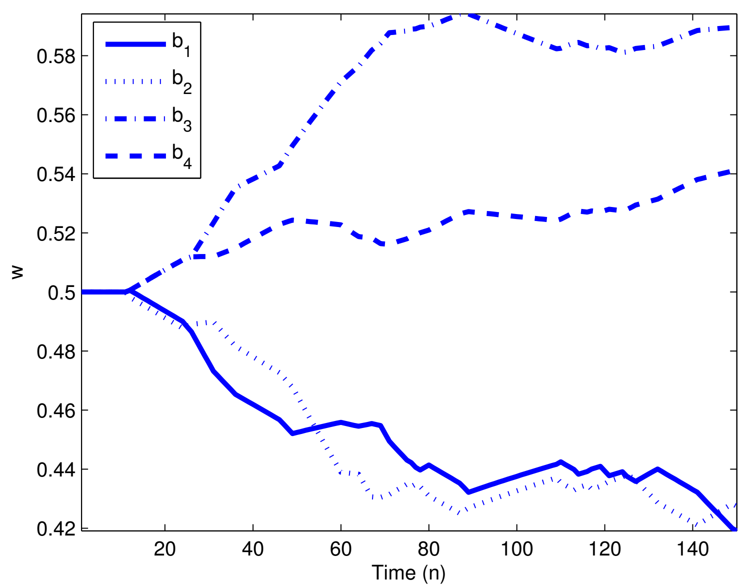

Figure 4.4: Example of SO-DSM weight dynamics of Fig. 4.3, reproduced with $\eta_2 = 0.005$. The rate of weight changes is slower than Fig. 4.3 and the effect of using the channel b_3 is not completely cleared in this case.

as in Fig. 4.3 when η_2 was changed from 0.05 to 0.005. By comparing the two figures, we can see that decreasing η_2 has also decreased the rate of learning. On the other hand, too large a η_2 would result in a very fast learning and sensitive system which would lose organization due to unnecessary responses to input data. Therefore, this parameter must be chosen according to the expected rate of changes in the environment.

4.3.3 Parameterization for Quality level signals β_1 and β_2

These two parameters are important in shaping the weight dynamics in SO-DSM. In general, we would like to have a large β_1, i.e. close to 1, and a small β_2, close to 0, to have more separation between signal levels for the sub-bands used by other CRs and free sub-bands. Increased separation tends to increase the self-amplification of the Hebbian learning and helps forming the SOM. However, these parameters can not get too close to limits (e.g. 1 for β_1 and 0 for β_2).

The difference between β_1 and 1, causes a bigger growth for the weights of sub-bands that are used by the CR unit compared to available sub-bands. Therefore, for the next links, a CR unit would use a previously used sub-band with higher probability. A value for β_1 closer to 1 would result in a smaller weight difference between used sub-bands and available ones and also faster forgetting of the history of sub-band utilization.
For example, Fig. 4.5 (a) and (b), show weights for a similar scenario with two different values of β_1. As can be seen in the figures, a smaller value of β_1 in Fig. 4.5 (a) has resulted in more weight separation between b_3 and b_4 and slower forgetting of sub-band utilization history.

Similarly, the weight dynamics for the case that all sub-bands are used by neighbouring CRs is formed by β_2. A smaller β_2 results in slower forgetting rate for such situation. For example, Fig. 4.6 (a) and (b) illustrate weights of

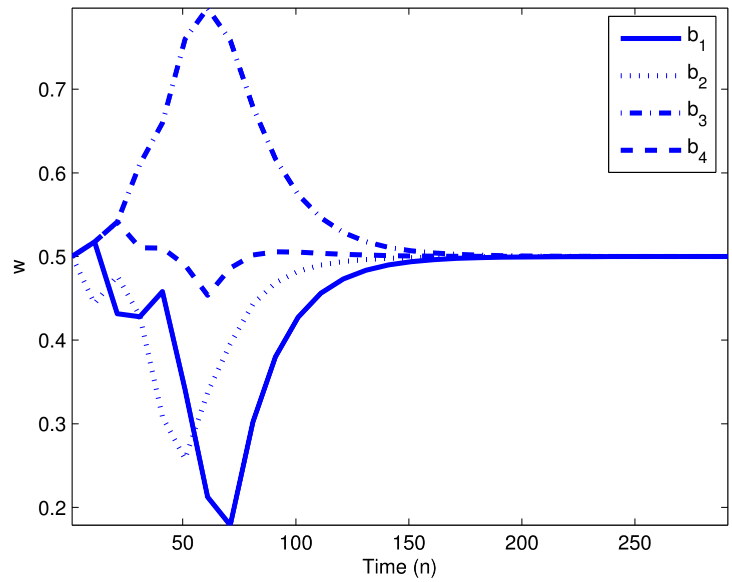

(a)

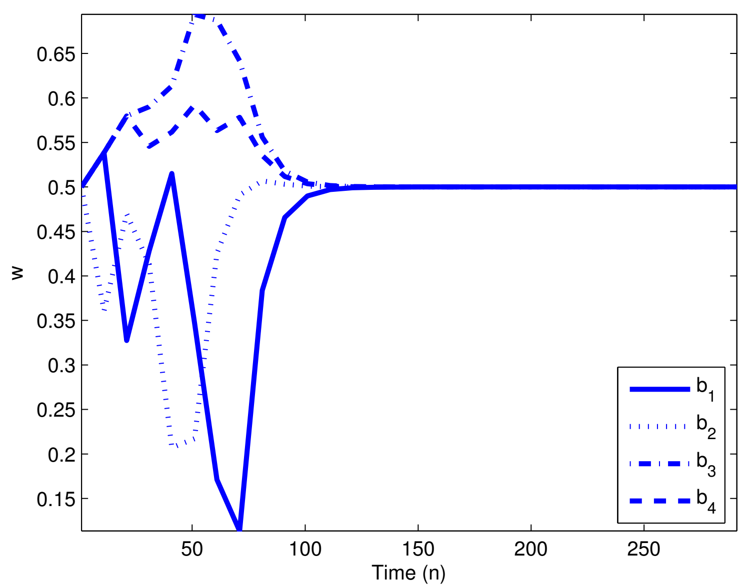

(b)

Figure 4.5: An example of SO-DSM weight dynamics showing the effect of β_1. Sub-bands b_1 and b_2 were used by neighbouring CRs from $n = 1$ to $n = 70$. Sub-band b_3 was used by the CR unit from $n = 20$ to $n = 70$ and all sub-bands were free after $n = 70$ (a)$\beta_1 = 0.5$ (b) $\beta_1 = 0.8$.

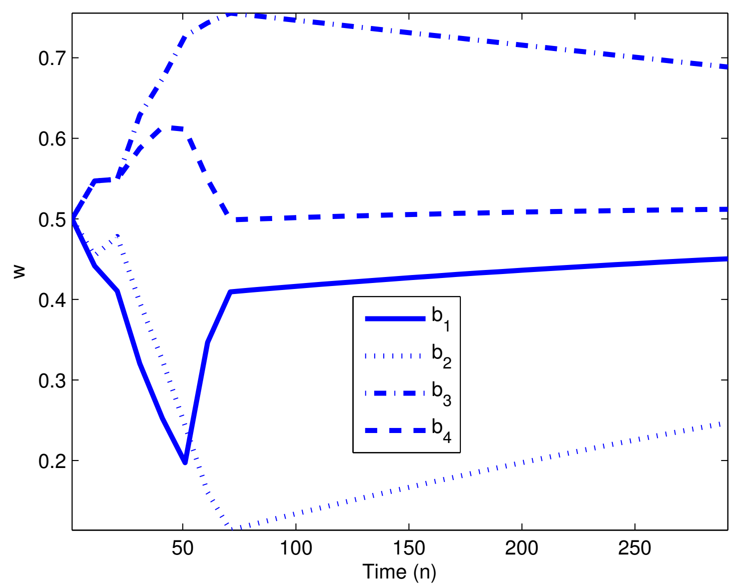

(a)

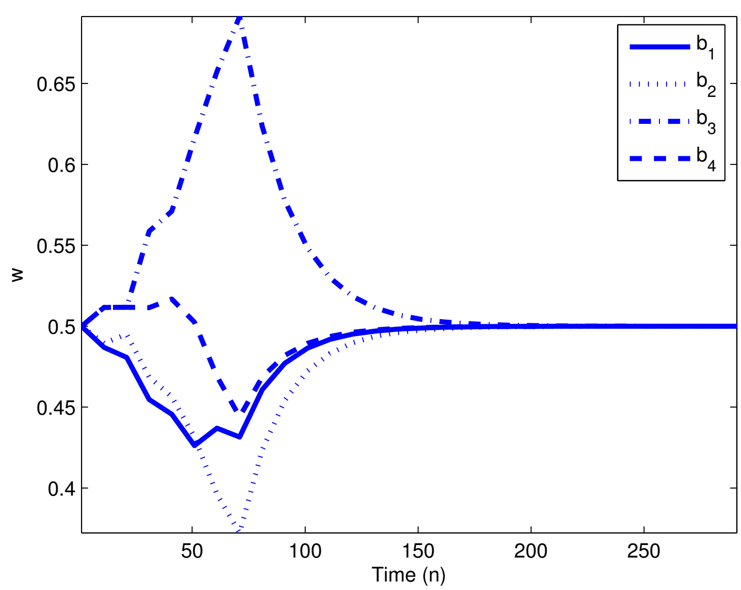

(b)

Figure 4.6: An example of SO-DSM weight dynamics showing the effect of β_2. Sub-bands b_1 and b_2 were used by neighbouring CRs from $n = 1$ to $n = 70$. Sub-band b_3 was used by the CR unit from $n = 20$ to $n = 70$ and all sub-bands were used by neighbouring CRs after $n = 70$ (a)$\beta_2 = 0.1$ (b) $\beta_2 = 0.5$.

a CR unit for a such scenario with two different values of β_2. As these figures show, the smaller value of β_2 in Fig. 4.6 (a) has resulted in slower learning and updating the weights.

4.4 Summary

In this chapter, a novel DSM scheme for CR networks, termed self-organizing DSM, is proposed and explained. This scheme is the first brain inspired DSM scheme for cognitive radios. Empowered by self-organizing map formation in the human brain, this scheme tries to find the patterns of spectrum utilization of other radio units and modify the channel assignment of CR radios to match that pattern. The obtained knowledge is stored in an array of weights that are updated using a form of Hebbian learning. When a new link is required, using a similar algorithm to TK-SOM model, a link that optimizes the energy function of the system is selected i.e. a sub-band that minimizes the gradient of energy function is selected. The mathematical equations of the gradient descent of energy function for TK model were derived. The system architecture for a CR ad hoc network employing SO-DSM was explained. Degrees of freedom for SO-DSM system design were discussed and its complexity was analyzed. The SO-DSM is a decentralized scheme, thus, its complexity depends on the number of neighbours, thus the network density, and not the total number of CRs. Furthermore, Hebbian learning rule is computationally simple and its memory requirement is also relatively low.

5

Simulation Results

In order to evaluate the emergent behaviour of CR network using the SO-DSM technique, an agent-based software test-bed has been developed. This testbed is implemented with C++ and is currently deployed on the Sharcnet [105], a network of high performance computers. It is capable of simulating a CR *ad hoc* network along with legacy network and users, and measures the spectrum utilization efficiency, probability of collision and probability of CR link interruption over the scope of simulation. The software test-bed is also capable of simulating centralized DSM (CDSM) CR network using LDO algorithm as described in Sec. 2.3.2 and minority game DSM (MG-DSM) CR network described in Appendix A.

5.1 Simulations Setup

The primary network has two types of radios: base station and mobile units. Similar to GSM systems, it is assumed that when mobile users are operating, one sub-band is used for up-link and another one for the down-link and both are occupied as long as the mobile user is active.

In order to decrease the probability of collision and shadowing, RSA data received from a neighbouring CR is relayed to other neighbouring CRs. The spectrum is monitored through a grid of probes. At each time instance, each probe counts the number of sub-bands occupied by radios that are in its interference range. The interference range is obtained by requiring at least 15 dB of signal to noise and interference ratio (SINR) for the received signal, as in [106], to be detectable. Define $S_{\text{cr}}(i,n)$ as the number of the sub-bands used by the CR network at time n and ith probe Prob_i. Similarly, $S_{\text{leg}}(i,n)$ is the number of the sub-bands occupied by the primary network; then, the spectrum utilization efficiency at Prob_i is defined as:

$$\gamma_i(n) = \frac{S_{\text{cr}}(i,n) + S_{\text{leg}}(i,n)}{N_{ch}}$$

After running the simulation for T_{tot} time-steps, $\hat{e}_i$, the average spectrum utilization at Prob_i and $\hat{\gamma}_{\text{network}}$, average spectrum utilization over the whole simulated area are calculated respectively from:

$$\hat{\gamma}_i = \frac{\sum_{n=1}^{T_{tot}} e_i(n)}{T_{tot}}, \quad \hat{\gamma}_{\text{network}} = \frac{\sum_{i=1}^{N_{\text{prob}}} \hat{\gamma}_i}{N_{\text{prob}}}$$

Another metric that the software testbed measures is P_{col}, *probability of collision*. Collision happens when a PU is operating on a sub-band and a CR unit in the interference range of the PU also operates on that band. For the ith

PU, $P_{col,i}$ is defined as:

$$P_{col,i} = \frac{T_{col,i}}{T_{use,i}}$$

where $T_{col,i}$ is total collisions happened in ith PR and $T_{use,i}$ is the total time-sub-bands it has used during the simulation. Any CR network should ideally have it equal to zero; however in practice due to RSA delay D_{RSA}, P_{col} is always larger than zero. Thus, one of the objectives in the DSM design is to minimize this probability.

Finally, define P_{intr} as the average number of interruptions during the CR communications due to PUs starting to use the same band. In order to have a more reliable communications in the CR network, we would like to have P_{intr} as small as possible, ideally zero.

The simulated area, shown in Fig. 5.1, is a 700×700 m^2 square with four base stations covering approximately all the area. From the total of 30 sub-bands, 6 sub-bands are TV white spaces and are always available and 24 sub-bands are used by a cellular network that uses 3 sub-bands for up-link and 3 sub-bands for down-link in each cell. The number of CR units, N_{CR}, was 300 and the number of PUs, N_{PU}, was 30, 80, 130 and 180. The channel noise level was set to -100 dBm, the maximum transmit power for transmitters was 50 dBm and the channel model used was of degree 4, as in [106, 107]. A robust transmit-power controller as described in [34,35] with 10% safety power margin was used in the simulations. Each simulation was run for 1×10^5 time steps. As explained in Chp. 4, assuming a fast RSA unit such as the one in [94],

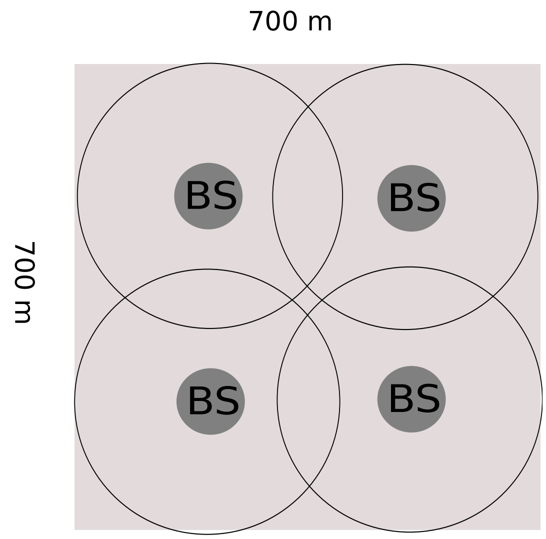

Figure 5.1: The simulated area with four base stations.

Parameter	Value
η_1	0.05
η_2	0.0005
D_{RSA}	1
β_1	0.7
β_2	0.2
PUs (μ_1, μ_2)	(0.01,0.05)
CRs (μ_1, μ_2)	(0.1,0.1)

Table 5.1: SO-DSM parameters used in simulations.

the algorithm is much faster than radio units' movements and radio units are considered to be still during the simulated time. In order to determine the network behaviour for different set ups, each simulation was repeated at least 1000 rounds and in each round of simulation, CR units and PUs were randomly placed in the simulated area. Each simulation was performed with two number of CR units. One time low density where $N_{\text{CR}} = 50$ and another time high density where $N_{\text{CR}} = 300$. The SO-DSM parameters used for simulations are listed in Table 5.1

5.2 Results

To evaluate our DSM scheme, we have used the testbed to simulate a wireless network using SO-DSM versus a LDO centralized DSM network, as described in Sec. 2.3.2, and a decentralized DSM method based on *minority game* (MG).

5.3 SO-DSM vs MG-DSM

In the first round of simulations, CR network is simulated using SO-DSM and a MG-DSM (see appendix A) with memory length $L_h = 200$. The simulation results are presented in Fig. 5.2 to 5.9.

5.3.1 Spectrum Utilization

Figure 5.2 shows γ_{PU}, the spectrum utilization of legacy network which is equal for all simulations because the legacy network is independent of the CR network. As N_{PU}increases from 30 to 180, γ_{PU}increases, therefore, average number and duration of spectrum hole decrease. Figure 5.3 demonstrates the CR network spectrum efficiency γ_{CR}. For $N_{\mathrm{PU}} = 30$, $\gamma_{\mathrm{CR}}$for SO-DSM is about 50% lower than MG-DSM. As N_{PU}increases, spectrum holes vanish and the difference between two scheme decreases. As Fig. 5.2 (a) shows, the SO-DSM achieves slightly higher spectrum efficiency in the tough condition of high density PU network when $N_{\mathrm{PU}} = 180$.

DSM	SO N_{CR}=50	SO N_{CR}=300	MG N_{CR}=50	MG N_{CR}=300
N_{PU}=30	3.373E-02	3.293E-02	3.373E-02	3.291E-02
N_{PU}=80	7.835E-02	7.641E-02	7.835E-02	7.642E-02
N_{PU}=130	9.258E-02	9.140E-02	9.259E-02	9.148E-02
N_{PU}=180	9.370E-02	9.257E-02	9.370E-02	9.268E-02

(a)

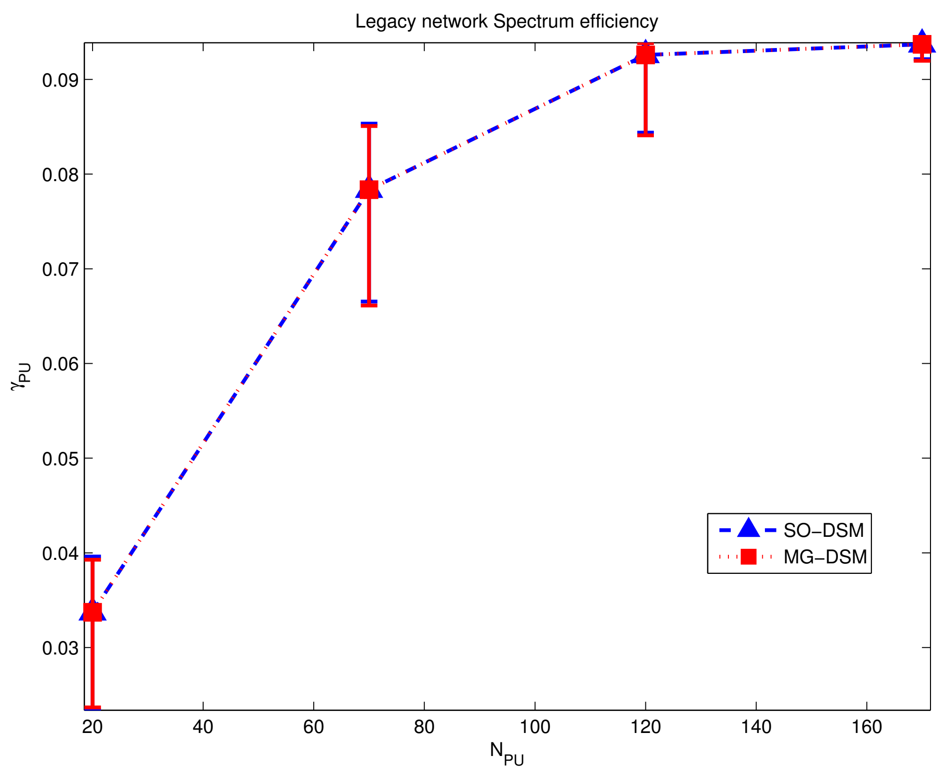

(b)

Figure 5.2: Legacy network spectrum utilization. (a) numerical results (b) graphical plot. As the number of PUs increase, the spectrum utilization of legacy network increases. The legacy network is independent of CR network, thus, the results are approximately equal for all simulations.

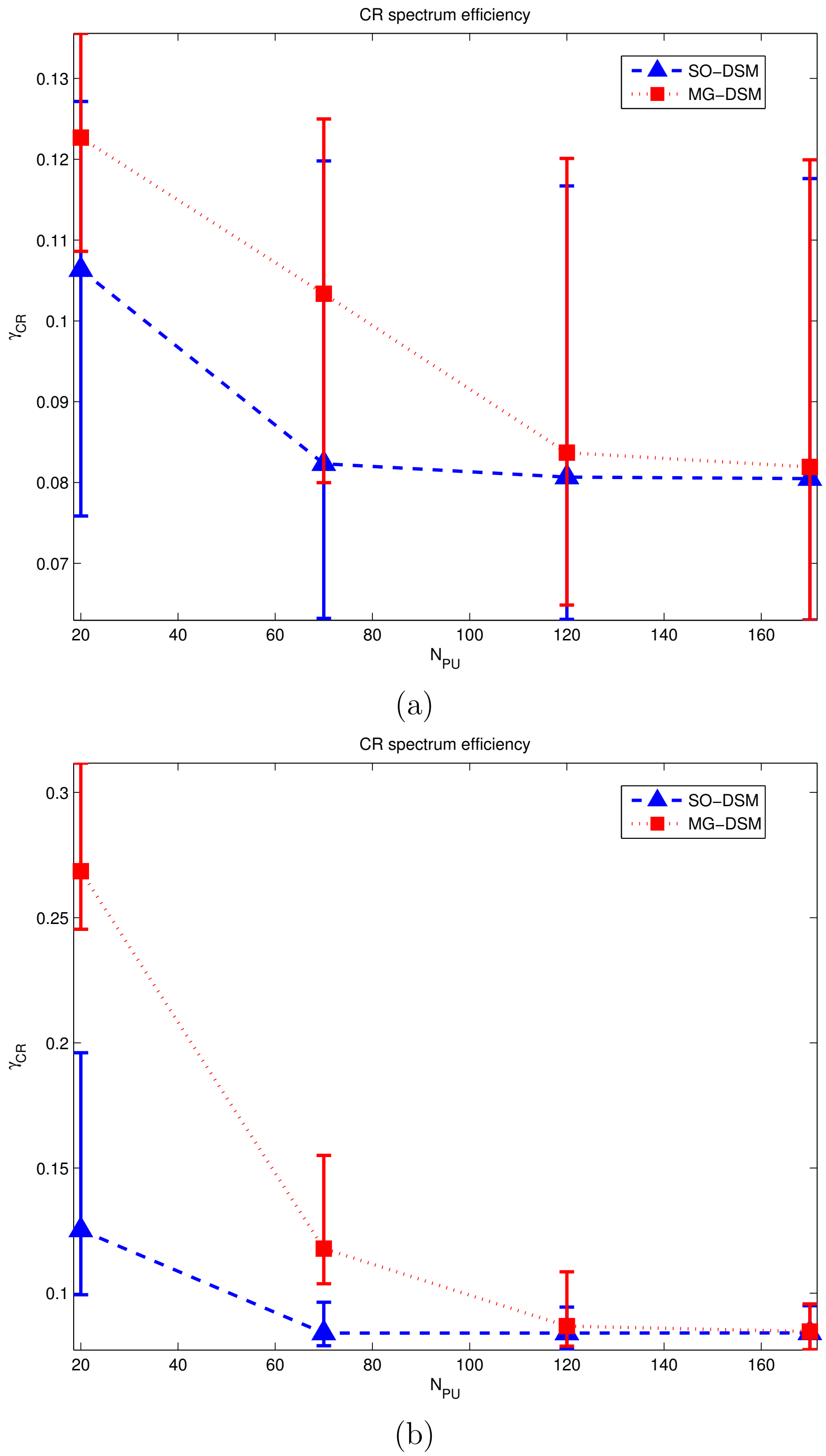

Figure 5.3: The CR network spectrum utilization. (a) N_{CR}=50 (b) N_{CR}=300. γ_{CR} at worst case is about 50% lower for SO-DSM. As the number of PUs increases, γ_{CR} decreases for both schemes due to vanishing of spectrum holes.

DSM	SO N_{CR}=50	SO N_{CR}=300	MG N_{CR}=50	MG N_{CR}=300
N_{PU}=30	0.106	0.125	0.123	0.267
N_{PU}=80	0.082	0.084	0.102	0.115
N_{PU}=130	0.081	0.084	0.081	0.083
N_{PU}=180	0.080	0.084	0.079	0.081

Table 5.2: The simulation results for SO-DSM and MG-DSM: The numerical results for the average CR network spectrum utilization.

5.3.2 Probability of Collision and CR Link Interruption

Figure 5.4 shows the probability of collision for Pus. As can be seen in this figure, the SO-DSM has significantly decreased this probability. At $N_{\mathrm{PU}} = 30$ where $\gamma_{\mathrm{CR}}$for SO-DSM is about half of $\gamma_{\mathrm{CR}}$for MG-DSM, $P_{\mathrm{col}}$is about 10 times lower for SO-DSM when $N_{\mathrm{CR}} = 50$. and 33 times lower when $N_{\mathrm{CR}} = 300$. As N_{PU}increases, for the low density CR network, P_{col}remains approximately equals for both cases of SO-DSM and MG-DSM. However, for high density CR network where $N_{\mathrm{CR}} = 300$, the SO-DSM decreases P_{col}significantly and for $N_{\mathrm{PU}} = 180$, there is no collisions for SO-DSM.

Figure 5.5 shows the probability of CR link interruption for these two schemes. Similar to P_{col}, for low density CR network, the SO-DSM network has experienced about 10 times fewer interruptions for $N_{\mathrm{PU}} = 30$ and their as N_{PU}approaches 180, P_{intr}becomes approximately equal for both schemes. For high density CR network, i.e. $N_{\mathrm{CR}} = 300$, $P_{\mathrm{intr}}$is lower about 10 times for SO-DSM when $N_{\mathrm{PU}} = 30$. When $N_{\mathrm{PU}} = 180$, CR links using SO-DSM have experienced 500 times fewer interruptions.

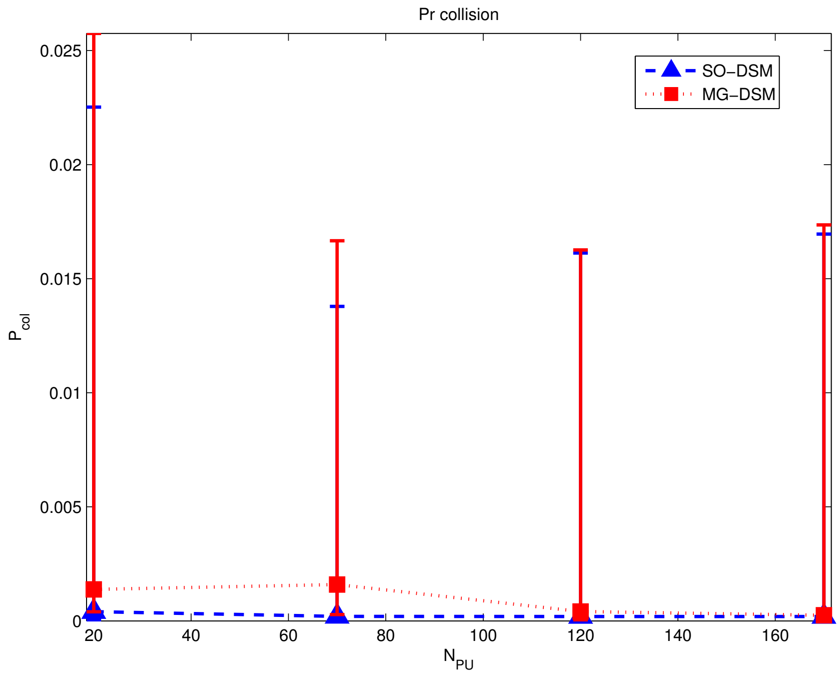

(a)

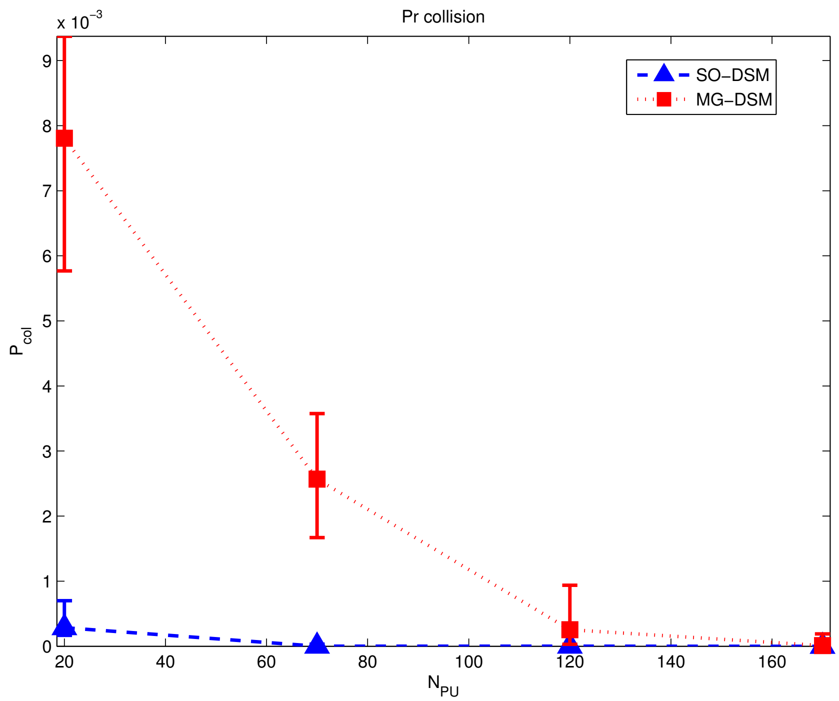

(b)

Figure 5.4: Probability of collision for PUs. (a) N_{CR}=50 (b) N_{CR}=300. $P_{\text{col}}$is significantly lower for SO-DSM. SO-DSM imposes about 33 times less collisions on PUs for $N_{\text{CR}} = 300$ and $N_{\text{PU}} = 30$; and at $N_{\text{PU}} = 180$ there is no collisions for SO-DSM with $N_{\text{CR}} = 300$.

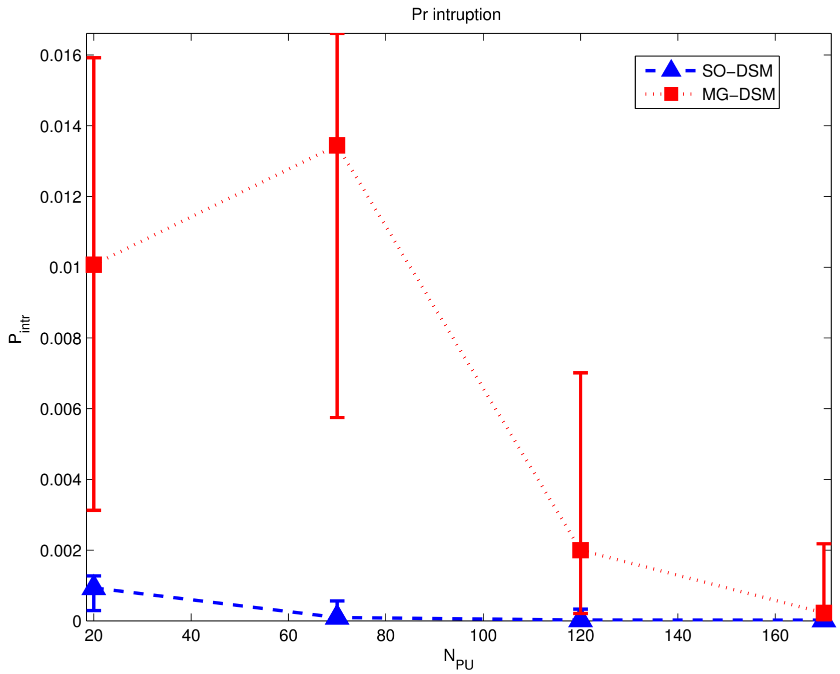

(a)

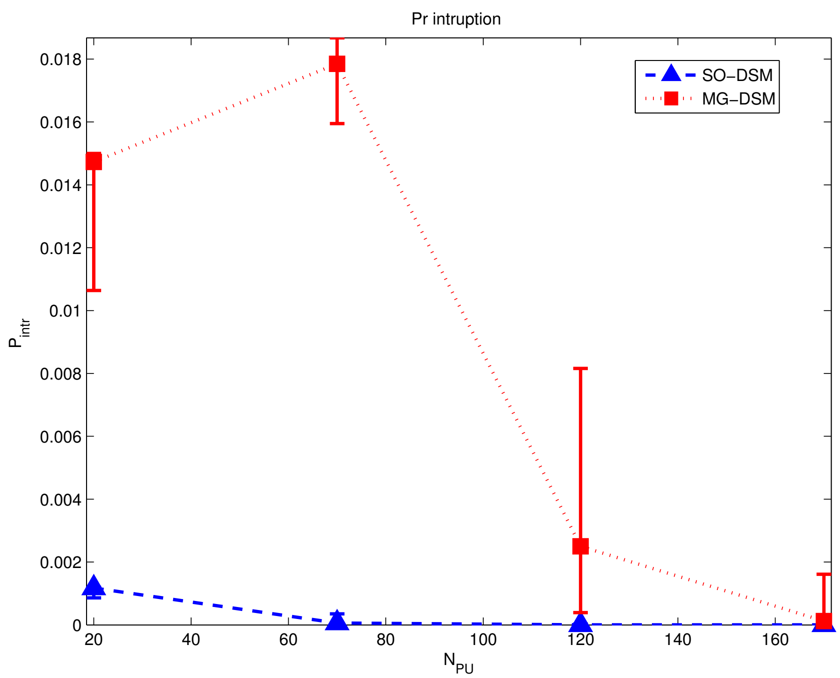

(b)

Figure 5.5: Probability of CR link interruption. (a) N_{CR}=50 (b) N_{CR}=300. The CR links experienced significantly fewer interruptions using SO-DSM. For $N_{\mathrm{PU}} = 30$ $P_{\mathrm{intr}}$is about 10 times lower for SO-DSM while for $N_{\mathrm{PU}} = 180$ the difference is even higher

DSM	SO N_{CR}=50	SO N_{CR}=300	MG N_{CR}=50	MG N_{CR}=300
N_{PU}=30	4.035E-04	2.853E-04	4.601E-03	1.019E-02
N_{PU}=80	1.972E-04	8.434E-07	2.547E-03	2.986E-03
N_{PU}=130	1.937E-04	2.566E-09	3.971E-04	2.760E-04
N_{PU}=180	1.891E-04	0.000E+00	1.636E-04	1.153E-05

Table 5.3: Numerical simulation results for SO-DSM and MG-DSM: Average probability of collision for PUs.

DSM	SO N_{CR}=50	SO N_{CR}=300	MG N_{CR}=50	MG N_{CR}=300
N_{PU}=30	9.345E-04	1.176E-03	1.167E-02	1.420E-02
N_{PU}=80	9.724E-05	5.786E-05	1.400E-02	1.728E-02
N_{PU}=130	2.529E-05	1.968E-06	1.990E-03	2.423E-03
N_{PU}=180	2.030E-05	2.876E-07	1.911E-04	1.229E-04

Table 5.4: Numerical simulation results for SO-DSM and MG-DSM: Average probability of CR link interruption.

5.3.3 PU's Received Interference

Figure 5.6 and 5.7 illustrate the received interference from CR by active PUs during TX and RX ($\mathcal{I}_{TX}$and $\mathcal{I}_{RX}$). As shown in these figures, for low number of PUs, the SO-DSM has imposed less interference on PUs. However, for the high number of PUs, the average interference becomes higher for SO-DSM because the SO-DSM has higher γ_{CR}, as shown in Fig. 5.5, and less P_{col}, as illustrated in Fig. 5.4. In other words, for $N_{\mathrm{PU}} = 180$, CRs have successfully chosen sub-bands with no PU in their neighbourhood that resulted in higher $\gamma_{\mathrm{CR}}$and lower P_{col}. As a result, PUs have received slightly higher interference from CR for SO-DSM which is an acceptable price to have much lower collisions.

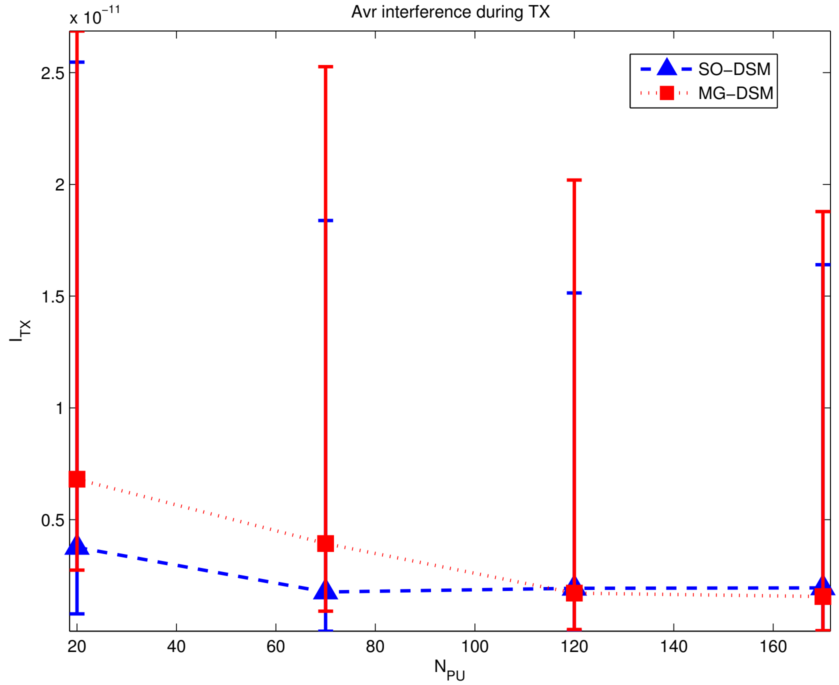

(a)

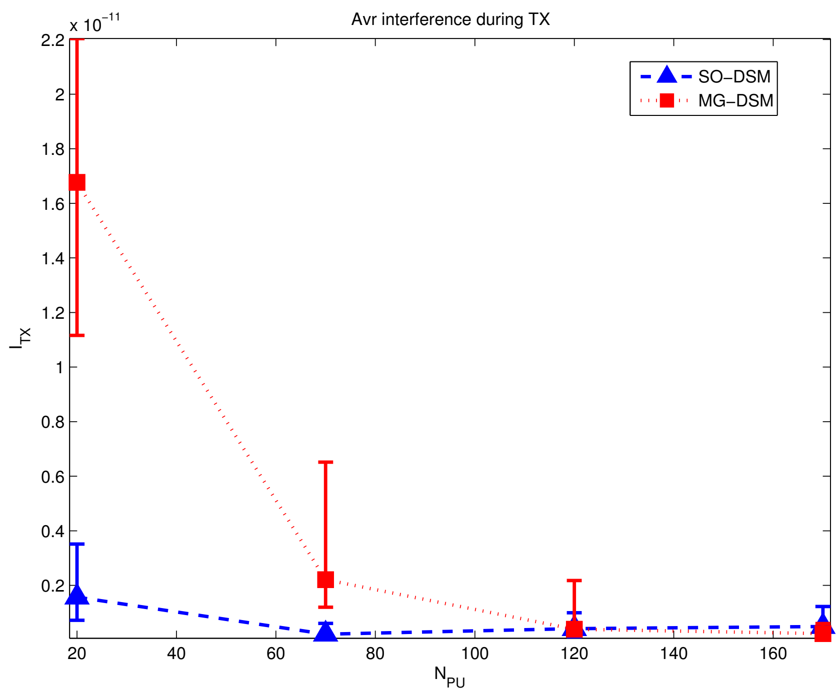

(b)

Figure 5.6: Average received interference by TX PUs. (a) N_{CR}=50 (b) N_{CR}=300. For $N_{\text{PU}} = 30$, $\mathcal{I}_{TX}$is about 10 times lower for SO-DSM. However, for $N_{\text{PU}} = 180$ $\mathcal{I}_{TX}$is slightly higher for SO-DSM. This is due to slightly higher $\gamma_{\text{CR}}$and much lower P_{col} of SO-DSM in this case.

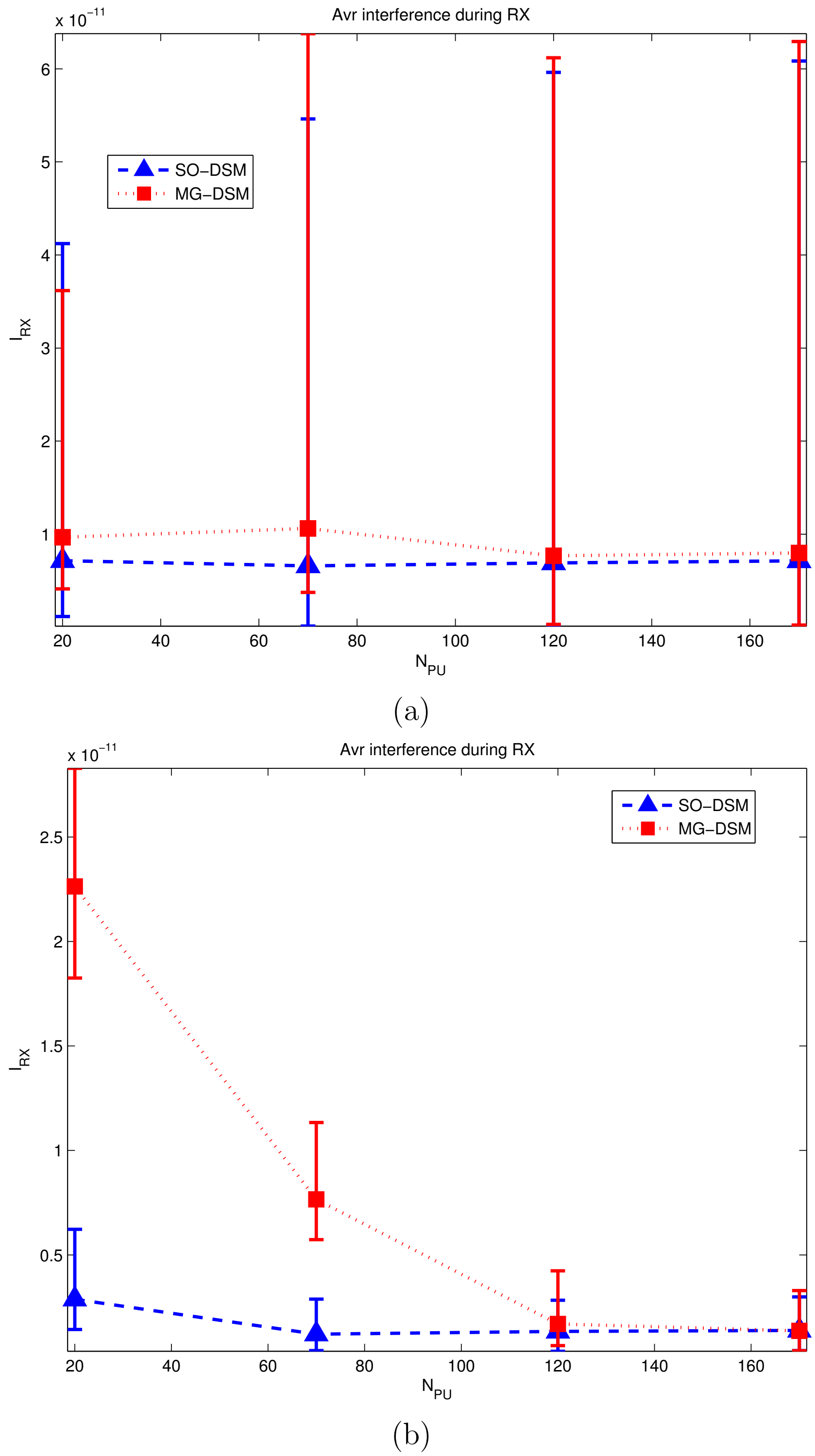

Figure 5.7: Average received interference by RX PUs. (a) N_{CR}=50 (b) N_{CR}=300. For $N_{\mathrm{PU}} = 30$, $\mathcal{I}_{RX}$is about 10 times lower for SO-DSM. However, for $N_{\mathrm{PU}} = 180$ $\mathcal{I}_{RX}$is slightly higher for SO-DSM. This is due to slightly higher $\gamma_{\mathrm{CR}}$and much lower P_{col} of SO-DSM in this case.

DSM	SO N_{CR}=50	SO N_{CR}=300	MG N_{CR}=50	MG N_{CR}=300
N_{PU}=30	3.755E-12	1.574E-12	7.924E-12	1.811E-11
N_{PU}=80	1.761E-12	2.065E-13	3.943E-12	2.394E-12
N_{PU}=130	1.926E-12	4.157E-13	1.459E-12	3.971E-13
N_{PU}=180	1.943E-12	4.899E-13	1.273E-12	2.011E-13

Table 5.5: Numerical simulation results for SO-DSM and MG-DSM: Average received interference by TX PUs.

DSM	SO N_{CR}=50	SO N_{CR}=300	MG N_{CR}=50	MG N_{CR}=300
N_{PU}=30	7.151E-12	2.880E-12	1.011E-11	2.398E-11
N_{PU}=80	6.591E-12	1.195E-12	9.573E-12	7.867E-12
N_{PU}=130	6.903E-12	1.345E-12	5.746E-12	1.538E-12
N_{PU}=180	7.126E-12	1.385E-12	5.737E-12	1.118E-12

Table 5.6: Numerical simulation results for SO-DSM and MG-DSM: Average received interference by RX PUs.

5.3.4 Mean and Variance of Sub-band Distribution

Figure 5.8 and 5.9 show the mean $\mathcal{M}_s$and variance $\mathcal{V}_s$of sub-band assignment distribution for these two schemes. Figure 5.8 illustrates the average number of different sub-bands used by radio units. As this figure shows, using SO-DSM radio units have used lower number of sub-bands which one indication of formation of a temporal organization in sub-band assignment. Furthermore, the higher variance of sub-band distribution for SO-DSM, shown in Fig. 5.9, as the second indication, confirms the formation of such temporal organization formation using SO-DSM.

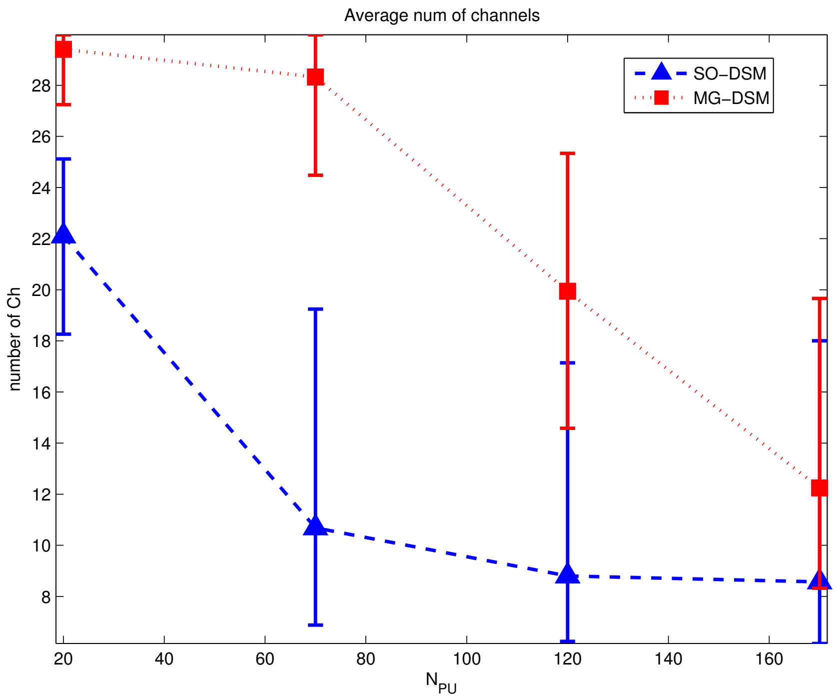

(a)

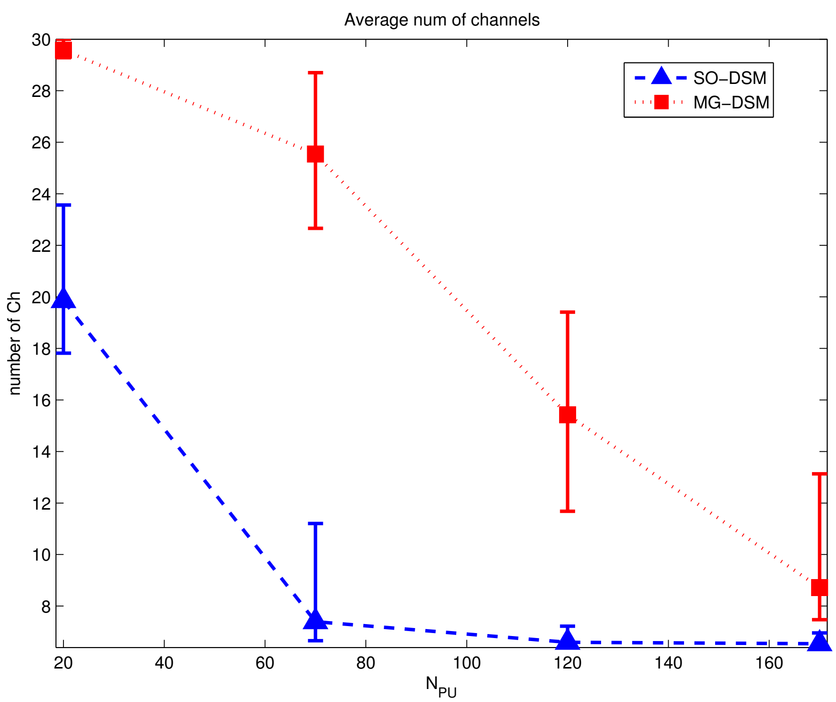

(b)

Figure 5.8: Mean of CR sub-band utilization distribution. (a) N_{CR}=50 (b) N_{CR}=300. The CRs have used lower number of sub-bands for SO-DSM which is an indication of map formation in SO-DSM.

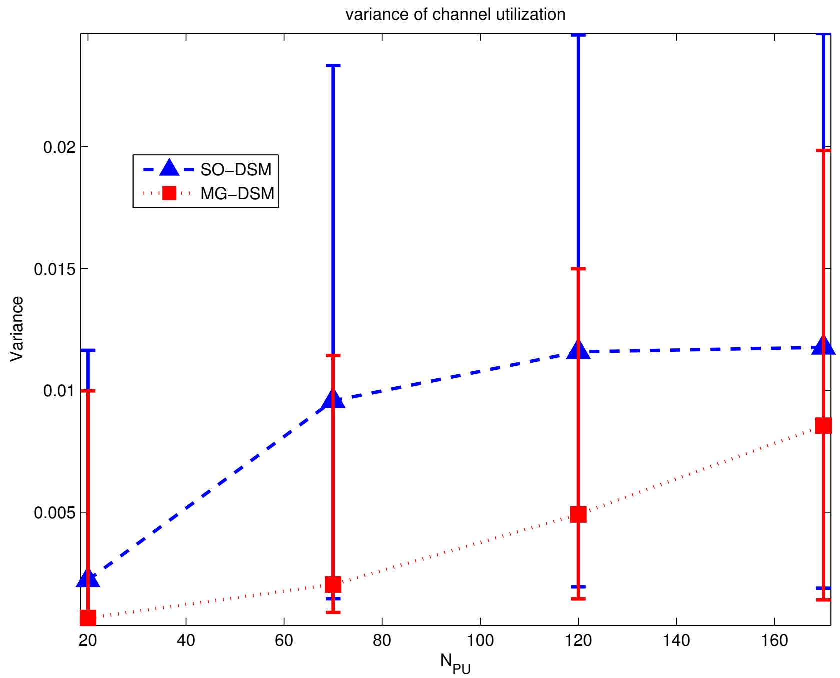

(a)

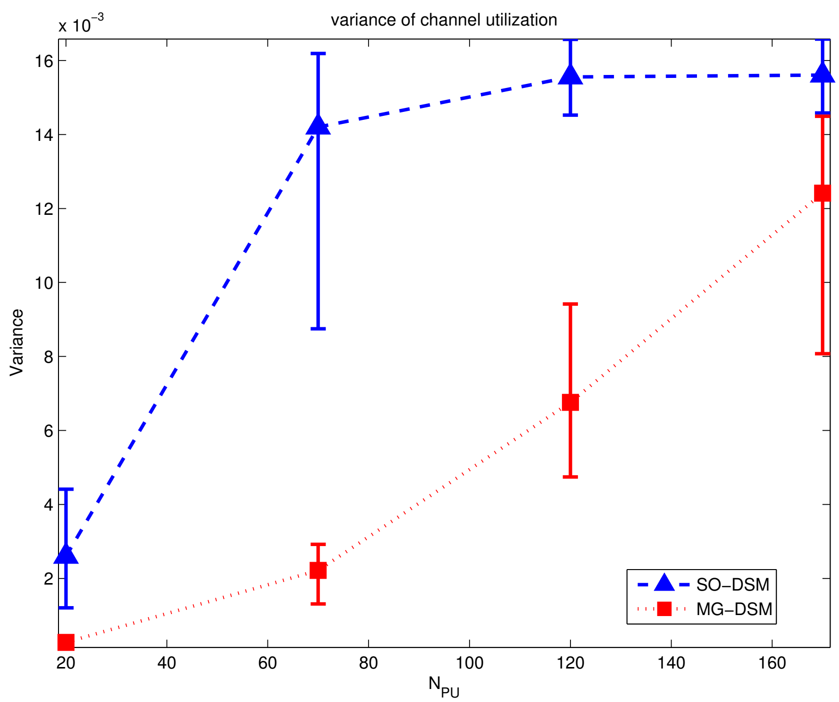

(b)

Figure 5.9: Variance of CR sub-band utilization distribution. (a) N_{CR}=50 (b) N_{CR}=300. $\mathcal{V}_s$is higher for SO-DSM which demonstrates CRs have successfully built temporal organization.

DSM	SO N_{CR}=50	SO N_{CR}=300	MG N_{CR}=50	MG N_{CR}=300
N_{PU}=30	22.109	19.830	29.928	29.402
N_{PU}=80	10.682	7.382	29.188	25.509
N_{PU}=130	8.801	6.590	20.561	15.373
N_{PU}=180	8.572	6.531	12.168	8.554

Table 5.7: Numerical simulation results for SO-DSM and MG-DSM: Mean of CR sub-band utilization distribution.

DSM	SO N_{CR}=50	SO N_{CR}=300	MG N_{CR}=50	MG N_{CR}=300
N_{PU}=30	2.220E-03	2.585E-03	2.097E-04	1.984E-04
N_{PU}=80	9.577E-03	1.416E-02	1.680E-03	2.079E-03
N_{PU}=130	1.158E-02	1.553E-02	4.341E-03	6.630E-03
N_{PU}=180	1.176E-02	1.560E-02	7.967E-03	1.243E-02

Table 5.8: Numerical simulation results for SO-DSM and MG-DSM: Variance of CR sub-band utilization distribution.

These results show that using SO-DSM, the CR units are more robust and provide more reliable communication links; and by extracting PU spectrum utilization patterns and forming a temporal sub-band organization, they have experienced fewer interruptions from PUs and imposed less interference on PUs. The SO-DSM trades off a bit of spectrum efficiency to achieve significantly less collisions with PUs and CR link interruptions. Interestingly, for the tough condition of high density CR network and high density PU network, i.e. $N_{\text{CR}} = 300$ and $N_{\text{PU}} = 180$, the SO-DSM achieves a slightly higher spectrum efficiency while still decreases $P_{\text{col}}$and P_{intr}significantly.

5.4 SO-DSM vs CDSM

Figures 5.10 to 5.15 show the simulation results for LDO centralized CR network versus SO-DSM.

DSM	SO N_{CR}=50	SO N_{CR}=300	C N_{CR}=50	C N_{CR}=300
N_{PU}=30	3.373E-02	3.293E-02	3.372E-02	3.305E-02
N_{PU}=80	7.835E-02	7.641E-02	7.834E-02	7.672E-02
N_{PU}=130	9.258E-02	9.140E-02	9.259E-02	9.154E-02
N_{PU}=180	9.370E-02	9.257E-02	9.370E-02	9.271E-02

Table 5.9: Numerical simulation results for centralized DSM and SO-DSM. Legacy network spectrum utilization.

5.4.1 Spectrum Utilization

Figure 5.10 and 5.11 show the spectrum utilization of legacy and CR networks. Naturally, γ_{PU} is approximately not changing using different DSM schemes. Figure 5.11 demonstrates the CR network spectrum efficiency γ_{CR}. Using centralized DSM, as it was expected, the spectrum utilization efficiency of CR network is higher than SO-DSM and even MG-DSM. For $N_{\mathrm{PU}} = 30$, γ_{CR} for SO-DSM is about 20% lower than CDSM when $N_{\mathrm{CR}} = 50$ and for $N_{\mathrm{CR}} = 300$, it is 80% lower. The difference decreases when N_{PU} increases to 180 and becomes 50% for $N_{\mathrm{CR}} = 50$ and 30% for $N_{\mathrm{CR}} = 300$.

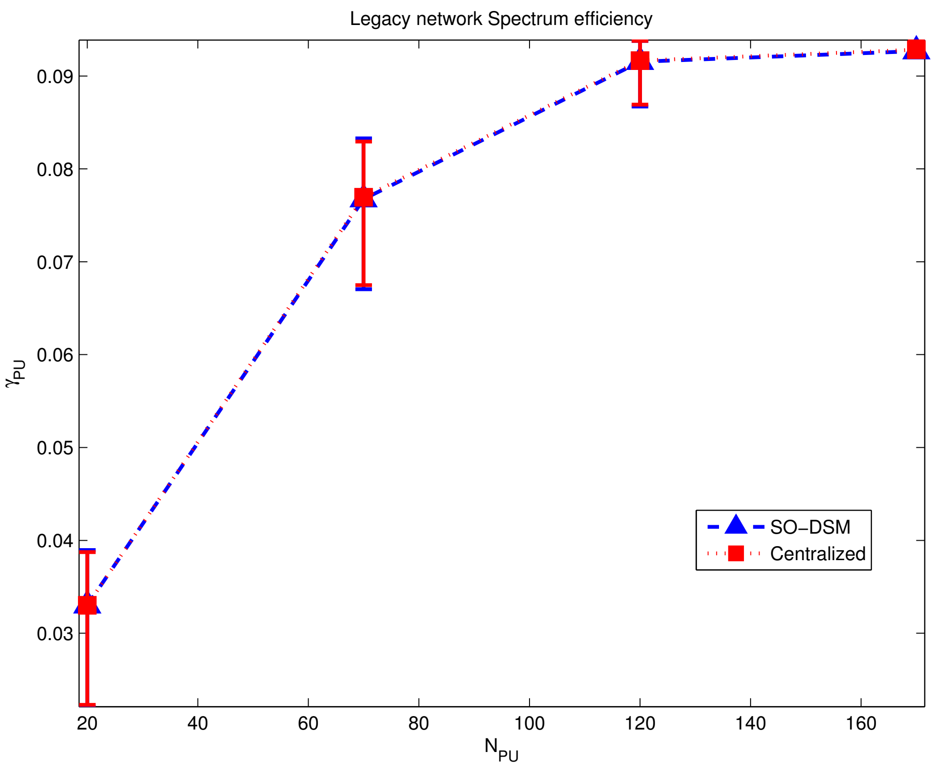

Figure 5.10: The simulation results for centralized DSM and SO-DSM. Legacy network spectrum utilization. As the number of PUs increase, the spectrum utilization of legacy network increases. The legacy network is independent of CR network, thus, the results are approximately equal for all simulations.

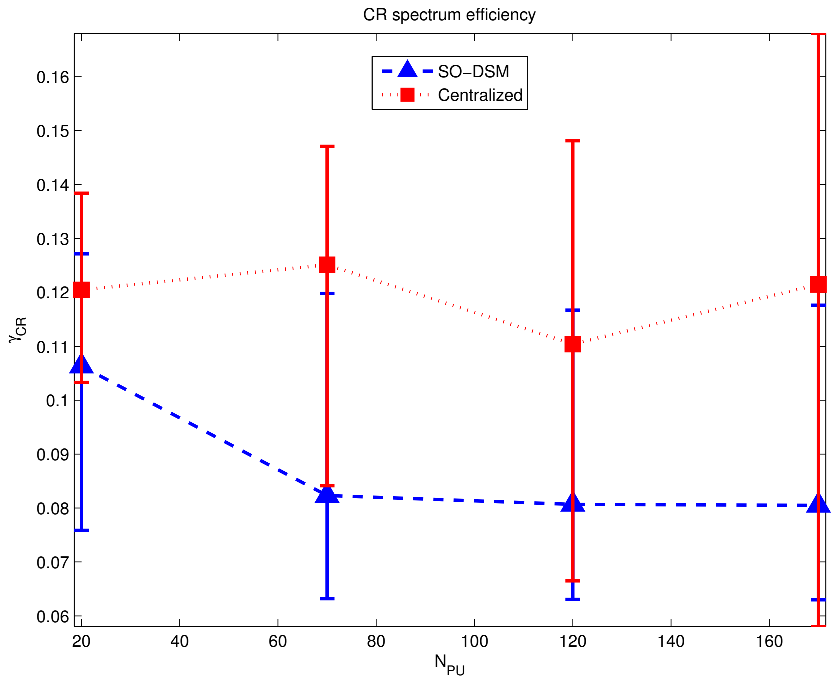

(a)

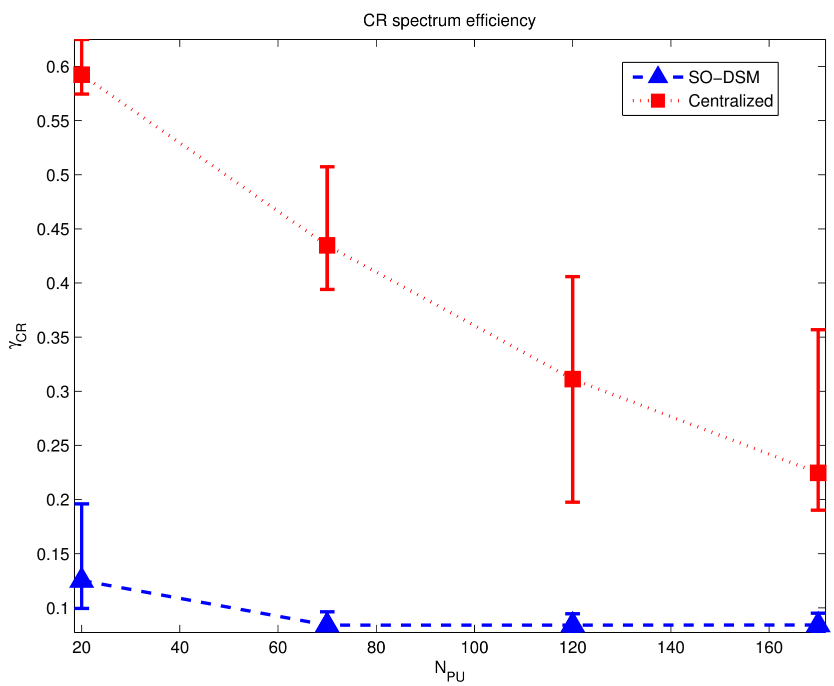

(b)

Figure 5.11: The CR network spectrum utilization. (a) N_{CR}=50 (b) N_{CR}=300. γ_{CR}at worst case is about 80% lower for SO-DSM. As the number of PUs increases, γ_{CR}decreases for both schemes due to vanishing of spectrum holes.

DSM	SO N_{CR}=50	SO N_{CR}=300	C N_{CR}=50	C N_{CR}=300
N_{PU}=30	0.106	0.125	0.120	0.591
N_{PU}=80	0.082	0.084	0.125	0.434
N_{PU}=130	0.081	0.084	0.110	0.310
N_{PU}=180	0.080	0.084	0.121	0.225

Table 5.10: Numerical simulation results for centralized DSM and SO-DSM: The CR network spectrum utilization.

5.4.2 Probability of Collision and Link Interruption

Figures 5.12 and 5.13 show probability of collision and probability of CR link interruption for SO-DSM and CDSM. As Fig. 5.12 shows, the $P_{\mathrm{col}}$is higher for CDSM, specially for high density CR network $N_{\mathrm{CR}} = 300$ the difference is much more, at least 100 times. This is the price CDSM pays to achieve at best 5 times higher spectrum efficiency.

Fig. 5.13 shows the probability of CR link interruption. As these results demonstrate, $P_{\mathrm{intr}}$is significantly higher for CR link using CDSM. This is due to the propagation of changes in the network using centralized approach. In a centralized scheme, a change in one part of network can propagate to all around the network. On the other hand, in a decentralized network, any change is responded locally and can cause changes only in its neighbourhood. Therefore, using a decentralized scheme, as shown in Fig. 5.13, link experience much fewer interruptions.

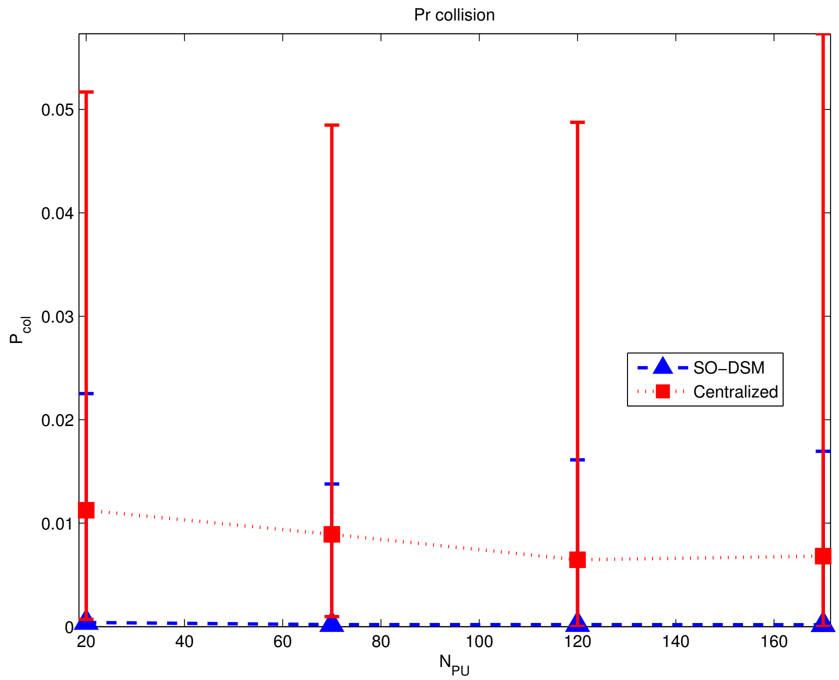

(a)

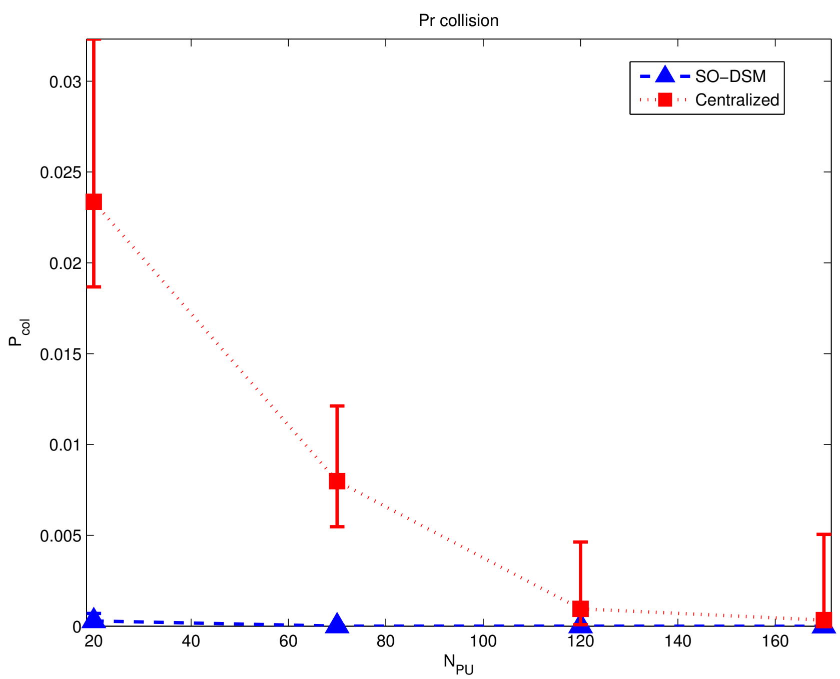

(b)

Figure 5.12: Probability of collision for PUs. (a) N_{CR}=50 (b) N_{CR}=300. $P_{\mathrm{col}}$is significantly lower for SO-DSM. SO-DSM imposes about 33 times less collisions on PUs for $N_{\mathrm{CR}} = 300$ and $N_{\mathrm{PU}} = 30$; and at $N_{\mathrm{PU}} = 180$ there is no collisions for SO-DSM.

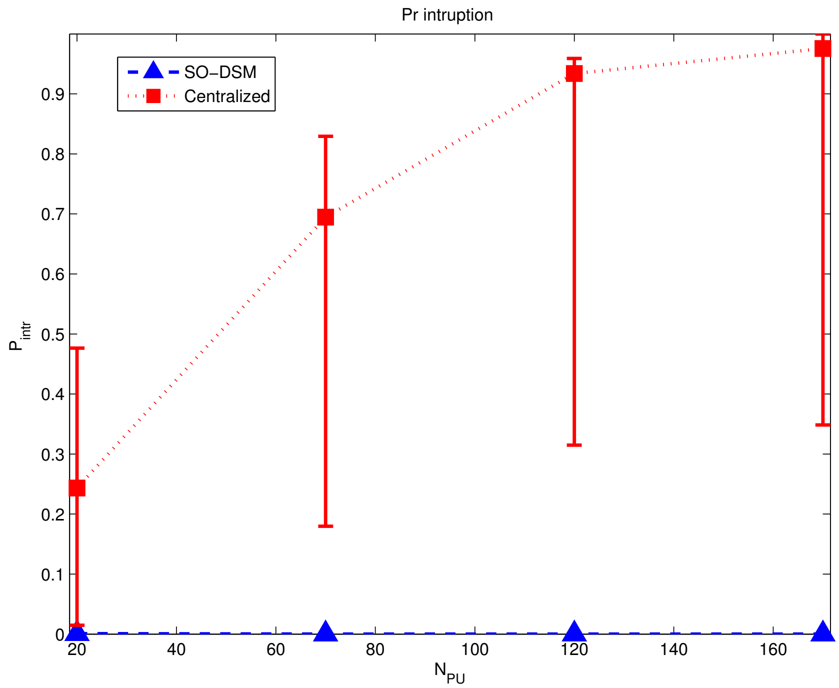

(a)

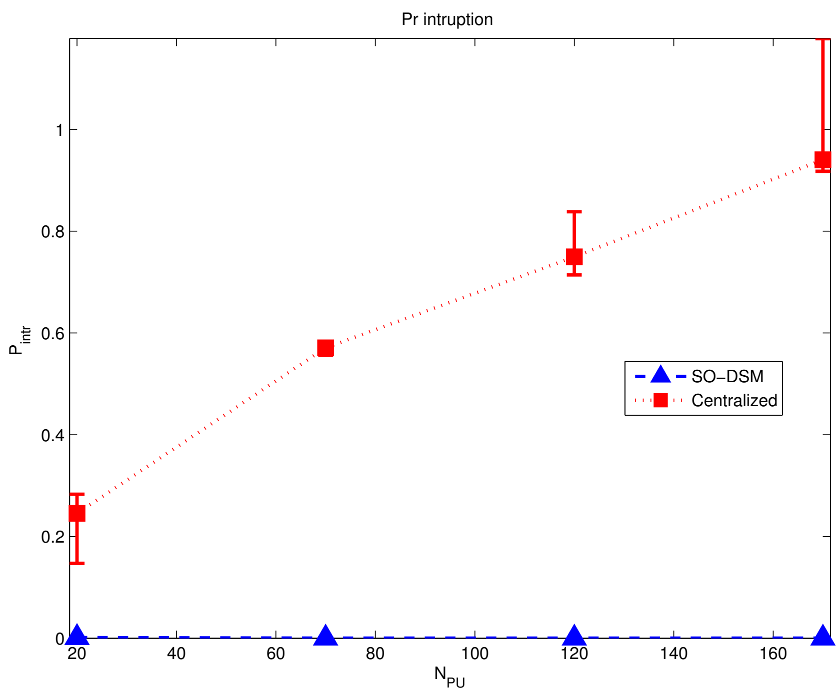

(b)

Figure 5.13: Probability of CR link interruption. (a) N_{CR}=50 (b) N_{CR}=300. The CR links experienced significantly fewer interruptions using SO-DSM. For $N_{\mathrm{PU}} = 30$ $P_{\mathrm{intr}}$is about 10 times lower for SO-DSM while for $N_{\mathrm{PU}} = 180$ the difference is even higher, as high as 500 times for $N_{\mathrm{CR}} = 300$.

DSM	SO N_{CR}=50	SO N_{CR}=300	C N_{CR}=50	C N_{CR}=300
N_{PU}=30	4.035E-04	2.853E-04	1.126E-02	2.330E-02
N_{PU}=80	1.972E-04	8.434E-07	8.916E-03	7.979E-03
N_{PU}=130	1.937E-04	2.566E-09	6.467E-03	9.399E-04
N_{PU}=180	1.891E-04	0.000E+00	6.822E-03	3.333E-04

Table 5.11: The simulation results for centralized DSM and SO-DSM: Probability of collision for PUs.

DSM	SO N_{CR}=50	SO N_{CR}=300	C N_{CR}=50	C N_{CR}=300
N_{PU}=30	9.345E-04	1.176E-03	2.433E-01	2.458E-01
N_{PU}=80	9.724E-05	5.786E-05	6.946E-01	5.705E-01
N_{PU}=130	2.529E-05	1.968E-06	9.340E-01	7.500E-01
N_{PU}=180	2.030E-05	2.876E-07	9.755E-01	9.400E-01

Table 5.12: The simulation results for centralized DSM and SO-DSM: Probability of CR link interruption.

5.4.3 PU's Received Interference

Figure 5.14 and 5.14 illustrate the received interference from CR by active PUs during TX and RX. As shown in these figures, the SO-DSM has imposed less interference on PUs. The main reason for significant lower imposed interference is the lower CR spectrum utilization using SO-DSM shown in Fig. 5.11.

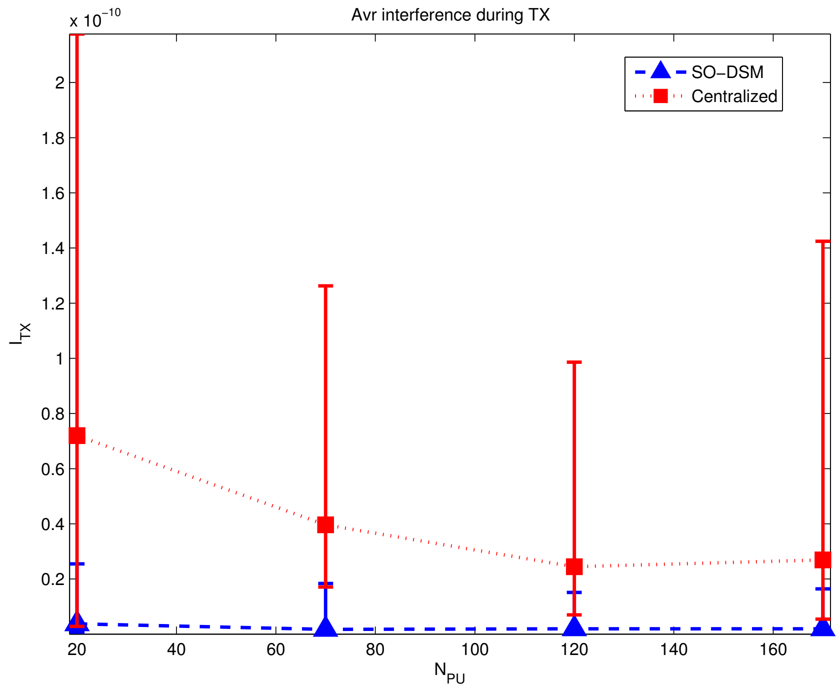

(a)

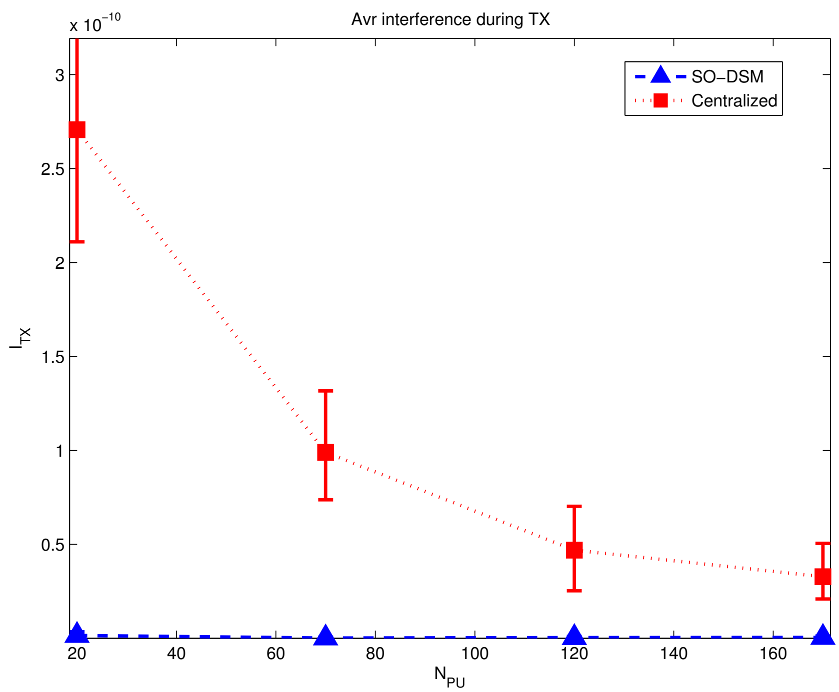

(b)

Figure 5.14: Average received interference by TX PUs. (a) N_{CR}=50 (b) N_{CR}=300. For $N_{\mathrm{PU}} = 30$, $\mathcal{I}_{TX}$is about 10 times lower for SO-DSM. However, for $N_{\mathrm{PU}} = 180$ $\mathcal{I}_{TX}$is slightly higher for SO-DSM. This is due to slightly higher $\gamma_{\mathrm{CR}}$and much lower $P_{\mathrm{col}}$of SO-DSM scheme for this case.

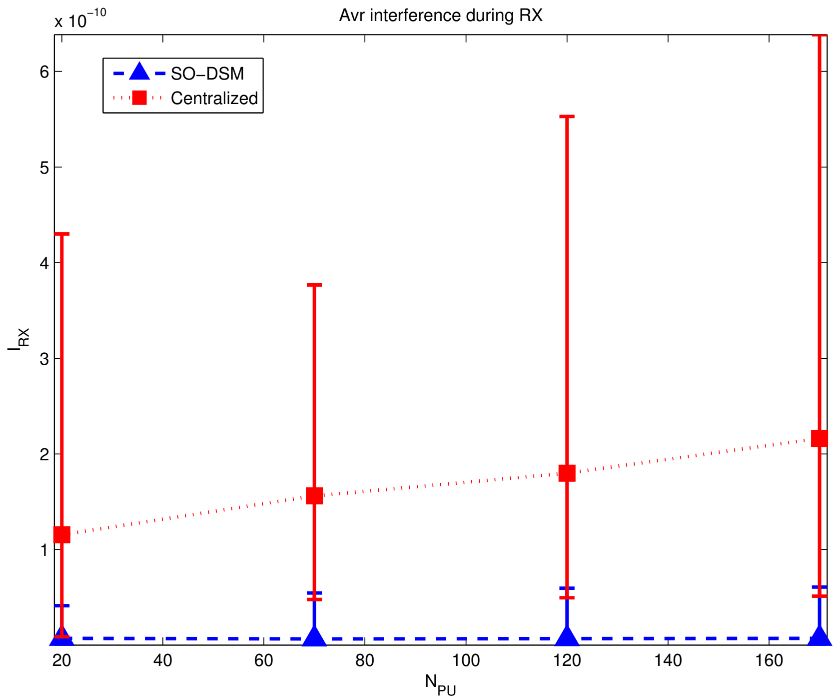

(a)

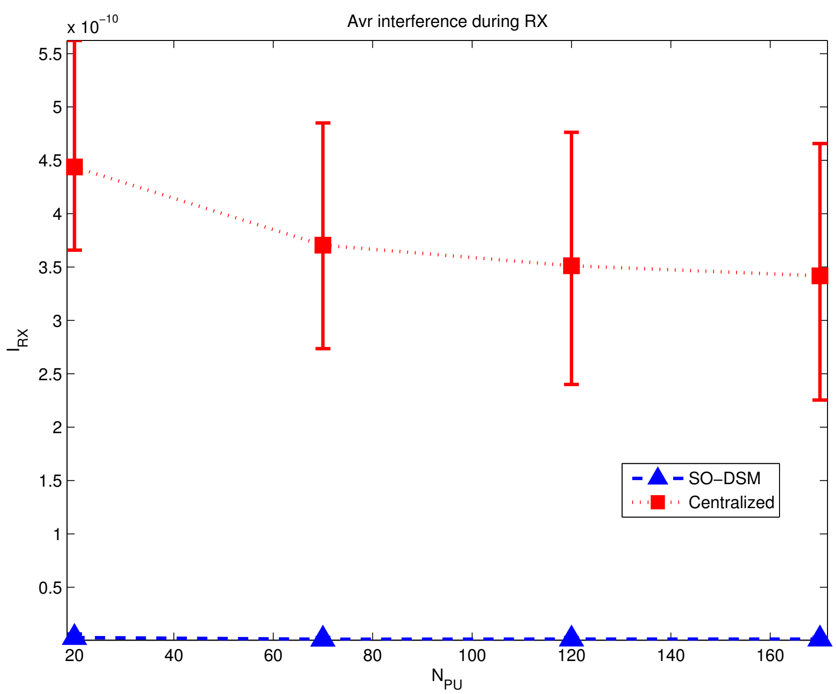

(b)

Figure 5.15: Average received interference by RX PUs. (a) $N_{\rm CR}$=50 (b) $N_{\rm CR}$=300. Similar to $\mathcal{I}_{TX}$, for $N_{\rm PU} = 30$, $\mathcal{I}_{RX}$is about 10 times lower for SO-DSM. However, for $N_{\rm PU} = 180$ $\mathcal{I}_{RX}$is slightly higher for SO-DSM. This is due to slightly higher $\gamma_{\rm CR}$and much lower $P_{\rm col}$of SO-DSM scheme for this case.

DSM	SO N_{CR}=50	SO N_{CR}=300	C N_{CR}=50	C N_{CR}=300
N_{PU}=30	3.755E-12	1.574E-12	7.199E-11	2.693E-10
N_{PU}=80	1.761E-12	2.065E-13	3.962E-11	9.918E-11
N_{PU}=130	1.926E-12	4.157E-13	2.444E-11	4.674E-11
N_{PU}=180	1.943E-12	4.899E-13	2.691E-11	3.295E-11

Table 5.13: Numerical simulation results for centralized DSM and SO-DSM: Average received interference by TX PUs.

DSM	SO N_{CR}=50	SO N_{CR}=300	C N_{CR}=50	C N_{CR}=300
N_{PU}=30	7.151E-12	2.880E-12	1.154E-10	4.406E-10
N_{PU}=80	6.591E-12	1.195E-12	1.561E-10	3.694E-10
N_{PU}=130	6.903E-12	1.345E-12	1.798E-10	3.493E-10
N_{PU}=180	7.126E-12	1.385E-12	2.163E-10	3.405E-10

Table 5.14: Numerical simulation results for centralized DSM and SO-DSM: Average received interference by RX PUs.

5.4.4 Mean and Variance of Sub-band Distribution

Figures 5.16 and 5.17 illustrate the mean and variance of channel assignment for SO-DSM and CDSM schemes. The SO-DSM has lower average number of used sub-bands. However, for the $N_{\mathrm{CR}} = 300$, the variance of sub-band utilization distribution is higher than CDSM, while for $N_{\mathrm{CR}} = 50$, $\mathcal{V}_s$is lower than CDSM. These results show that the SO-DSM has successfully created a temporal sub-band assignment organization while sub-band assignment in CDSM is more random for $N_{\mathrm{CR}} = 300$. For $N_{\mathrm{CR}} = 50$, which is low density CR network where more spectrum holes are available for CRs, the CDSM has also resulted in a temporal organization in sub-band assignment demonstrated by higher $\mathcal{V}_s$of CDSM for this case.

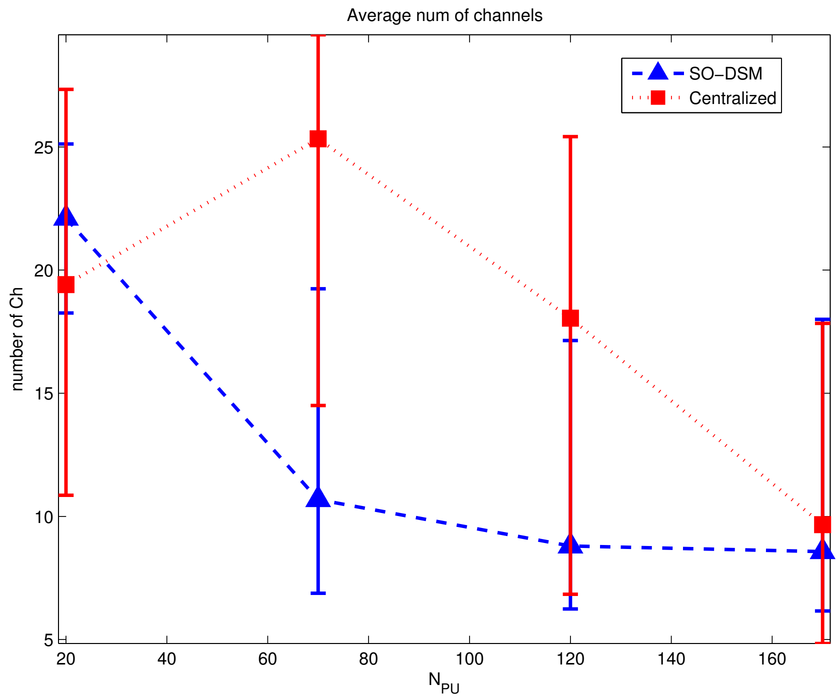

(a)

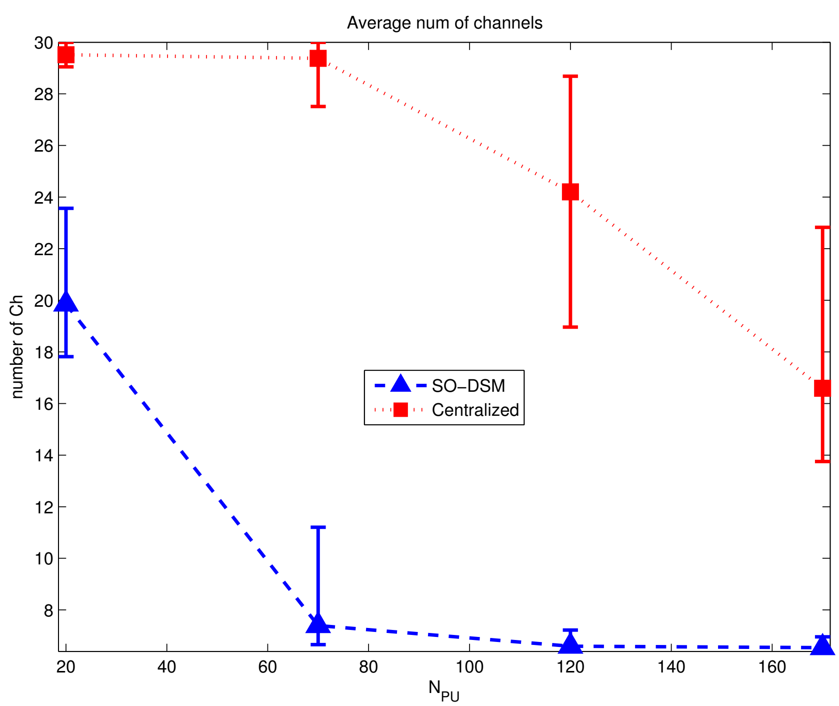

(b)

Figure 5.16: Mean of CR sub-band utilization distribution. (a) N_{CR}=50 (b) N_{CR}=300. The CRs have used lower number of sub-bands for SO-DSM which is an indication of map formation in SO-DSM.

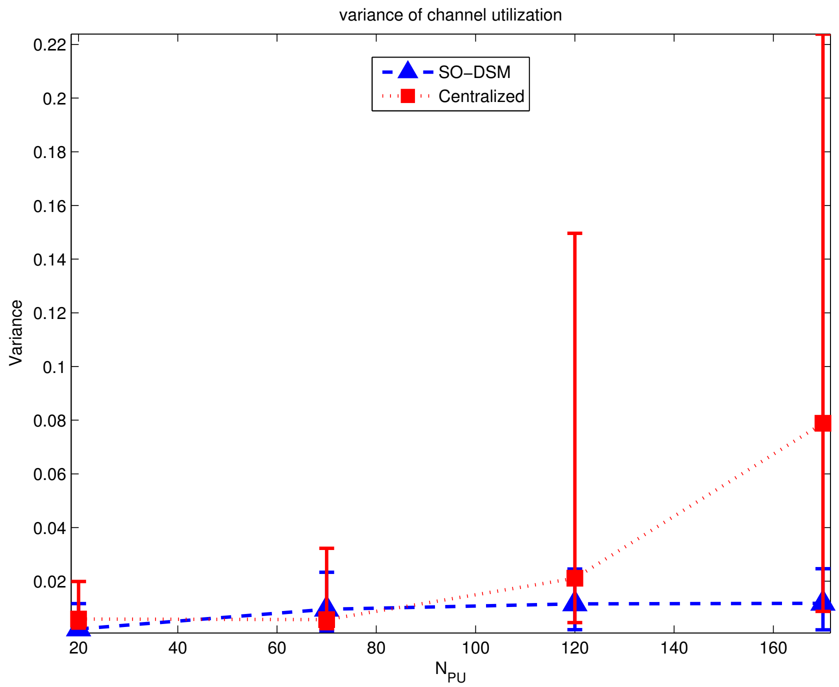

(a)

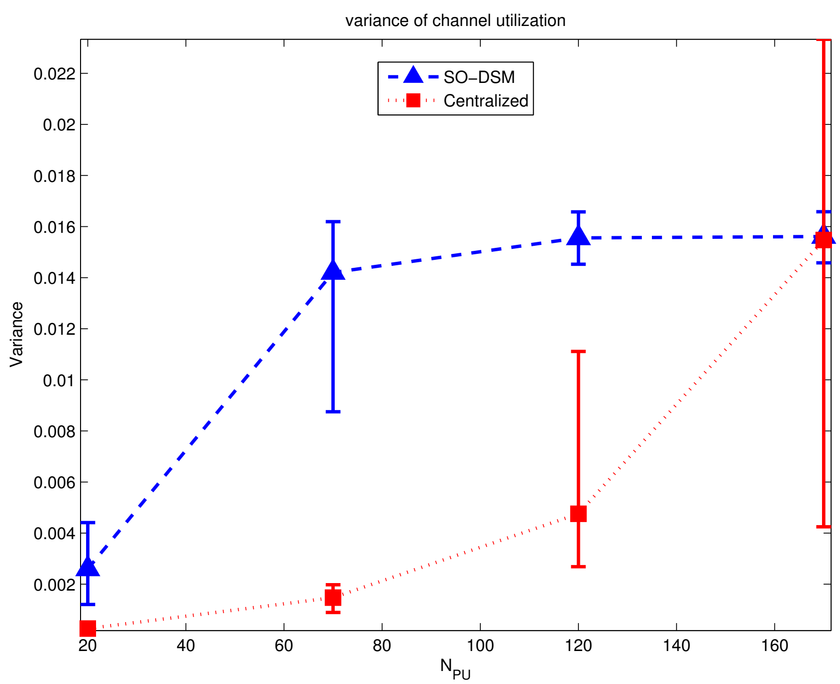

(b)

Figure 5.17: Variance of CR sub-band utilization distribution. (a) N_{CR}=50 (b) N_{CR}=300. $\mathcal{V}_s$is higher for SO-DSM which demonstrates CRs have successfully built temporal organization.

DSM	SO N_{CR}=50	SO N_{CR}=300	C N_{CR}=50	C N_{CR}=300
N_{PU}=30	22.109	19.830	19.409	29.462
N_{PU}=80	10.682	7.382	25.333	29.319
N_{PU}=130	8.801	6.590	18.047	24.169
N_{PU}=180	8.572	6.531	9.666	16.556

Table 5.15: Numerical simulation results for centralized DSM and SO-DSM: Mean of CR sub-band utilization distribution.

DSM	SO N_{CR}=50	SO N_{CR}=300	C N_{CR}=50	C N_{CR}=300
N_{PU}=30	2.220E-03	2.585E-03	5.894E-03	2.626E-04
N_{PU}=80	9.577E-03	1.416E-02	5.677E-03	1.469E-03
N_{PU}=130	1.158E-02	1.553E-02	2.110E-02	4.768E-03
N_{PU}=180	1.176E-02	1.560E-02	7.886E-02	1.550E-02

Table 5.16: Numerical simulation results for centralized DSM and SO-DSM: Variance of CR sub-band utilization distribution.

The simulation results for CDSM and SO-DSM CR networks confirmed that as described in Sec. 2.4, the centralized schemes result in higher CR spectrum utilization. However, this gain in $\gamma_{\mathrm{CR}}$is achieved with paying a significant price in terms of much higher collisions with PUs and much higher interruptions in the CR links. Therefore, comparing CDSM and SO-DSM, the SO-DSM trades off some spectrum efficiency to achieve significantly more gain in collisions and link interruptions.

5.5 SO-DSM parameters

The SO-DSM CR network was simulated with different values for η_1 and η_2 to study the effect of these parameters on the emergent behaviour of the network.

5.5.0.1 Learning-rate Parameter η_1

Figures 5.18 to 5.22 show the simulation results for SO-DSM CR network simulated with different values of η_1 and parameters listed in Table. 5.17. As

Parameter	Value
N_{PU}	80
η_2	0.05
D_{RSA}	1
β_1	0.6
β_2	0.1
PUs (μ_1, μ_2)	(0.01,0.05)
CRs (μ_1, μ_2)	(0.1,0.1)

Table 5.17: SO-DSM parameters used in $\eta_1$simulations.

Fig. 5.18 shows, as η_1 increases CR units forget PUs' activities faster and the CR network spectrum utilization increases. However, by increasing η_1, the CR network becomes more aggressive and consequently, as Fig. 5.19 illustrates, the probability of collision with PUs increases. Figure 5.20 shows the probability of CR link interruption. Figures 5.21 and 5.22 show the mean and variance of CR sub-band assignment distribution. As shown in these figures, as η_1 increases, the temporal organization vanishes.

Similar to probability of collision, the probability of CR link interruption increases as η_1 increases. These figures show the trade off between optimality and stability in this problem. If we increase η_1, spectrum efficiency increases

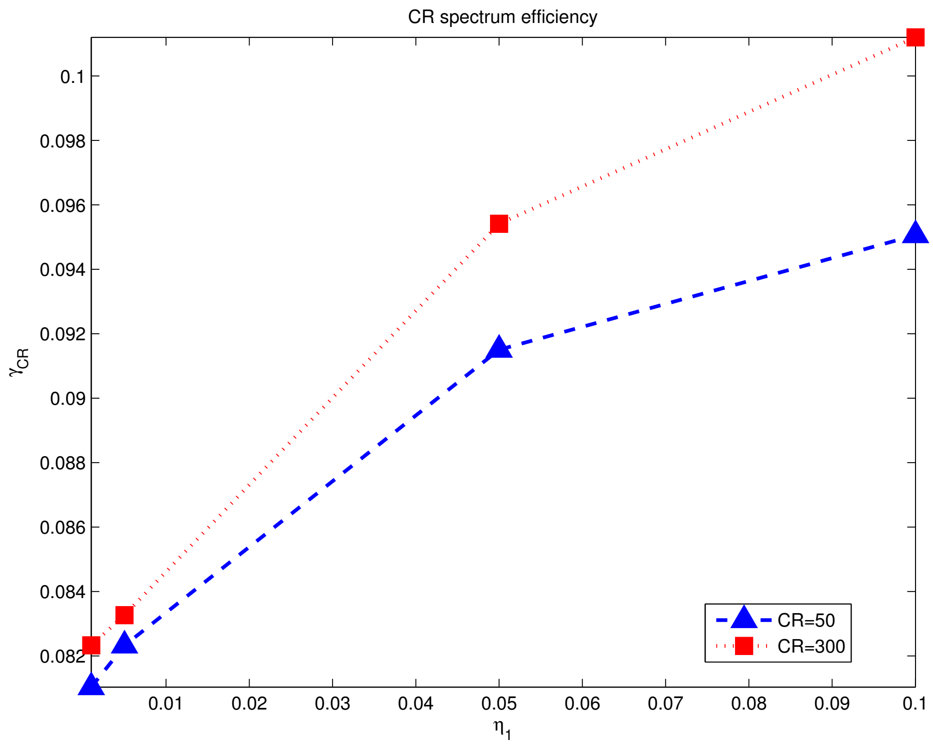

Figure 5.18: The simulation results for SO-DSM using different values of η_1. CR network spectrum utilization.

but at same time CR units will face more interruptions and PUs will experience more collisions. The SO-DSM CR network can become more aggressive, i.e. γ_{CR}, $P_{\text{col}}$and P_{intr}, or more conservative, i.e. lower γ_{CR}, $P_{\text{col}}$and P_{intr}, by tuning η_1.

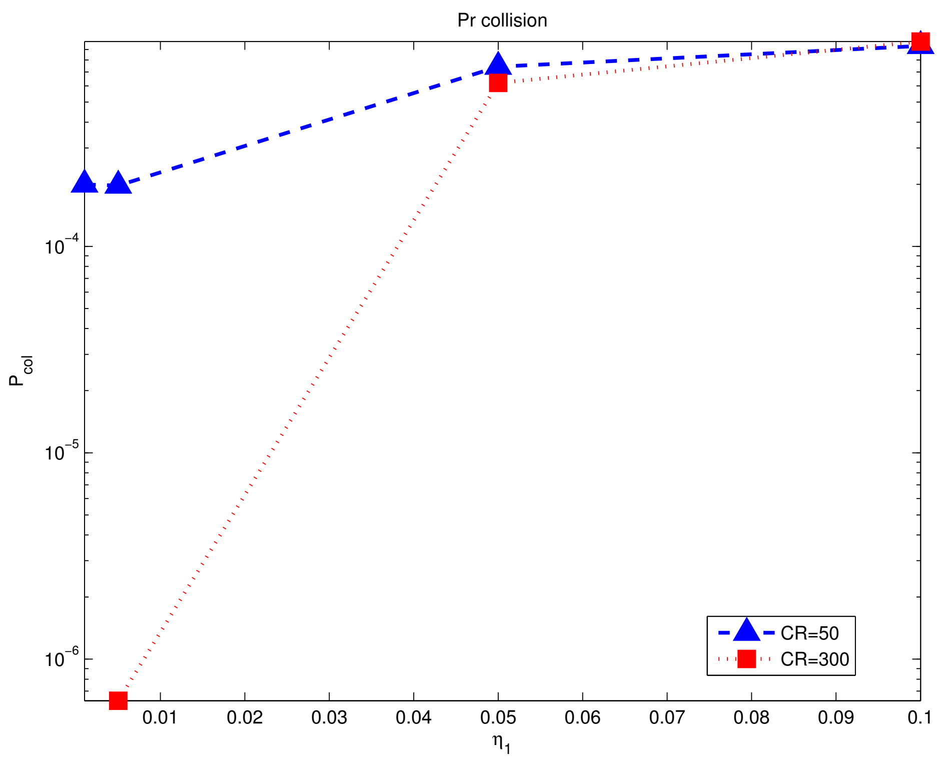

Figure 5.19: The simulation results for SO-DSM using different values of η_1. Probability of collision for PUs.

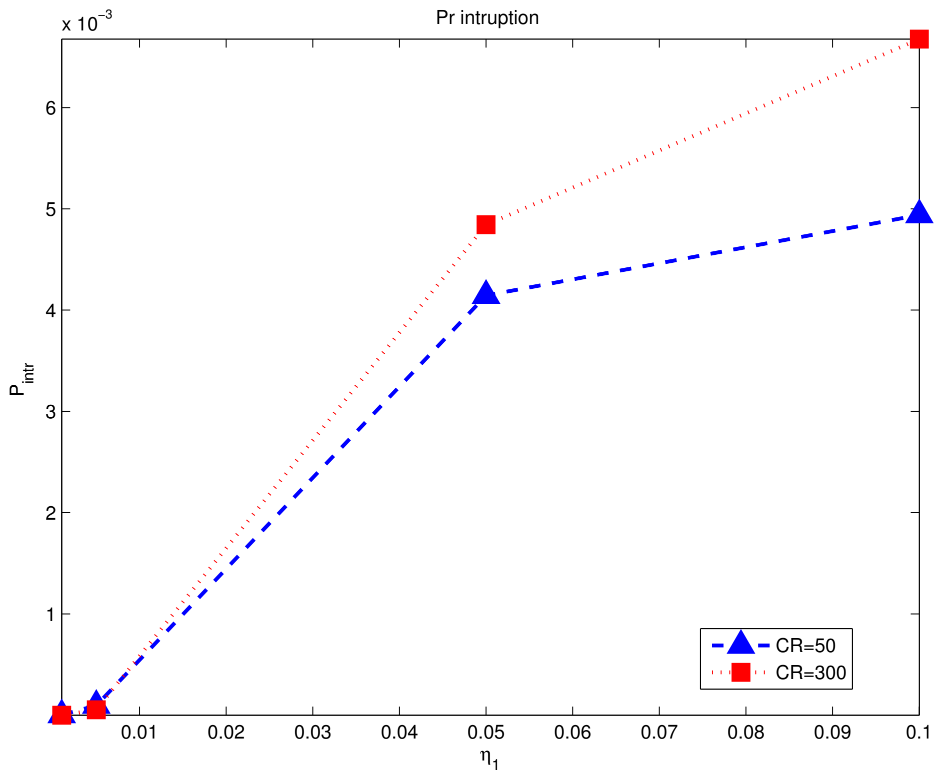

Figure 5.20: Probability of CR link interruption for SO-DSM using different values of η_1. Probability of CR link interruption.

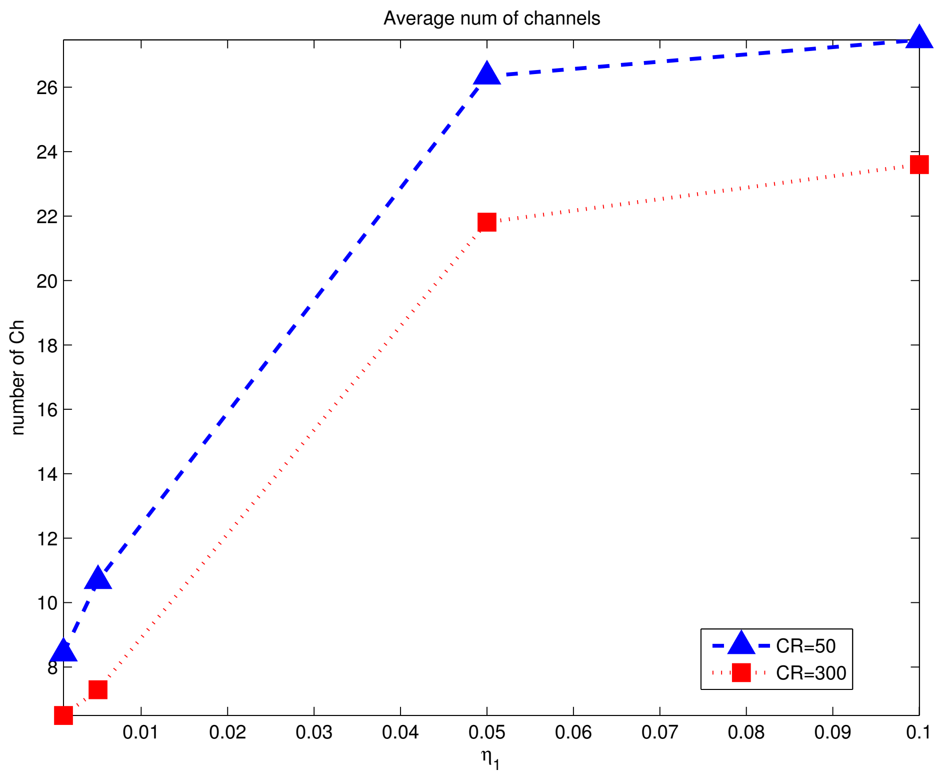

Figure 5.21: The simulation results for SO-DSM using different values of η_1. Average number of sub-bands used by CRs.

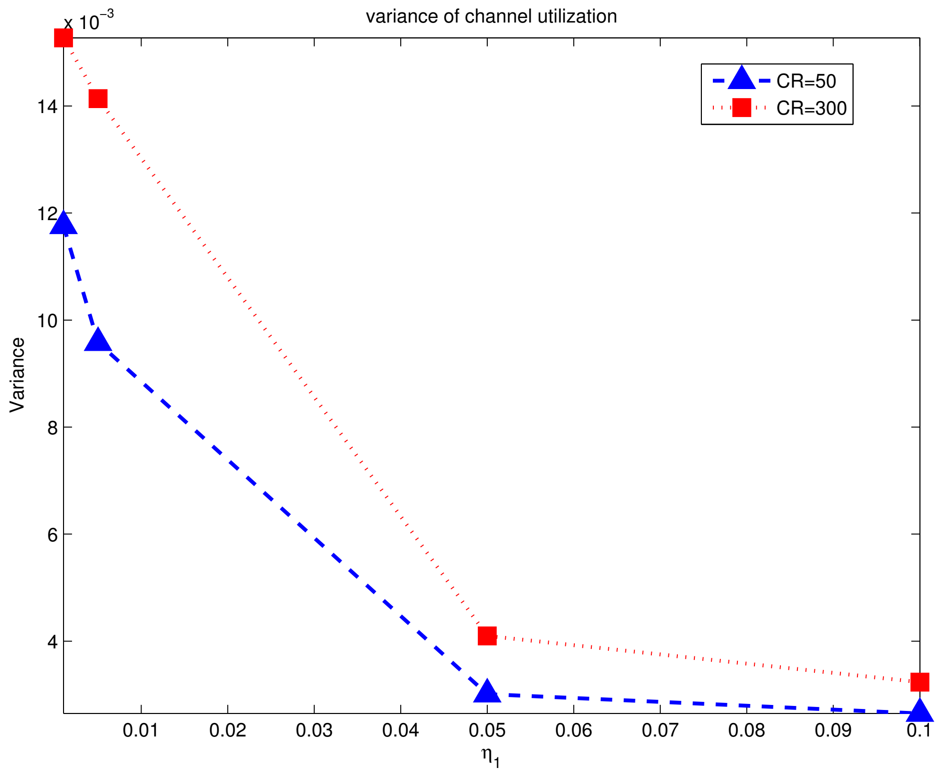

Figure 5.22: The simulation results for SO-DSM using different values of η_1. Average variance of CR sub-band utilization distribution.

Parameter	Value
N_{PU}	80
η_1	0.05
D_{RSA}	1
β_1	0.6
β_2	0.1
PUs (μ_1, μ_2)	(0.01,0.05)
CRs (μ_1, μ_2)	(0.1,0.1)

Table 5.18: SO-DSM parameters used in η_2 simulations.

5.5.0.2 Learning-rate Parameter η_2

The next set of simulations demonstrate how the emergent behaviour of CR network changes by changing η_2. The system parameters used in simulations are listed in Table. 5.18.

Figures 5.23 and 5.25 show the CR network spectrum utilization efficiency, probability of PU collision and probability of CR link interruption for various values of η_2. For a very small value of η_2, the CR sub-band assignment becomes more static and learns and evolves by time more slowly. Therefore, it demonstrates an emergent behaviour close to a random selection of sub-bands, i.e. higher spectrum efficiency and also, higher probability of collision and interruption. Figures 5.26 and 5.27 show the mean and variance of the sub-band distribution in the CR network. These figures demonstrate that by increasing η_2, the sub-band assignment organization becomes more dynamic and variance slightly decreases while the average number of used sub-bands approximately remains constant.

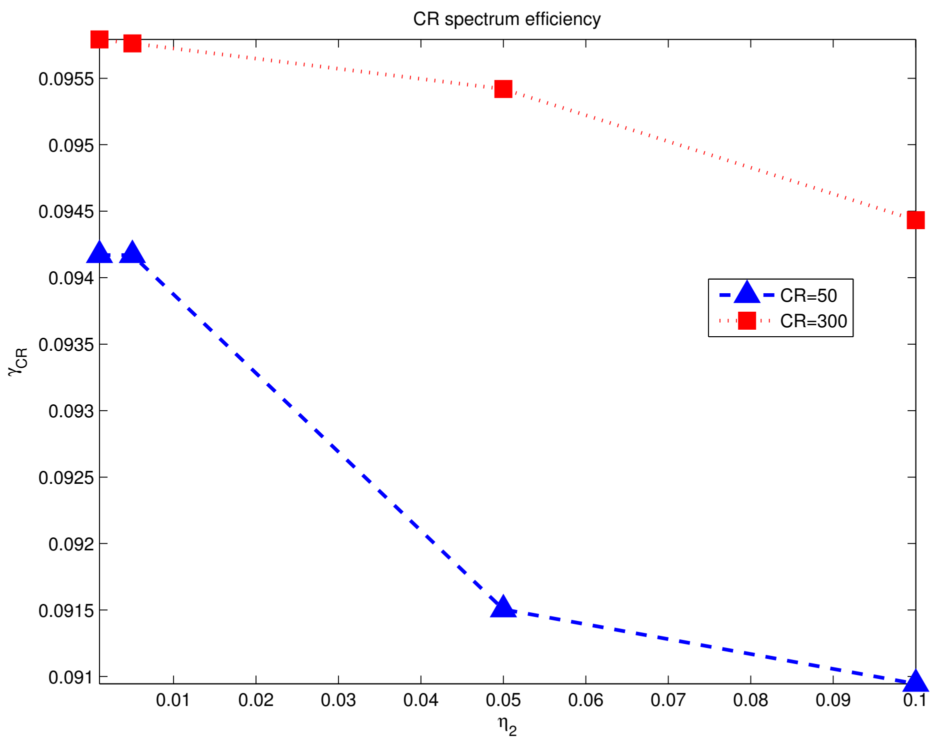

Figure 5.23: The simulation results for SO-DSM using different values of η_2. CR network spectrum utilization.

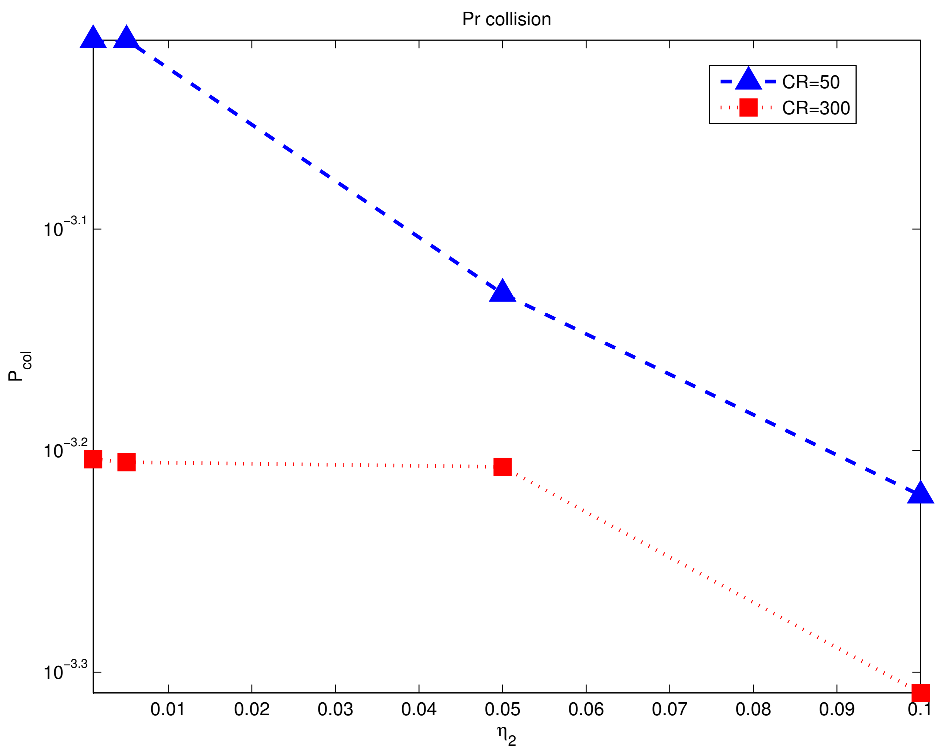

Figure 5.24: The simulation results for SO-DSM using different values of η_2. Probability of collision for PUs.

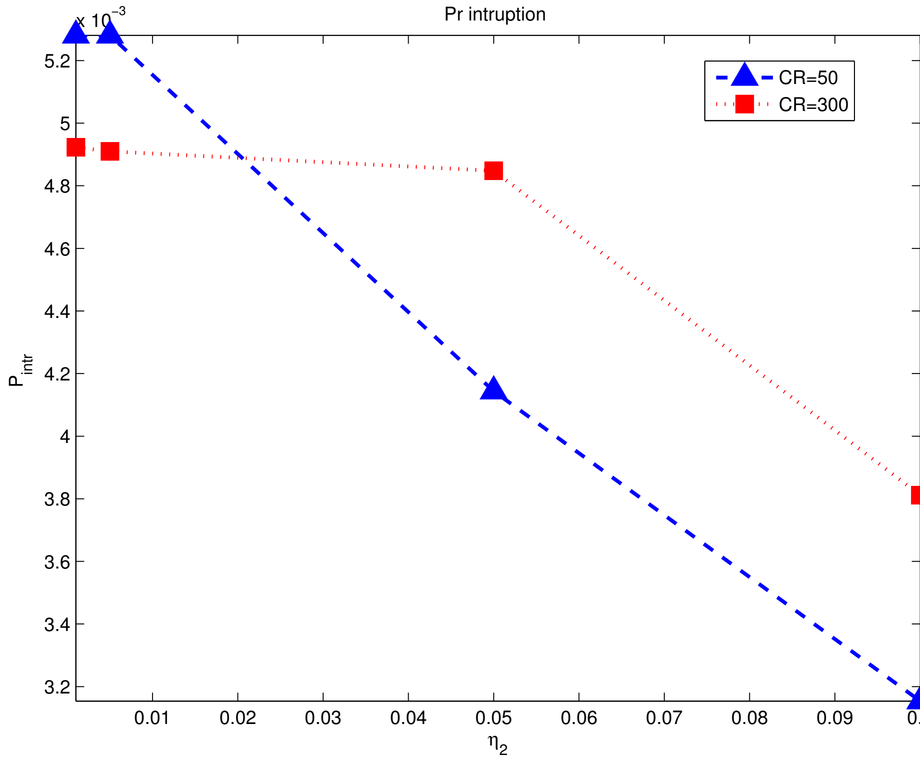

Figure 5.25: Probability of CR link interruption for SO-DSM for different values of η_2. Probability of CR link interruption.

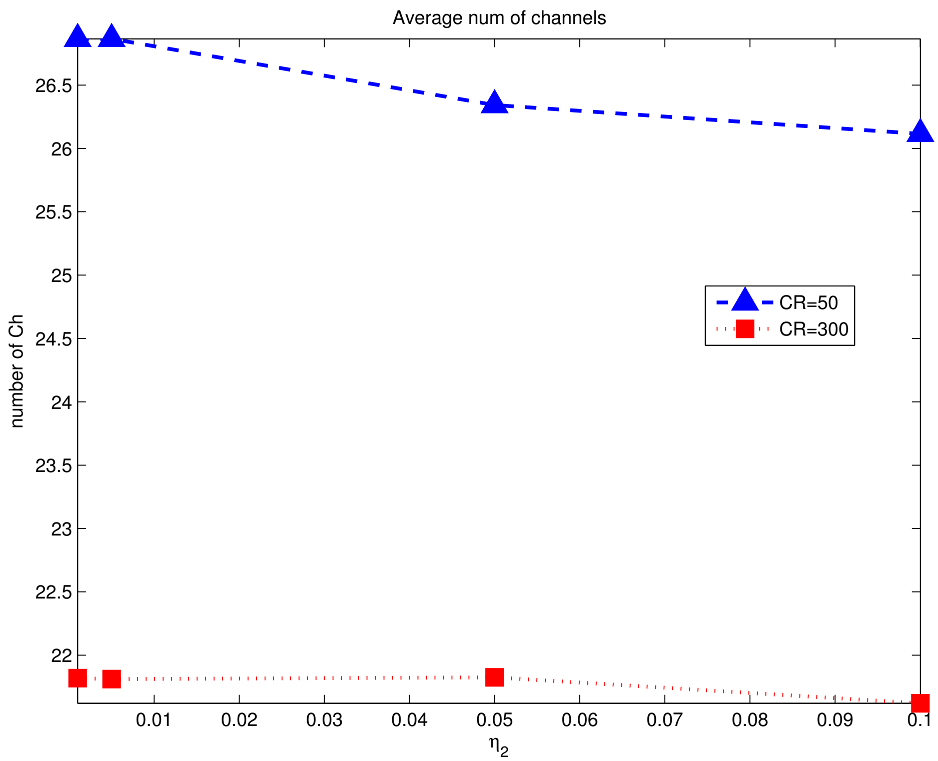

Figure 5.26: The simulation results for SO-DSM using different values of η_2. Average number of sub-bands used by CRs.

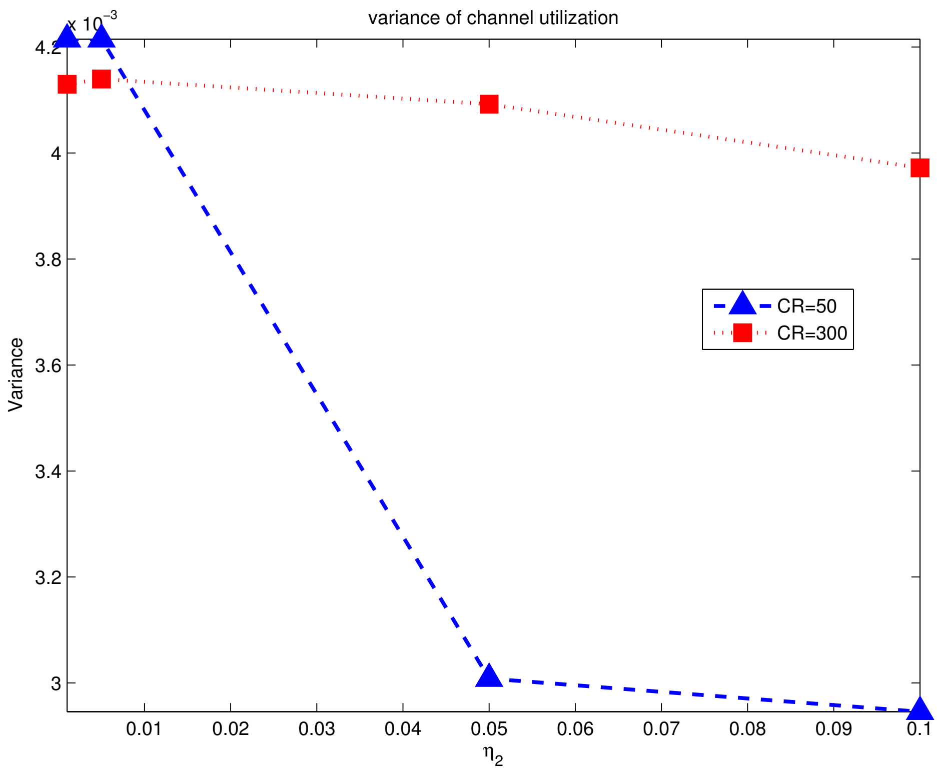

Figure 5.27: The simulation results for SO-DSM using different values of η_2. Average variance of CR sub-band utilization distribution.

Parameter	Value
N_{PU}	80
η_1	0.005
η_2	0.05
D_{RSA}	1
β_2	0.1
PUs (μ_1, μ_2)	(0.01,0.05)
CRs (μ_1, μ_2)	(0.1,0.1)

Table 5.19: SO-DSM parameters used in β_1 simulations.

5.6 Quality Level Signal Parameters

In the last set of simulations, the SO-DSM CR network is simulated for various values of β_1 and β_2.

5.6.1 Parameter β_1

The CR network using SO-DSM is simulated for different values of β_1. The system parameters used in the simulations are listed in Table. 5.19. The results are shown in Figs. 5.28- 5.32. As these figures show, increasing β_1 results in increases spectrum utilization, however, simultaneously probability of interruption and collision increases. As explained in Sec. 4.3.3, a more separation between β_1 and β_2 increases the self-amplification of the Hebbian learning and helps formation of the SOM. Figures 5.31 and 5.32 shows the mean and variance of sub-band utilization distribution of SO-DSM. These figures confirm that the formed SOM becomes more dynamic by increasing β_1.

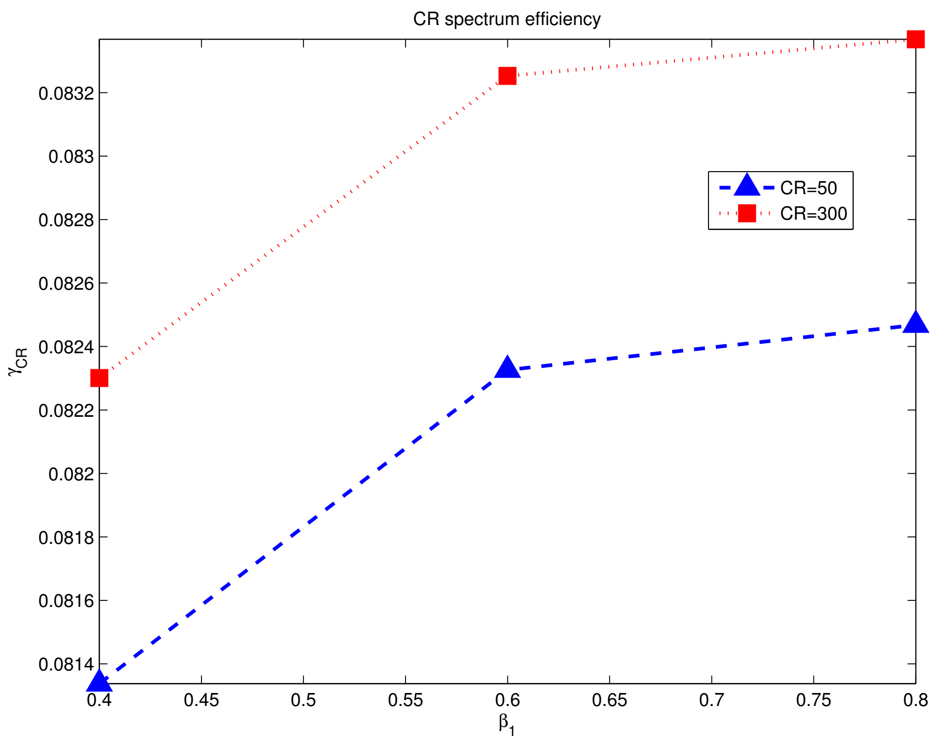

Figure 5.28: The simulation results for SO-DSM using different values of β_1. The CR network spectrum utilization.

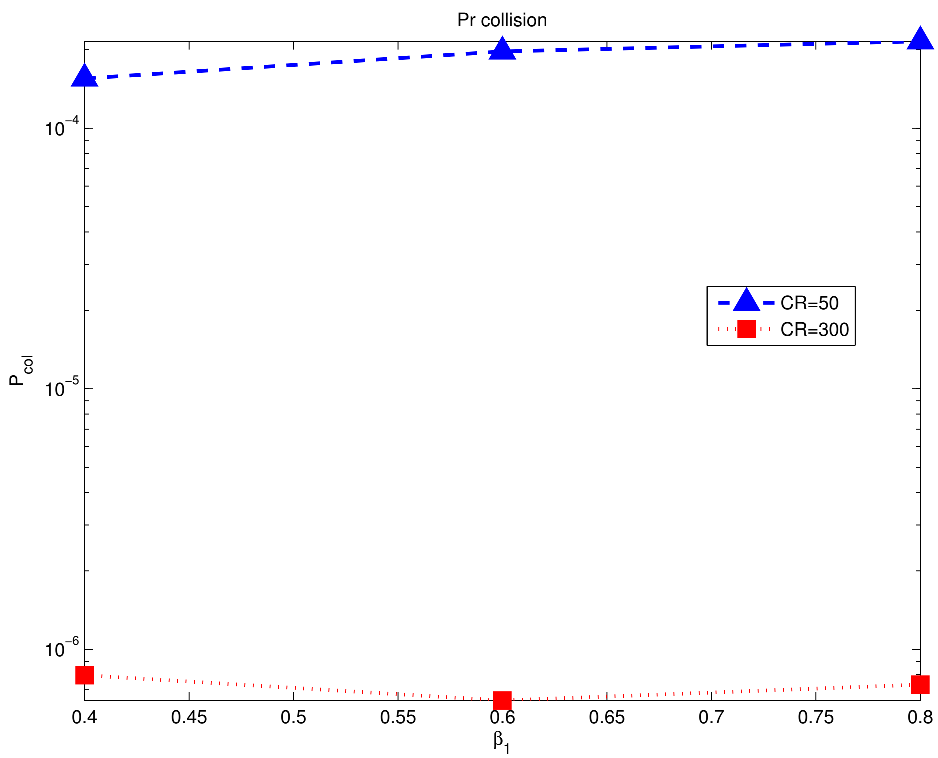

Figure 5.29: The simulation results for SO-DSM using different values of β_1. Probability of collision for PUs.

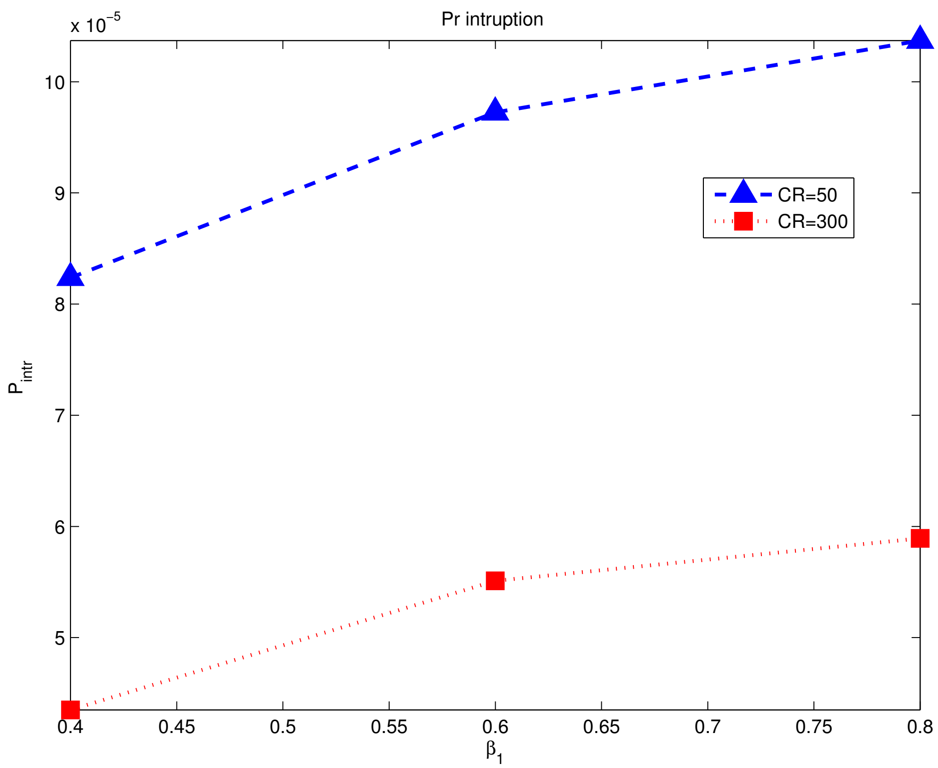

Figure 5.30: Probability of CR link interruption for SO-DSM using different values of β_1.

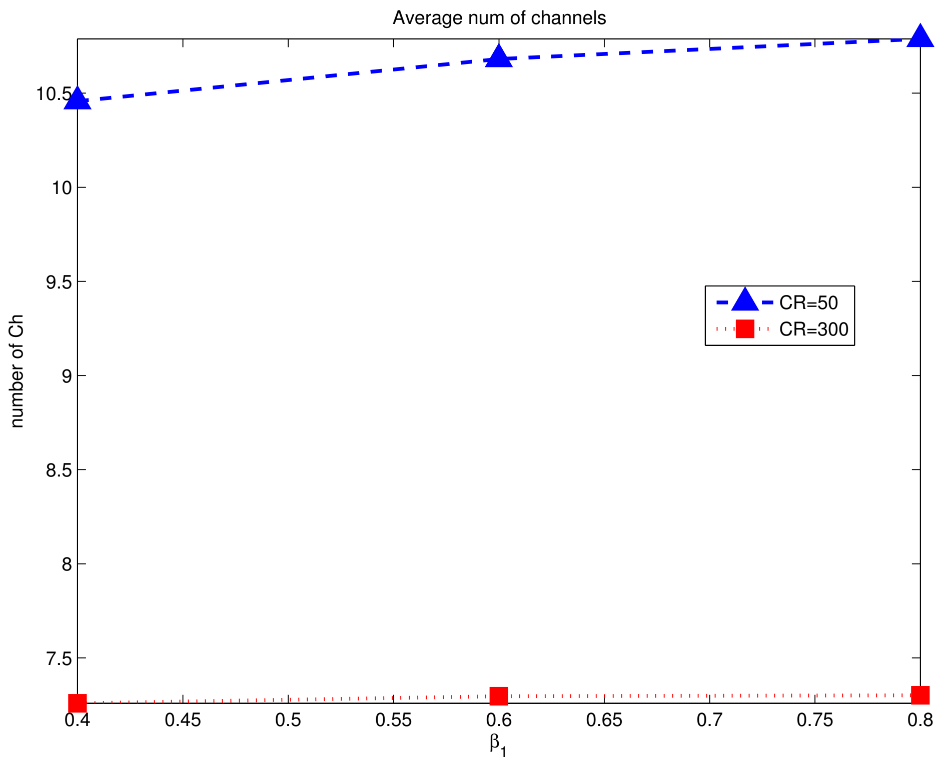

Figure 5.31: The simulation results for SO-DSM using different values of β_1. Average number of sub-bands used by CRs.

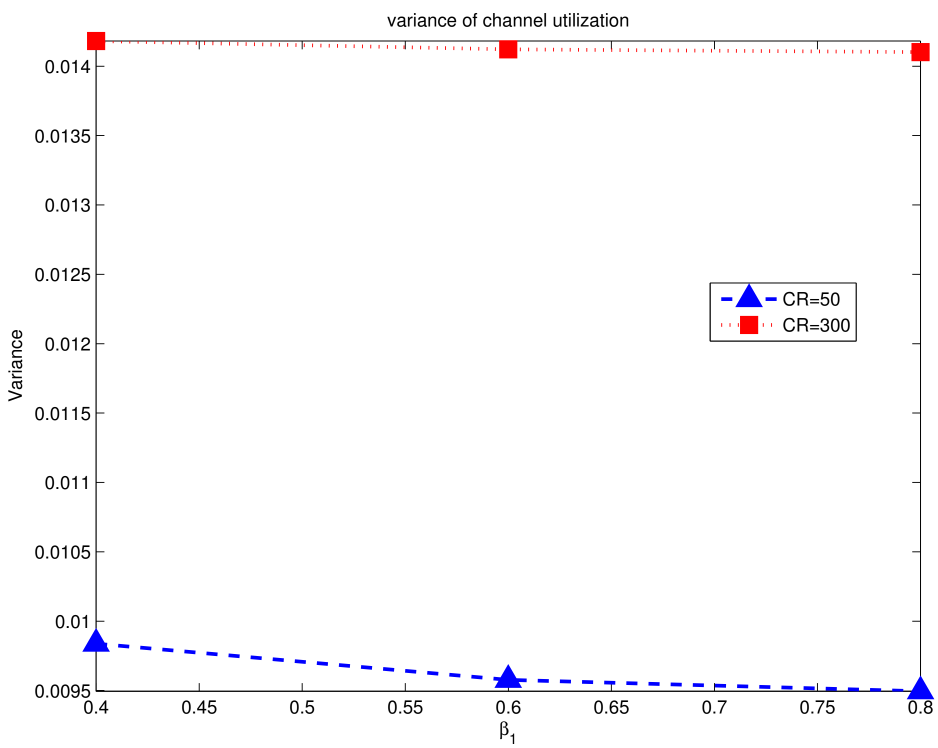

Figure 5.32: The simulation results for SO-DSM using different values of β_1. Average variance of CR sub-band utilization distribution.

Parameter	Value
N_{PU}	80
η_1	0.005
η_2	0.05
D_{RSA}	1
β_1	0.6
PUs (μ_1, μ_2)	(0.01,0.05)
CRs (μ_1, μ_2)	(0.1,0.1)

Table 5.20: SO-DSM parameters used in β_2 simulations.

5.6.2 Parameter β_2

In the last round of simulations, the CR network is simulated with various values of β_2. The system parameters used in the simulations are listed in Table. 5.20. The simulation results are illustrated in figures 5.33- 5.37. As shown in the figures, these results also confirm that more separation between β_1 and β_2 improves the dynamics of the SOM. As β_2 increases, and therefore gets close to β_1, the spectrum utilization of the CR network decreases. Consequently, the probability of collision with PUs and interruption in CR links decreases. Figures 5.36 and 5.37 illustrates the mean and variance of sub-band distribution. As this figure shows, a smaller β_2 results in a more dynamic system.

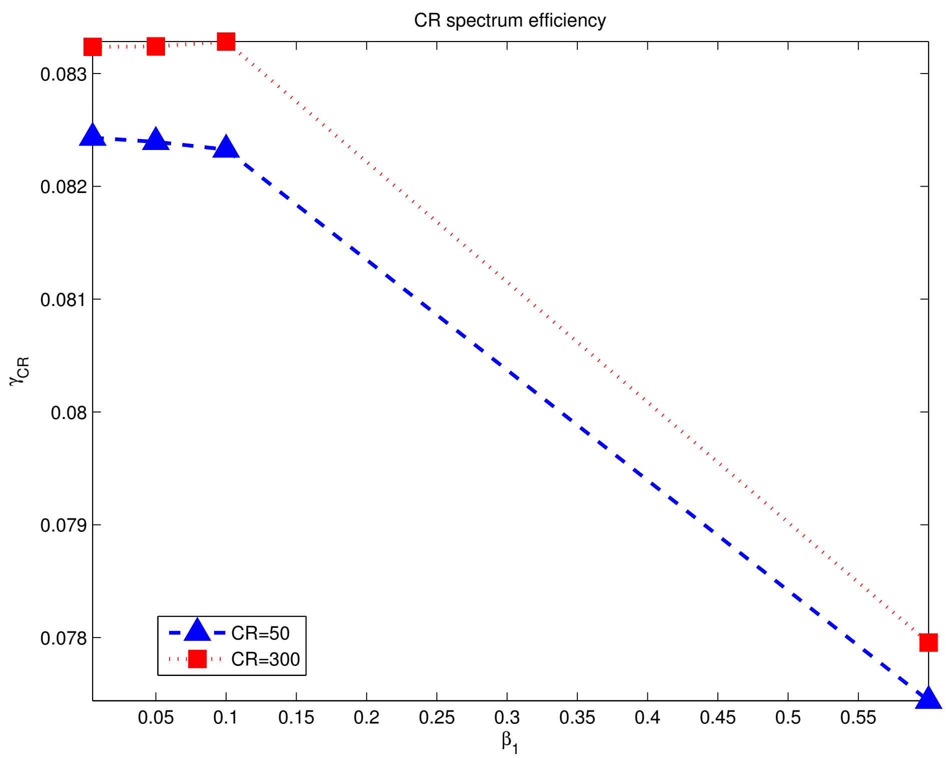

Figure 5.33: The simulation results for SO-DSM using different values of β_2. The CR network spectrum utilization.

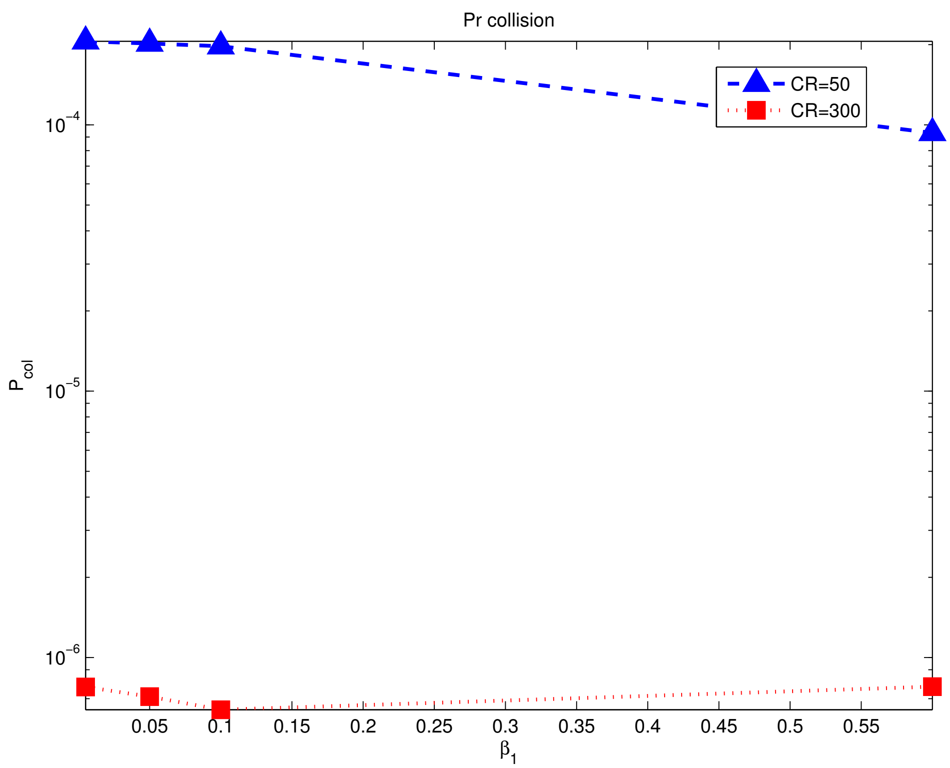

Figure 5.34: The simulation results for SO-DSM using different values of β_2. Probability of collision for PUs.

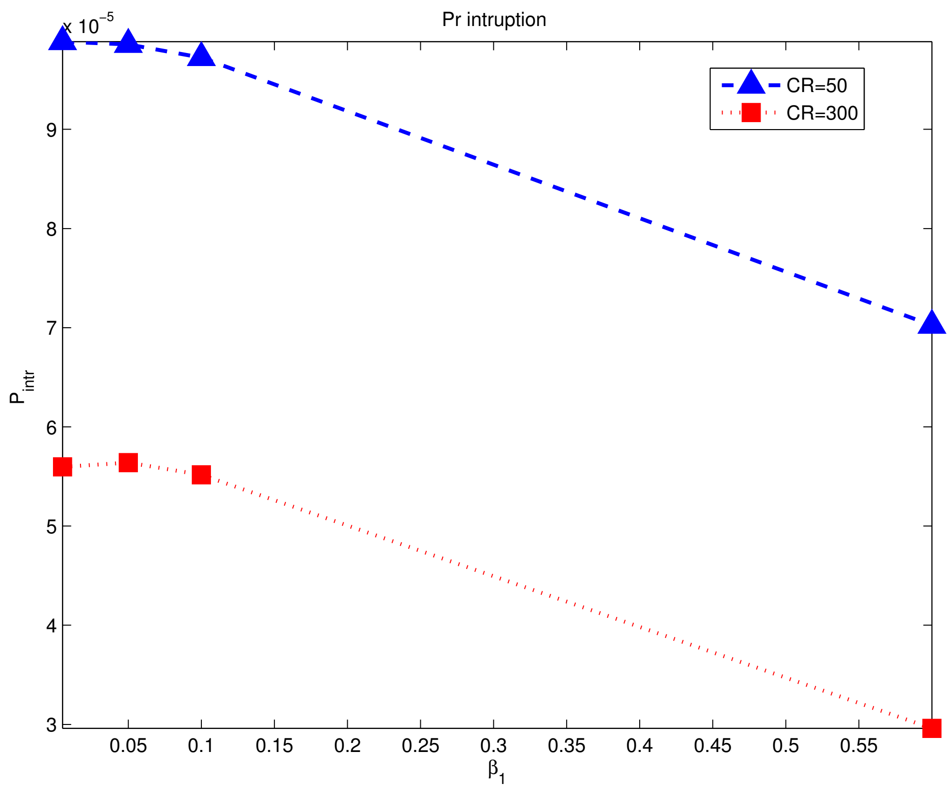

Figure 5.35: Probability of CR link interruption for SO-DSM using different values of β_2.

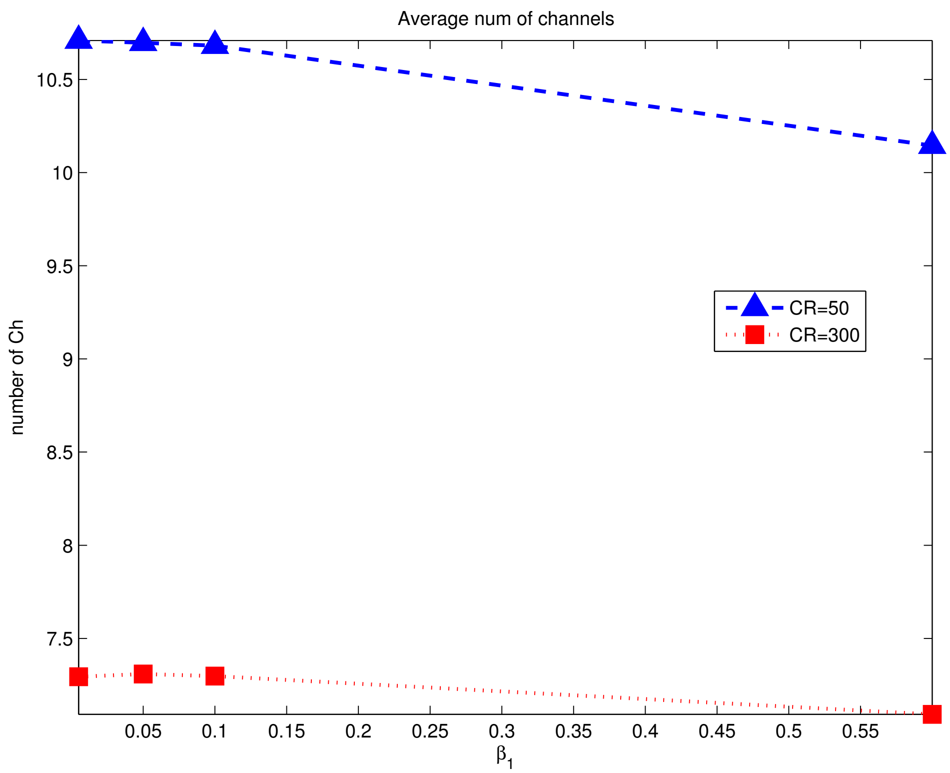

Figure 5.36: The simulation results for SO-DSM using different values of β_1. Average number of sub-bands used by CRs.

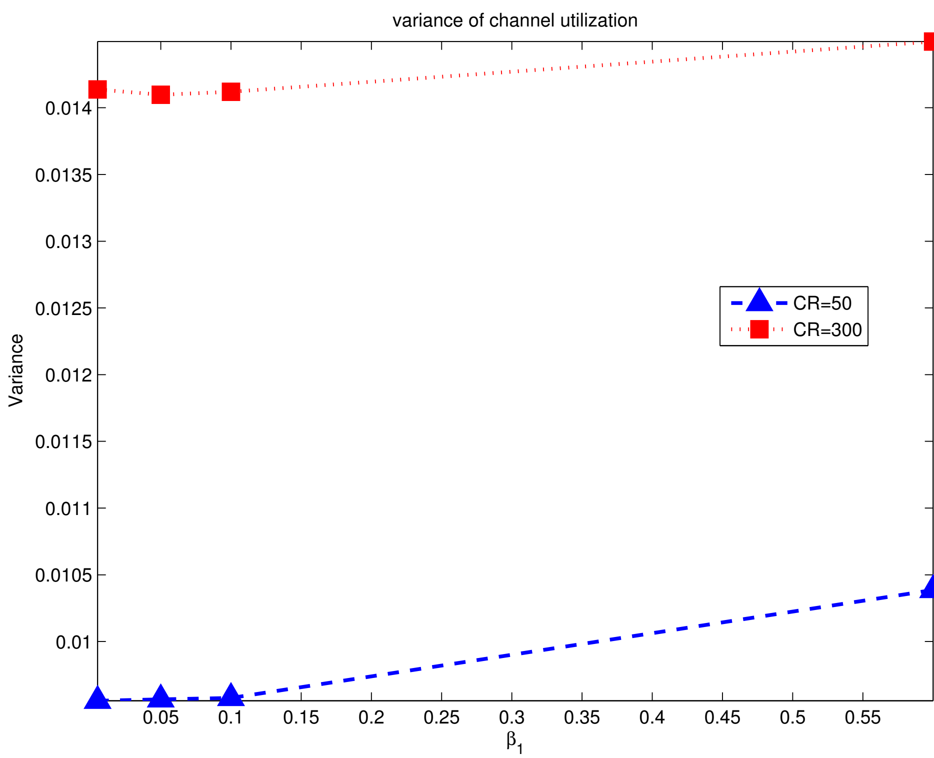

Figure 5.37: The simulation results for SO-DSM using different values of β_2. Average variance of CR sub-band utilization distribution.

5.7 Summary

In this chapter, large scale simulations were conducted to study the emergent behaviour of CR network and results where presented for CR network using three different DSM schemes, namely SO-DSM, CDSM and MG-DSM. The simulation setup having four cells for PUs was explained. All simulations were performed for two cases of CR numbers, namely 50 that represents a low density network and 300 that represents a high density CR network. The simulation results confirmed that having more CRs in the network improves the SO-DSM learning process and CRs can avoid collision with PUs more successfully.

In the first set of simulations, the SO-DSM system was compared to a MG-DSM system. The results showed that the SO-DSM achieves lower spectrum efficiency. However, the probability of collision with PUs and CR link interruption are significantly lower in the SO-DSM case.

In the second set of simulations, a centralized DSM system was compared to the SO-DSM. The results confirms that the centralized scheme achieves a higher spectrum utilization than both SO-DSM and MG-DSM. However, using CDSM, the CR link experience a much higher interruption and collision with PUs.

The results show that using SO-DSM, the CR network provides much more reliable links for CR units. Furthermore, the main objective in designing CR networks is minimizing (ideally avoiding) collisions with PUs and also minimizing the imposed interference on PUs' links. The SO-DSM achieves both objective and decreases the received interference by PU links and probability of collision with PUs significantly by trading off a relatively small amount of spectrum efficiency.

The emergent behaviour of the CR network depends on the SO-DSM systems parameters. Simulations results were presented to demonstrate the effect of each parameter on the network's emergent behaviour.

6

Robustness

6.1 Robustness

Much too often in the literature, optimality is considered as the driving force for obtaining the best performance possible. When considering small-scale applications or applications in a static environment, such an objective may well work satisfactorily. However, when the application of interest is of a complex or large-scale kind and/or the environment is highly dynamic, exemplified by a cognitive radio network, we find ourselves confronted with a much more pressing system requirement: robustness.

Most, if not all, control design strategies exemplified by dynamic spectrum manager, are based on the selection of a model for the plant, a generic term used to describe part of a dynamic system that is supposed to be controlled. Selection of the model is influenced by mathematical tractability and prior knowledge that we may have about the plant. Unfortunately, no matter how hard we try and irrespective of all the prior knowledge we may have about the system, there will always be some discrepancy between the actual physical behaviour of the plant and the corresponding behaviour of the hypothetical model. The response produced at the output of the plant due to a prescribed input signal is determined by the underlying physics of the plant. On the other hand, when the corresponding behaviour of the plant is considered, the response of the model due to the same input signal deviates invariably from the actual response of the plant due to unavoidable model uncertainty. The challenge in designing the controller is, regardless of all operating conditions that are likely to arise in practice, to make sure that the errors are kept small enough to be acceptable from an operational viewpoint.

6.1.1 Optimality-Robustness Dilemma

Due to uncertainties in the environment, achieving both robustness and optimality in adaptive systems is usually impossible in practice. Therefore, in designing adaptive systems, we face a dilemma between optimality and robustness. If we make a system optimal, it may not be robust. On the other hand, if we make it robust it is highly likely sub-optimal. This interplay between optimality and robustness leads us to postulate the optimality-robustness dilemma in adaptive systems. This postulate states [108]:

> When working in a nonstationary environment, the optimality of an adaptive system is achieved at the expense of robustness, and vice versa.

From a practical perspective when there is a choice between optimality and robustness, the decision should be made in favour of robustness for obvious practical reasons.

6.2 Robustness of SO-DSM

The SO-DSM is a decentralized DSM scheme that, as explained in Sec. 2.4 and validated by simulation results in Sec. 5.4, it achieves a sub-optimal solution. Thus, we have already accepted sub-optimality in the SO-DSM and in the light of Optimality-Robustness Dilemma, it is highly likely to be robust. Furthermore, the SO-DSM is based on the Tsigankov-Koulakov model [55]. The original model was based on the brain and was validated further by work done by Stryker [56]. We know that the brain is very robust and can handle uncertainty without becoming unstable, therefore, intuitively this model has the elements of robustness.

Robustness is very hard to verify mathematically. There is a lot of literature on robustness, a lot of it is for linear systems [109, 110], but nonlinear systems are hard to verify. What makes verifying the robustness of SO-DSM even harder is the fact that the CR network is also very complex and is a system of systems. In this problem we are dealing with a complex nonlinear system which is a system of systems. Therefore, we can not take the analytical approach to robustness for this problem. The most sensible way to justifying it is to use Monte-Carlo simulations.

6.3 Simulation Results

In order to perform Monte-Carlo simulations for validating robustness of SO-DSM, we perturb environment parameters and study the system behaviour. In order to have a robust system, a bounded perturbation in system parameters must result in a bounded fluctuation in the system output. In the SO-DSM system, there may be two sources of perturbations:

- **initial state:** The initial state of the radio units is not known to CR units. Therefore, for a particular configuration of the wireless network, the SO-DSM must result in consistent behaviour for any initial state.

- **change in PUs' parameters:** Another source of perturbations in this system is change of PU's parameters. CR units may have a estimation of PU's parameters which can be inaccurate. Furthermore, as discussed in Chp. 4, these parameters are changing slowly by time. Thus, the SO-DSM must be robust against perturbations in PU's parameters.

Two sets of simulations are performed for these two sources of perturbations. In each simulation, the fluctuations in the system output are measured and presented through two lines, one of which represents the minimum value measured and the other one represents the maximum value measured. The area between these two lines in the fluctuations in the output as a result of perturbations in the input.

6.3.1 Initial State

In the first round of simulations, the CR network is simulated using SO-DSM for various different initial state of the system. The location of radio units are the same in all simulations and the only difference between each set is the different initial state. The system parameters used in simulations are listed in Table. 6.1. Two sets of simulations were performed, in the first set 50 CR units were used and in the second set 300 CR units were used in simulations.

The simulation results are presented in Fig. 6.1- 6.7. As these figures show, perturbing the initial state has resulted in bounded fluctuations in the system output. These results show a noticeable difference between fluctuations for CR=50 case with CR=300 case. In all figures, we see more fluctuations in the CR=50 case which is the result of less information obtained from the environment. As it was discussed in Chp. 4, the information sharing of CR units results in an improved learning process. These results confirms that having more CR units in environment, CR units obtain a more precise image of their environment and the CR network become more robust.

Parameter	Value
η_1	0.005
η_2	0.05
D_{RSA}	1
β_1	0.6
β_2	0.1
PUs (μ_1, μ_2)	(0.01,0.05)
CRs (μ_1, μ_2)	(0.1,0.1)

Table 6.1: SO-DSM parameters used in random initial state simulations.

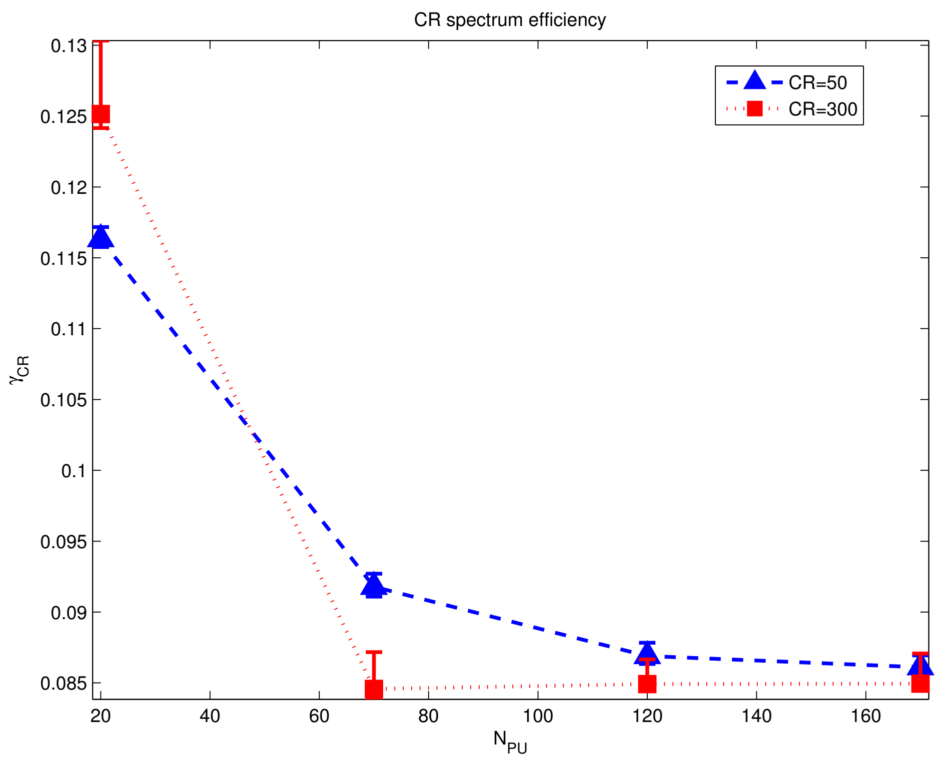

Figure 6.1: The simulation results for random initial state. The CR network spectrum utilization.

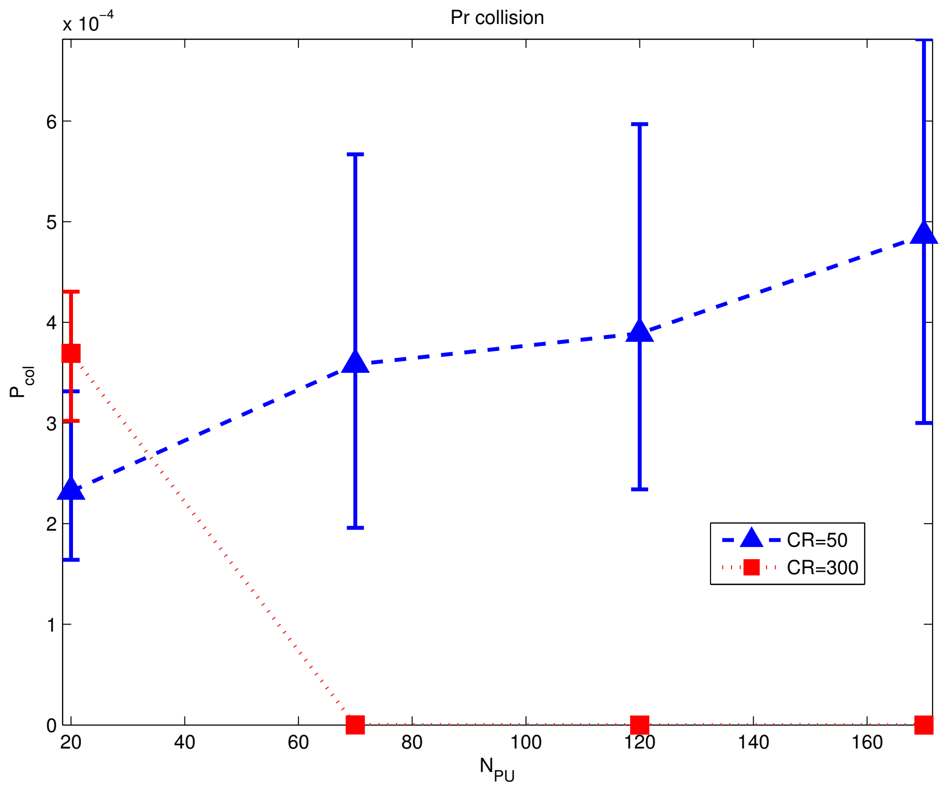

Figure 6.2: The simulation results for random initial state. The Probability of collision for PUs.

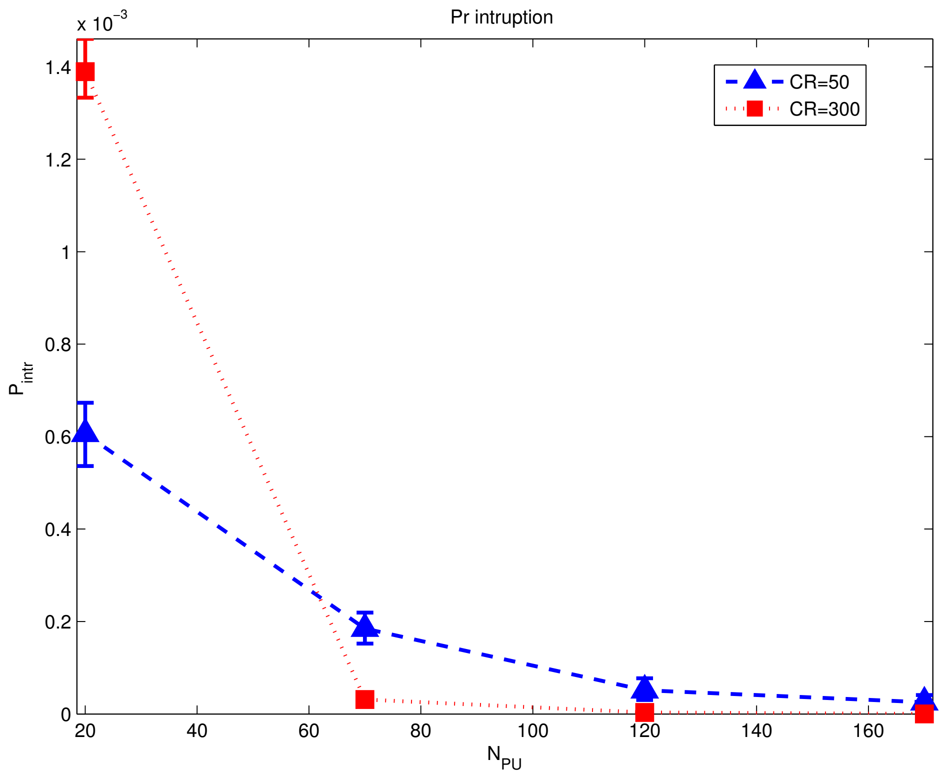

Figure 6.3: The simulation results for random initial state. Probability of CR link interruption.

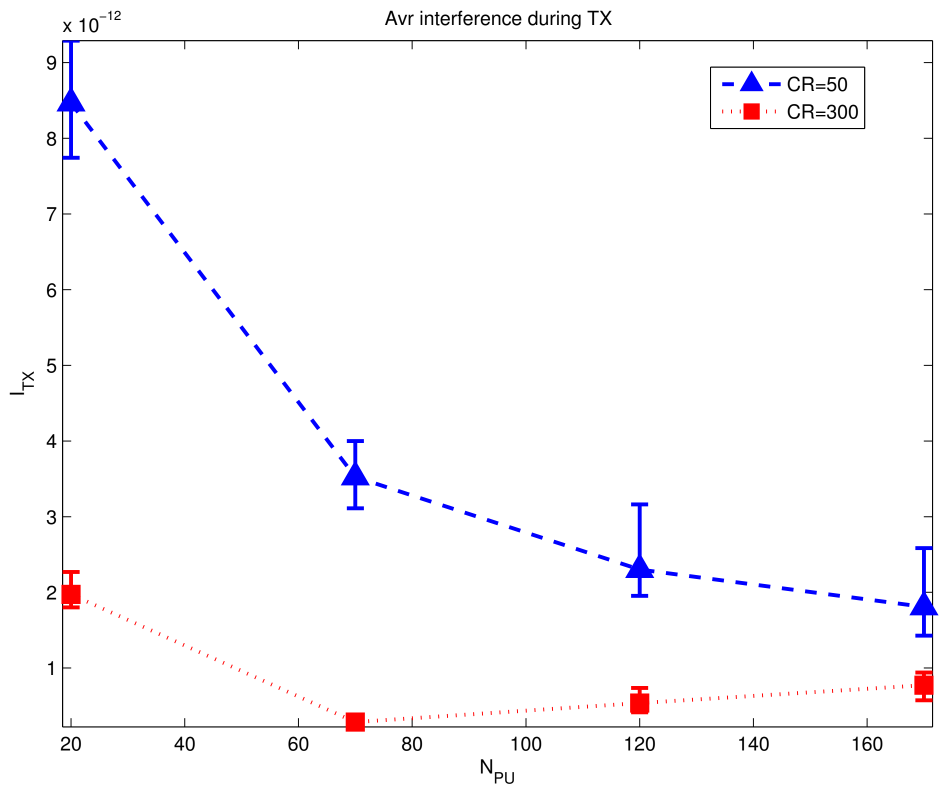

Figure 6.4: The simulation results for random initial state. Average received interference by TX PUs.

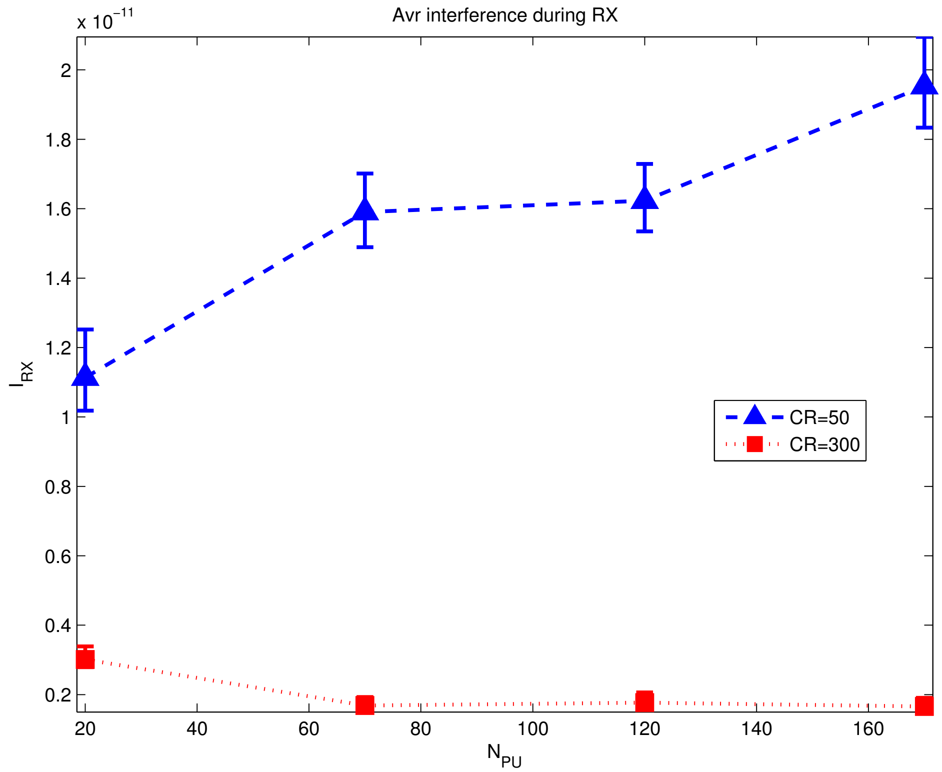

Figure 6.5: The simulation results for random initial state. Average received interference by RX PUs.

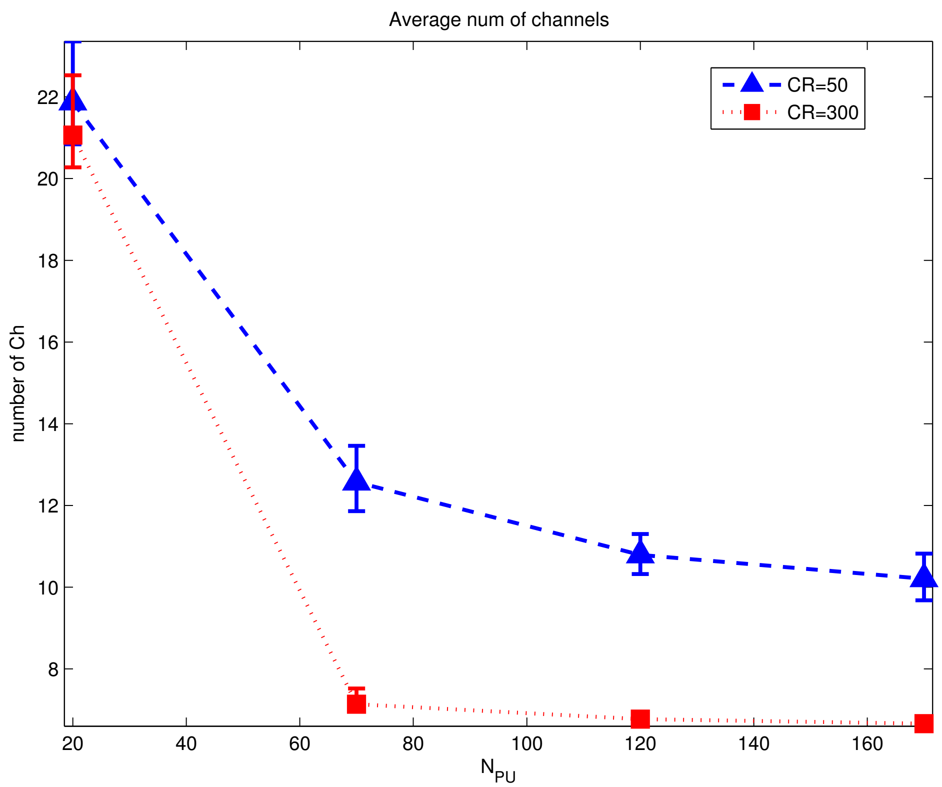

Figure 6.6: The simulation results for random initial state. Average number of sub-bands used by CRs.

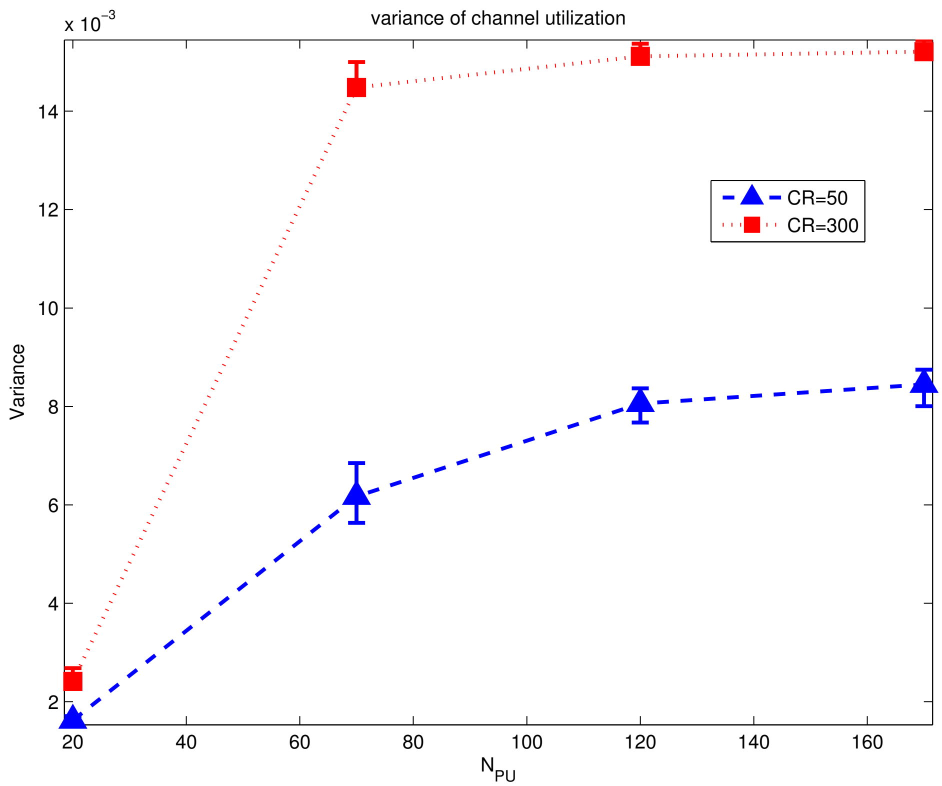

Figure 6.7: The simulation results for random initial state. Average variance of CR sub-band utilization distribution.

6.3.2 Change of PUs Parameters

In the second round of simulations, the PUs' traffic parameters, p_1 and p_2, are perturbed at each time step by adding a normal distributed random variable $\mathcal{X}_{tr} = \mathcal{N}(0, 0.015)$ to them.

The simulation results are plotted in Fig. 6.8- 6.14. The results show that the SO-DSM is also robust against perturbations in PUs' parameters. Similar to the results in the previous section, the fluctuations in the system output is more in the case of CR=50. Therefore, these simulations also confirm that having more CR units in the environment results in the improved learning process and a more robust network.

Parameter	Value
η_1	0.005
η_2	0.05
D_{RSA}	1
β_1	0.6
β_2	0.1
PUs (μ_1, μ_2)	(0.01,0.05)
CRs (μ_1, μ_2)	(0.1,0.1)

Table 6.2: SO-DSM parameters used in noisy PUs' parameters simulations.

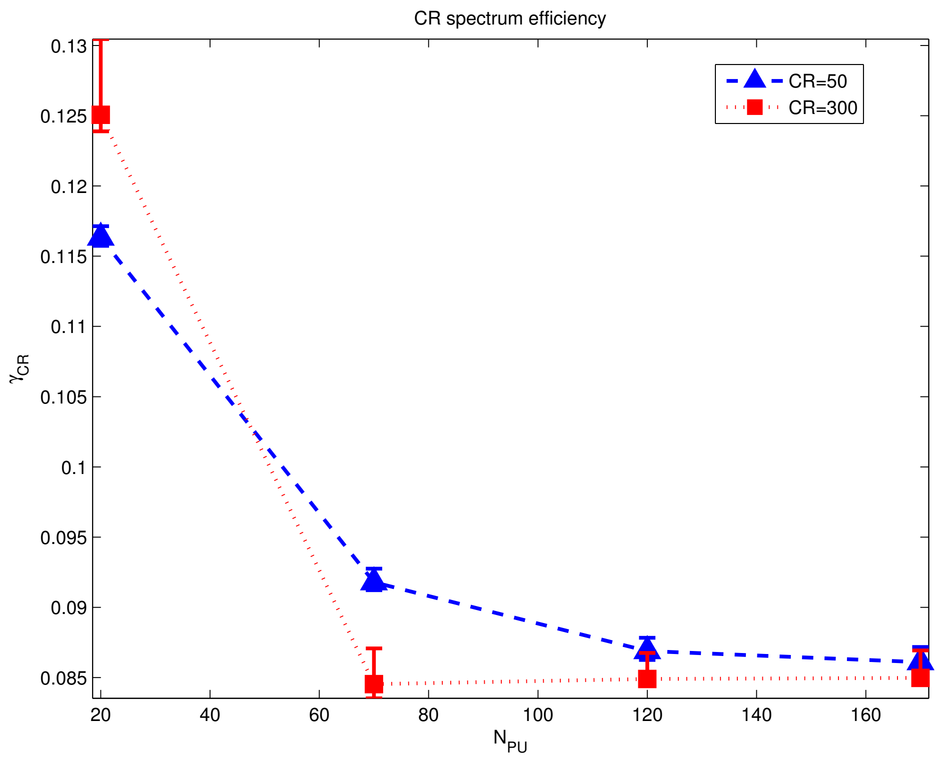

Figure 6.8: The simulation results for noisy PUs' parameters. The CR network spectrum utilization.

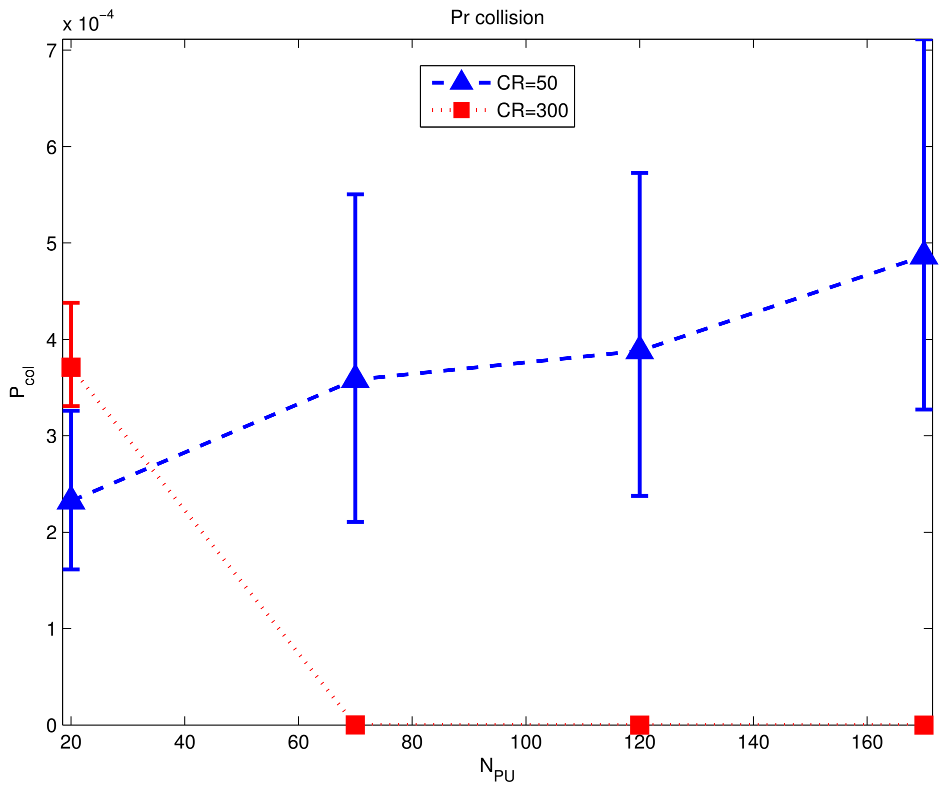

Figure 6.9: The simulation results for noisy PUs' parameters. The Probability of collision for PUs.

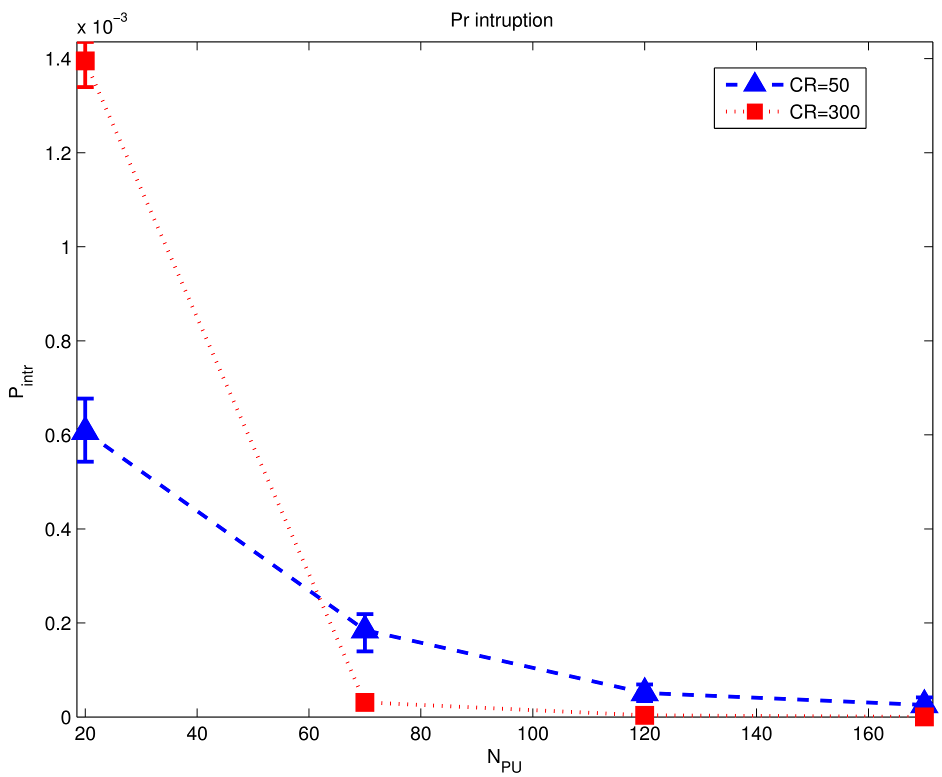

Figure 6.10: The simulation results for noisy PUs' parameters. Probability of CR link interruption.

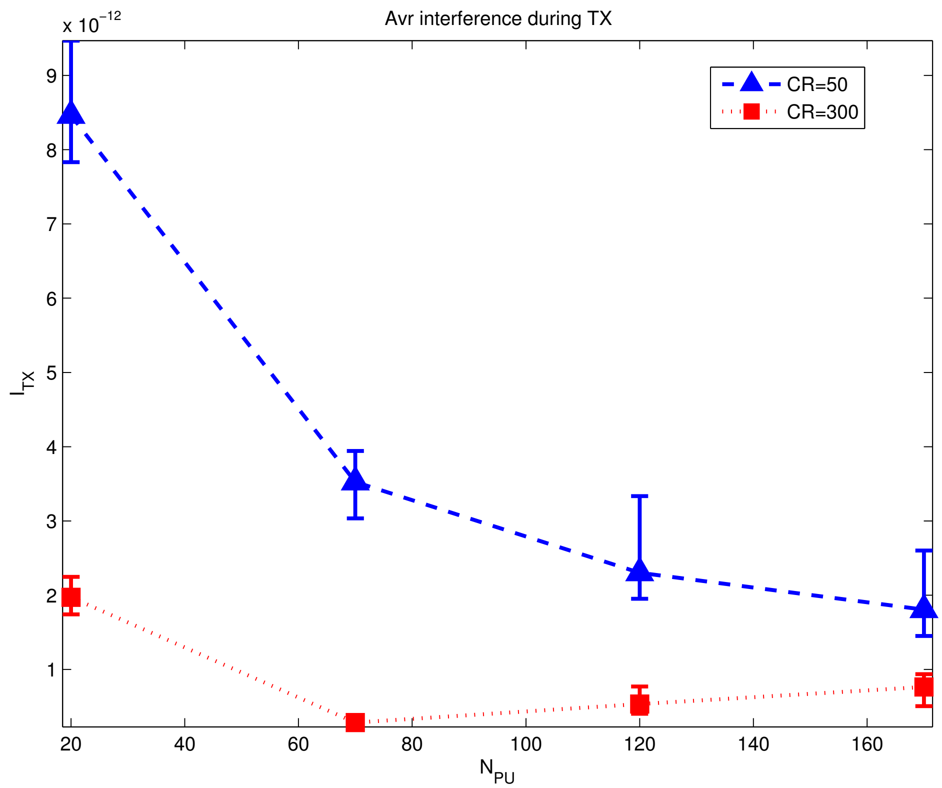

Figure 6.11: The simulation results for noisy PUs' parameters. Average received interference by TX PUs.

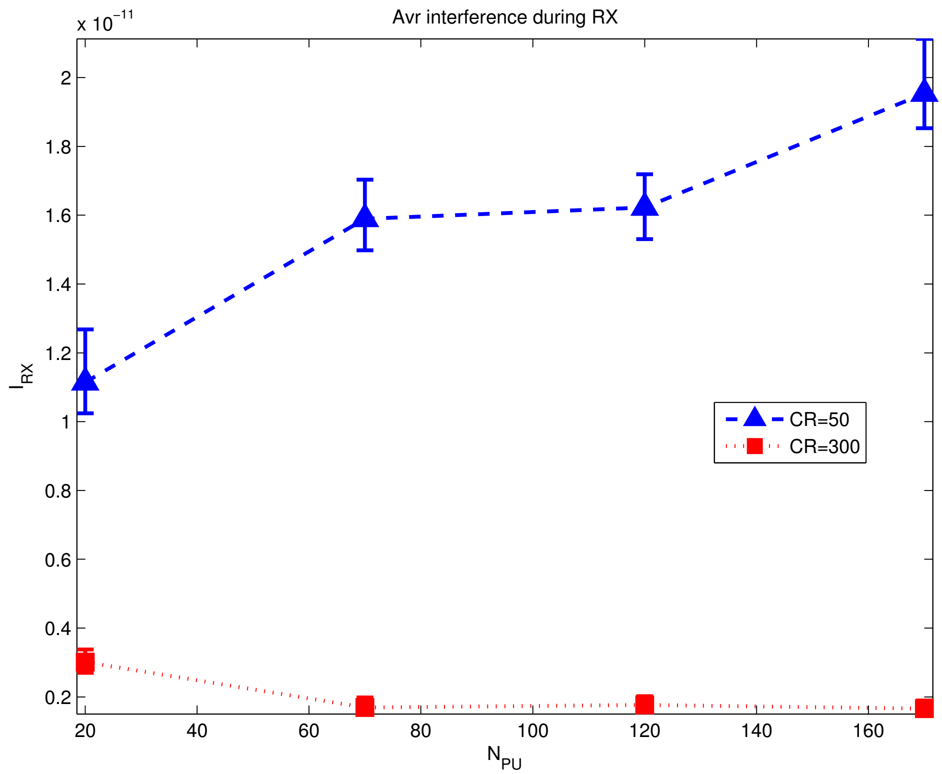

Figure 6.12: The simulation results for noisy PUs' parameters. Average received interference by RX PUs.

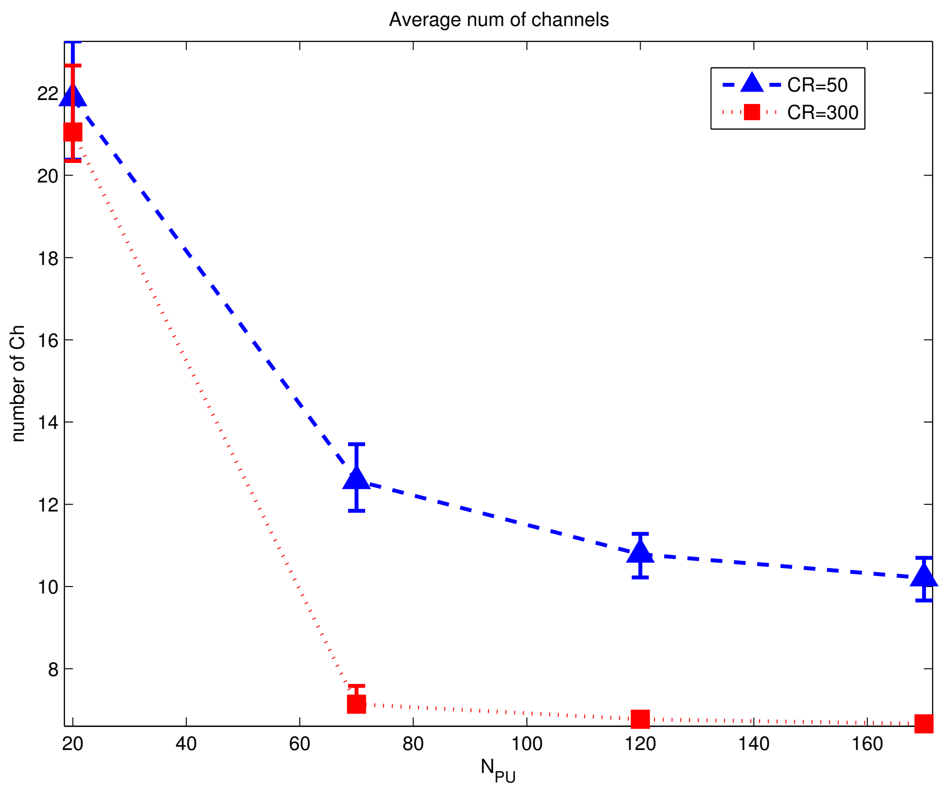

Figure 6.13: The simulation results for noisy PUs' parameters. Average number of sub-bands used by CRs.

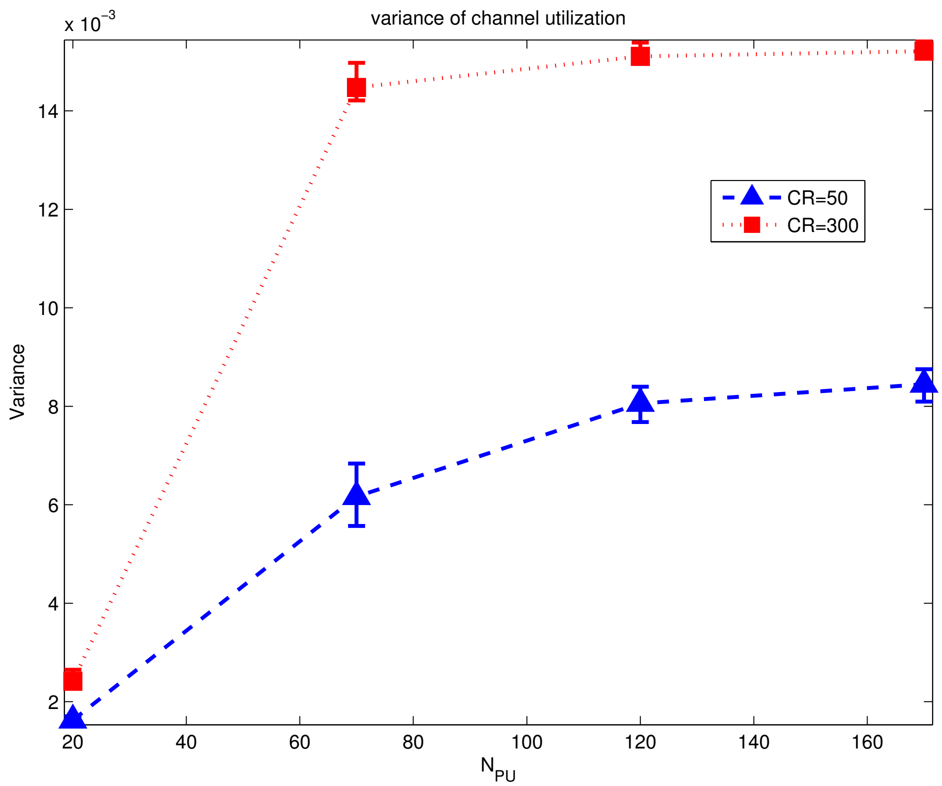

Figure 6.14: The simulation results for noisy PUs' parameters. Average variance of CR sub-band utilization distribution.

6.4 Summary

The concept of robustness and its formal definition were reviewed. Two sources of perturbations in the CR network using SO-DSM were discussed. Large scale simulation results were conducted for each source of perturbation. The results confirm that the CR network using SO-DSM is robust and perturbations have caused bounded fluctuations in the output of the system. Furthermore, the results showed that having more CR units in the environment improves the learning process in CR units by providing them with more information about their environment. Therefore, the SO-DSM is more robust when more CR units are participating in the network.

7

Contributions to the Literature

Research in this thesis was focused on dynamic spectrum management problem in cognitive radio ad hoc networks. A novel decentralized method termed self-organizing dynamic spectrum management was proposed which is the first brain-inspired DSM scheme for cognitive radio. This method embodies an important element of cognition, namely memory and learning. It uses the same learning rule that occurs in the brain and is known to be one of essences of self-organizing maps. The SO-DSM adapts a SOM model developed by Tsigankov and Koulakov [55]; however, our model is adopted for a problem that is entirely different from how the brain does it. Using the SO-DSM scheme, CR units extract the spectrum utilization pattern of PUs and neighbouring CR units and choose sub-bands to match the extracted pattern.

The low complexity of the Hebbian learning rule used in this method and decentralized nature of SO-DSM makes the CR network scalable, using the SO-DSM. Unlike centralized schemes in which complexity of the DSM algorithm depends on total number of radio units, the SO-DSM is a decentralized scheme and its complexity depends on the number of neighbouring CR units and total number of sub-bands. The SO-DSM scheme only converges and builds temporal organization of sub-bands assignments if the CR units are equipped with fast spectrum analyzers that are able to perform radio scene analysis much faster than the change rate of PUs' traffic patterns and physical movements. The MTM [94] method is an example of such a spectrum sensing method that is able to perform spectrum sensing very fast and reliably.

In order to evaluate the SO-DSM scheme, a complex software test-bed has been developed which can simulate a network of CR units along with one or several primary networks. This test-bed measures various critical metrics of the emergent behaviour of a CR network such as spectrum utilization efficiency and probability of collision with primary users. In addition to SO-DSM, this test-bed is capable of simulating CR network having centralized DSM and MG-DSM. Moreover, the test-bed is deployed on Sharcnet parallel computing clusters to run large scale simulations, adding more insight into the information-processing of the SO-DSM.

Simulations were performed using three DSM schemes, namely SO-DSM, CDSM and MG-DSM. The results show that the SO-DSM scheme, using memory and Hebbian learning, was able to decrease the probability of collision with primary users and also probability of CR link interruption compared to CDSM and MG-DSM. The price paid to achieve more robust and stable communications was a decrease in spectrum utilization. However, the decrease in the spectrum utilization efficiency was much lower than the achieved decrease in probability of collision and interruption. The very important requirement of opportunistic CR networks is minimizing (ideally avoiding) collision with PUs. Using SO-DSM, the probability of collision with PUs was decreased significantly.

Furthermore, in this work, the DSM problem in cognitive radio networks was studied and a complete mathematical model of the problem based on graph theory was proposed. Two different methods of spectrum sharing, namely price based and opportunistic, were discussed and compared. Additionally, two approaches, namely centralized and decentralized, were explained and discussed for solving DSM problem in CR networks. Decentralized schemes were identified as the method of choice for solving the DSM problem in CR networks.

To conclude, as complexity is increasingly growing in technology and its applications, self-organization has gained a lot of attention for solving challenging problems. In particular, a self-organized wireless network offers several advantages:

- ease of installation,
- high reliability,
- and low cost,
- robustness.

In this context, cognitive radios – a new frontier in wireless communications – are required to provide reliable communications whenever and wherever needed while decreasing the collision with PU network to ideally zero or at an tolerable level. The SO-DSM is an attractive DSM scheme for CR networks since it is robust, scalable and computationally simple, and can increase the spectrum efficiency while decreasing the collision with primary network. With these attributes in mind, CRs should be self-organized so as to operate in infrastructure-free environments as described in this work.

7.1 Future Directions

Much has been written on cognitive radio as a novel idea for improved utilization of the radio spectrum. Specifically, cognitive radio provides the means for this improved utilization by making it possible for secondary (cognitive radio) users to access sub-bands of the radio spectrum whenever and wherever the primary (legacy) users are not utilizing their sub-bands. It is, therefore, not surprising to find that papers written on cognitive radio have been growing exponentially in number over the past ten years.

A distinctive characteristic of a traditional cognitive radio network is the involvement of two kinds of users [111]:

- Legacy users, who have paid for the employment of specific sub-bands and therefore have the right to use those sub-bands whenever and wherever they are needed for their own use.

- Secondary users, who are opportunistic in the sense that they continually monitor the radio spectrum so as to identify underutilized sub-bands whenever and wherever they become available.

Accordingly, the dynamics of a cognitive radio network may be viewed as a double-layer system of systems [35]. Another way of viewing such an environment is that of a "master-slave" kind of relationship, where the legacy users are the masters of the network and the secondary users are its slaves.

7.1.1 Beyond Traditional Cognitive Radio

Cognitive radio can increase spectrum utilization efficiency by exploiting spectrum holes available in the environment and therefore, it can be inferred that applicability of cognitive radio will be confined to localized areas through short range communication links. Furthermore, as the availability of spectrum holes is not always guaranteed, it should be used as a complementary technology to other systems to increase system capacity whenever spectrum holes are available. We can therefore imagine two paths for cognitive radio to find real world applications in future:

1. Cognitive short range ad hoc networks.

2. Cognitive femtocells.

7.1.1.1 Cognitive Ad Hoc Networks

There is a growing demand for high speed short range point to point communication links. Several new electronic devices and applications now require to connect to other devices and transfer high amount of data. For example, users may want to play a high definition video clip from their iphone on the TV through a wireless link. The current 802.11 standard which operates on unlicensed band may soon not be able to cater this demand due to low efficiency and also increased traffic on this limited band. Therefore, one of the potential applications of cognitive radio is high speed short range point to point communications. Cognitive radios will use spectrum holes for such short range links whenever possible. When no spectrum holes is available, links will use only unlicensed band. This application of CR is very beneficiary for consumers because will improve their communication links when spectrum holes are available. On the other hand, service providers have no interest in this application unless they provide a service that also uses unlicensed band. This application of CR faces two challenges which needs to be addressed:

- requires fast and reliable spectrum sensing because legacy users are not collaborating with CRs.
- fairness between CRs.

7.1.1.2 Cognitive Femtocell

For cognition to impact the world of wireless communications at the global level, the principles of cognition will have to be applied to wireless networks owned by service providers. As such, there will only be one common group of users throughout the network. Indeed, it is here where cognitive principles will be tested in terms of the difference that could be made to the improved utilization of the radio spectrum.

Over and above the advantages to be gained from application of the principles of cognition, the new vision for the world of wireless communications will incorporate a new layer of femtocells dedicated to homes and small offices.

For users, femtocells will provide the following advantages:

- improved indoor reception,
- higher data rates, and
- low power consumption leading to improved battery life.

The network providers will also benefit from the deployment of femtocells through improved spectrum utilization.

For cognitive femtocell networks, to function satisfactorily, we see the following requirements:

- scalability, which can be taken care of through network decentralization,
- stability, and
- heterogeneous coexistence community of different users.

Cognitive femtocells can operate very efficiently because there is no conflict of interest with legacy users in this network. Radio units have the right to use the spectrum and there is a high quality feedback channel through internet between femtocells.

Appendices

A

Minority Game DSM

Minority game theory, originally proposed by Challet and Zhang [112], is a branch of game theory for studying competition and self-imposed cooperation in a non-cooperative game with limited resources. Players in this game usually play with binary strategy set and do not interact or negotiate with each other directly regarding the strategy set. Classical Minority game or the El Farol bar problem was first proposed in [112]. In the bar problem, a group of n persons have to decide independently and at the same time if they want to go to the El Farol bar on Friday night. At each step, a player has binary strategy set: to go or not to go to the bar. Going to the bar is enjoyable only if the bar is not too crowded. Now, if all n players decide not to go to the bar thinking that the bar will be crowded then the bar will be empty. However, if they all decide that the bar will be empty and decide to go, then the bar will be overcrowded.

Minority game (MG) is a class of non-cooperative games [113]. In MG, players are called agents and each agent selects one of two possible actions.

When agents successfully select the minority side where the number of agents selecting an action is less than the number of agents selecting another action, those agents win the game. A number of studies have already applied minority games to resource management in wireless communication systems [114–117]. The MG introduces self-organized behaviour in a decision-making process. It models a situation where belonging to the minority group is desirable.

In MG-DSM, each CR unit keeps the history of each sub-band for the last L_h time steps. When a link is required between two CRs, they select a sub-band based on MG strategy, i.e. they choose the sub-band with lowest activity in the last L_h time steps.

B

Robust Transmit Power Control

There are two primary resources in a cognitive radio network; channel bandwidth and transmit power. The operation of the transmit-power controller is complicated by a phenomenon that is peculiar to cognitive radio communication, namely, the fact that spectrum holes come and go, depending on the availability of sub-bands as permitted by licensed users. To deal with this phenomenon and thereby provide the means for improved utilization of the radio spectrum, a cognitive radio system must have the ability to fill the spectrum holes rapidly and efficiently. In other words, cognitive radios have to be frequency-agile radios with flexible spectrum shaping abilities. The information that transmitter receives through the feedback channel enables it to adaptively adjust the transmitted signal and update its transmit power over desired channels. A set of constraints must be imposed on each user's transmit power in each channel to maintain a limit on the interference produced.

The information capacity of sub-band k, a continuous channel of bandwidth B_k Hz, perturbed by additive white Gaussian noise of power spectral density

$N_0^k/2$ and limited in bandwidth to B_k, is given by

$$C_k = B_k \log_2 \left(1 + \frac{P_k}{B_k N_0^k}\right) \tag{B.1}$$

where P_k is the average transmitted power. However, received interference from other radio units operating on the same band adds to the noise level. Define I_k^i as the sum of received interference in sub-band k at receiver i:

$$I_k^i = \sum_{j \neq i} \alpha^{ij} p_k^j$$

where α^{ij} is the interference gain from transmitter j to receiver i on sub-band k and p_k^j denotes user is transmit power on sub-band k. We the rewrite Eqn. B.1 to include interference as:

$$C_k = B_k \log_2 \left(1 + \frac{P_k}{B_k N_0^k + I_k^i}\right) \tag{B.2}$$

The ratio

$$\frac{P_k}{B_k N_0^k + I_k^i}$$

is called *signal to noise plus interference ratio* (SNIR).

B.1 Iterative Waterfilling Controller (IWFC)

Several key attributes such as distributed implementation, low complexity, and fast convergence to a reasonably good solution, provide an intuitively satisfying framework for choosing and designing resource-allocation algorithms for cognitive radio. In a cognitive radio network, which is an infrastructure-less network, a central scheduling does not exist and also synchronization between the nodes is difficult. Therefore, users update their transmit powers in a totally asynchronous manner. It is with this kind of framework in mind that in [5, 15, 34], the IWFC has been proposed as a good candidate for finding a Nash equilibrium solution for resource allocation in cognitive radio networks. IWFC can be formulated in two ways:

- *Rate-adaptive waterfilling* in which the data rate is maximized subject to a constraint on the maximum allowable transmit power.
- *Margin-adaptive waterfilling* in which the transmit power is minimized subject to a constraint on the minimum acceptable data rate.

This way, the transmit power control problem is formulated as a *game*, where each user acts greedily to optimize its own performance based on local information. In other words, each user adjusts its transmit power based on the measured level of interference at its receiver, which is a measure of the combined effect of all active users in the network plus the environment noise. Hence, IWFC can be implemented without any knowledge about the number of active users in the network and the transmit power of individual users. Therefore, users do not need to communicate with each other to establish coordination between themselves. This tends to reduce the complexity.

When we consider the associated cognitive function of transmit-power control in the transmitter, the issue of prime interest is robustness versus optimality. Due to different uncertainty sources in a cognitive radio network, adjusting the transmit power of a cognitive radio requires solving an optimization problem under uncertainty.

B.2 Dominant Sources of Uncertainty

The dominant sources of uncertainty in a cognitive radio network are:

- *Primary Users:* In a cognitive radio network, spectrum holes come and go, depending on the availability of idle sub-bands. Therefore, primary users' activities are the cause of *supply-side risk*. Communication patterns of primary users determine the availability and the duration of availability of resources. The availability of the spectrum holes determines the joint feasible set of the resource-allocation optimization problems that are solved by individual secondary users. In other words, it determines the joint set of the action spaces of all secondary users in the corresponding game. The availability duration of spectrum holes determines the control horizon for the transmit-power controllers of secondary users. Depending on the sub-bands of interest and the dynamics of activities of primary users in those sub-bands, two different cases are observed:

  a) The activities of the primary users and therefore, their occupancy of the corresponding sub-bands are well-defined. A good example for this case would be the use of TV bands for cognitive radios.

  b) The activities of the primary users and therefore, the appearance and disappearance of spectrum holes are more dynamic and far less predictable than the former case. A good example for this case would be the use of cellular bands for cognitive radios.

- *Secondary Users:* Anytime users can leave the network and new users can join the network in a stochastic manner. This is the cause of *demand-side risk* in the network.

- *Mobility:* Users move all the time. Because of the mobility, the interference that a user causes on other users and mutually the interference that other users cause on that particular user in the network are time-varying.

- *Noise:* The ambient noise depends on different activities in the environment and is caused by both natural and man-made phenomena.

B.3 Dealing with Uncertainty

During the time intervals that the activity of primary users does not change and the available spectrum holes are fixed, two approaches can be taken to deal with the uncertainty caused by joining and leaving of other cognitive radios as well as their mobility; *stochastic optimization* and *robust optimization* [118]. The pros and cons of these two approaches are discussed here.

If there is good knowledge about the probability distribution of the uncertainty sources, then the uncertainty can be dealt with by means of probability and related concepts. In this case, calculation of the expected value will not be an obstacle and therefore, transmit-power control can be formulated as a stochastic optimization problem.

However, since in practice, little may be known about the probability distribution, the stochastic optimization approach that utilizes the expected value is not a suitable approach. In this case, robust optimization techniques that are based on worst-case analysis, without involving probability theory, are more appropriate, although such techniques may well be overly conservative in practice. Suboptimality in performance is, in effect, traded in favour of robustness.

Stochastic optimization guarantees some level of performance on average, and sometimes the desired quality of service may not be achieved, which means a lack of reliable communication. On the other hand, robust optimization guarantees an acceptable level of performance under worst-case conditions. It is a conservative approach because real-life systems are not always in their worst behaviour, but it can provide seamless communication even in the worst situations. Regarding the dynamic nature of the cognitive radio network, the statistics of interference that is used by the transmitter to adjust its power may not represent the real current situation of the network. In these cases, robust optimization is equipped to prevent permissible interference power level violation by taking into account the worst-case uncertainty in the interference and noise. Therefore, sacrificing optimality for robustness seems to be a reasonable proposition. However, the use of a predictive model may make it possible for the user to choose the uncertainty set adaptively according to environmental conditions and therefore, may lead to less conservative designs.

In order to take account of uncertainty in the IWFC formulation, the noise plus interference term is considered as the summation of two components: a nominal term, $\bar{I}$, which is the measured value provided by the receiver, and a perturbation term, ΔI. Then, the transmit power is adjusted based on the worst-interference scenario for ΔI. Therefore, Eqn. B.2 is modified as

$$C_k = B_k \log_2 \left(1 + \frac{\bar{P}_k}{B_k N_0^k + \bar{I}_k^i} \right) \tag{B.3}$$

Thus, for a fixed required data rate, transmitter spends more power than calculated by Eqn. B.2 to mitigate the uncertainties. *Safety power margin* is defined as :

$$S_p = \frac{\bar{P}_k}{P_k} \tag{B.4}$$

which is the ratio of robust transmitter power obtained from Eqn. B.3 to the power calculated from Eqn. B.2.

C

Autoregressive Model (AR)

The autoregressive model is one of a group of linear prediction formulas that tries to predict the output of a system based on the previous outputs. In recent years, the autoregressive models (AR models) are widely used to predict the fading channel state changes [103, 119]. Autoregressive models are commonly used to approximate discrete-time random processes [119]. An AR process of order p, noted by $[AR - p]$, can be expressed by

$$X(K) = -\sum_{j=1}^{p} \phi_k X[k-j] + \omega_k$$

where $X(k)$ and ω_k are the observed sample and noise values at the kth instant. The autocorrelation matrix of $X(k)$, R_{xx}, is defined as

$$R_{xx} = \begin{cases} -\sum_{j=1}^{p} \phi_k R_{xx}[k-j], & k \geq 1 \\ -\sum_{j=1}^{p} \phi_k R_{xx}[-j], & k = 0 \end{cases}$$

And the estimation of R_{xx} is given by

$$\hat{R}_{xx} = \begin{cases} R_{xx}[k], \quad p \geq k \geq 1 \\ -\sum_{j=1}^{p} \phi_k \hat{R}_{xx}[k-j], \quad k > p \end{cases}$$

$$\Phi = \mathbf{R}^{-1}\mathbf{v}$$

where

$$\Phi = [\phi_1 \ \phi_2 \ \ldots \ \phi_p]^T$$

,

$$\mathbf{v} = [R_{xx}(1) \ R_{xx}(2) \ \ldots \ R_{xx}(p)]^T$$

and

$$\mathbf{R} = \begin{bmatrix} 1 & R_{xx}(1) & R_{xx}(1) & \ldots & R_{xx}(p-2) & R_{xx}(p-1) \\ R_{xx}(1) & 1 & R_{xx}(1) & \ldots & R_{xx}(p-3) & R_{xx}(p-2) \\ & \vdots & & & \vdots & \\ R_{xx}(p-2) & R_{xx}(p-3) & R_{xx}(p-4) & \ldots & 1 & R_{xx}(1) \\ R_{xx}(p-1) & R_{xx}(p-2) & R_{xx}(p-3) & \ldots & R_{xx}(1) & 1 \end{bmatrix}$$

D

Proof of Theorem 1

This is an outline of the proof for Theorem 1 of Sec. 3.2. Proof of this theorem can be found in [52], Chapter 8. Essential outline of the proof is as follows.

The equation 3.6, can be written using vectors $\mathbf{x}(n)$ and $\mathbf{w}(n)$ as:

$$\mathbf{w}(n+1) = \mathbf{w}(n) + \eta y(n)[\mathbf{x}(n) - y(n)\mathbf{x}(n)]$$

where

$$y(n) = \mathbf{x}^T(n)\mathbf{w}(n) = \mathbf{w}^T(n)\mathbf{x}(n)$$

thus

$$\mathbf{w}(n+1) = \mathbf{w}(n) + \eta[\mathbf{x}(n)\mathbf{x}^T(n)\mathbf{w}(n) - \mathbf{w}^T(n)(\mathbf{x}(n)\mathbf{x}^T(n))\mathbf{w}(n)\mathbf{w}(n)] \quad \text{(D.1)}$$

Thus, the *characteristic matrix* defined by

$$\mathbf{w}(n+1) = \mathcal{M}\mathbf{w}(n)$$

for this algorithm is :

$$\mathcal{M} = \mathbf{I} + \eta[\mathbf{x}(n)\mathbf{x}^T(n) - \mathbf{w}^T(n)(\mathbf{x}(n)\mathbf{x}^T(n))\mathbf{w}(n)\mathbf{I}]$$

Provided η is small, using *Kushner's direct-averaging method*, we can replace the characteristic matrix by its expected value:

$$E\{\mathcal{M}\} = \mathbf{I} + \eta[\mathbf{R} - \mathbf{w}^T(n)\mathbf{R}\mathbf{w}(n)\mathbf{I}]$$

where

$$\mathbf{R} = E\mathbf{x}(n)\mathbf{x}^T(n)$$

The solution of the stochastic equation of Eqn. D.1 is close to the solution of the deterministic difference equation:

$$\mathbf{w}(n+1) = \mathbf{w}(n) + \eta[\mathbf{R} - \mathbf{w}^T(n)\mathbf{R}\mathbf{w}(n)\mathbf{I}]\mathbf{w}(n) \tag{D.2}$$

Let

$$\Delta\mathbf{w}(n) = \mathbf{w}(n+1) - \mathbf{w}(n)$$

we may say:

$$\frac{d\mathbf{w}(t)}{dt} \propto \Delta\mathbf{w}(n) \tag{D.3}$$

By eliminating the constant η and normalizing time, the evolution of the maximum eigenfilter over time can be described by *ordinary nonlinear differential equation*

$$\frac{d\mathbf{w}(t)}{dt} = \mathbf{R}\mathbf{w}(t) - \left(\mathbf{w}^T(t)\mathbf{R}\mathbf{w}(t)\right)\mathbf{w}(t) \tag{D.4}$$

We can expand $\mathbf{w}(t)$ in terms of the *complete orthonormal set of eigenvectors* of $\mathbf{R}$

$$\mathbf{w}(t) = \sum_{k=1}^{m} \theta_k(t)\mathbf{q}_k \tag{D.5}$$

where $\mathbf{q}_k$ is the kth normalized eigenvector of $\mathbf{R}$, and the coefficient $\theta_k(t)$ is the projection of the vector $\mathbf{w}(t)$ onto $\mathbf{q}_k$. Using basic definitions of eignevector and eigenvalue

$$\mathbf{R}\mathbf{q}_k = \lambda_k \mathbf{q}_k$$

and

$$\mathbf{q}_k.\mathbf{R}\mathbf{q}_k = \lambda_k$$

where λ_k is the eigenvalue associated with $\mathbf{q}_k$, and substituting Eqn. D.5 in Eqn. D.4 we get

$$\sum_{k=1}^{m} \frac{d\theta_k(t)}{dt}\mathbf{q}_k = \sum_{k=1}^{m} \lambda_k \theta_k(t)\mathbf{q}_k - \left[\sum_{l=1}^{m} \lambda_l \theta_l^2(t)\right] \sum_{k=1}^{m} \theta_k(t)\mathbf{q}_k \tag{D.6}$$

which can be stated as

$$\frac{d\theta_k(t)}{dt} = \lambda_k\, \theta_k(t) - \theta_k(t) \left[\sum_{l=1}^{m} \lambda_l\, \theta^2(l)(t)\right], \quad k = 1, 2, \ldots, m \tag{D.7}$$

This equation is a *nonlinear modified form of the Langevin equation without a driving force*, and therefore, we expect that the maximum eigenfilter will be absolutely convergent in an asymptotic sense.

We now consider two cases for the index k:

1. $\mathbf{1 < k \leq m}$

Define (assuming $\theta_1(t) \neq 0$)

$$\alpha_k(t) = \frac{\theta_k(t)}{\theta_1(t)}$$

then differentiating $\alpha_k(t)$ we get

$$\begin{aligned} \frac{d\alpha_k(t)}{dt} &= \frac{1}{\theta_1(t)}\frac{d\theta_k(t)}{dt} - \frac{\theta_k(t)}{\theta_1^2(t)}\frac{d\theta_1(t)}{dt} \\ &= \frac{1}{\theta_1(t)}\frac{d\theta_k(t)}{dt} - \frac{\alpha_k(t)}{\theta_1(t)}\frac{d\theta_1(t)}{dt} \quad 1 < k \leq m \qquad \text{(D.8)} \end{aligned}$$

now using Eqn. D.7 in Eqn. D.8, we obtain

$$\frac{d\alpha_k(t)}{t} = -(\lambda_1 - \lambda_k)\alpha_k(t), \quad 1 < k \leq m \qquad \text{(D.9)}$$

with the assumption of distinct eigenvalues of $\mathbf{R}$ and eigenvalues arranged in decreasing order we have

$$\lambda_1 > \lambda_2 > \cdots > \lambda_m > 0$$

therefore, $(\lambda_1 - \lambda_k)$ is positive and for this case of k we have

$$\alpha_k(t) \to 0 \quad \text{as } t \to \infty \quad \text{for } 1 < k \leq m \qquad \text{(D.10)}$$

2. $\mathbf{k=1}$

From Eqn. D.7

$$\begin{aligned}
\frac{d\theta_1(t)}{dt} &= \lambda_1\,\theta_1(t) - \theta_1(t)\,\sum_{l=1}^{m}\lambda_l\,\theta_l^2(t) \\
&= \lambda_1\,\theta_1(t) - \lambda_1\,\theta_1^3(t) - \theta_1(t) - \theta_1(t)\,\sum_{l=2}^{m}\lambda_l\,\theta_l^2(t) \\
&= \lambda_1\,\theta_1(t) - \lambda_1\,\theta_1^3(t) - \theta_1(t) - \theta_1^3(t)\,\sum_{l=2}^{m}\lambda_l\,\alpha_l^2(t) \quad \text{(D.11)}
\end{aligned}$$

we know that for $l \neq 1$, as $t \to \infty$ $\alpha_l(t) \to 0$. Thus, the last term on the right-hand side of Eqn. D.8 approaches zero as t approaches infinity. So

$$\frac{d\theta_1(t)}{dt} = \lambda_1\,\theta_1(t)[1-\theta_1^2(t)] \quad \text{for} t \to \infty \qquad \text{(D.12)}$$

Equation D.12 represents an *autonomous system* i.e. a system with no explicit time dependence. The stability of such a system can be handled using a *Lyapunov function.* Let $\mathbf{s}$ denote the state vector of an autonomous system and $V(t)$ denote a Lyapunov function of the system. An equilibrium state $\bar{\mathbf{s}}$ of the system is asymptotically stable if

$$\frac{d}{dt}V(t) < 0 \quad \text{for } \mathbf{s} \in \mathcal{U} - \bar{\mathbf{s}} \qquad \text{(D.13)}$$

where $\mathcal{U}$ is a small neighbourhood around $\bar{\mathbf{s}}$. The autonomous system of Eqn. D.12, has a Lyapunov function defined by

$$V(t) = [1-\theta_1^2(t)]^2$$

In order to validate this assertion, we should show that $V(t)$ satisfies two conditions:

$$1.\quad \frac{d}{dt}V(t) < 0 \quad \text{for all } t \tag{D.14}$$

$$2.\quad V(t) \text{ has a minimum} \tag{D.15}$$

Differentiating Eqn. D.12 with respect to time, and using Eqn. D.12 we get

$$\begin{aligned} \frac{d}{dt}V(t) &= 4\theta_1(t)[\theta_1(t) - 1]\frac{d\theta_1(t)}{dt} \\ &= -4\lambda_1\theta_1^2(t)[\theta_1^2(t) - 1]^2 \quad \text{as } t \to \infty \end{aligned} \tag{D.16}$$

Since λ_1 is positive, the first condition stated in Eqn. D.15 is true for t approaching infinity. Furthermore, from Eqn. D.16, we see that $V(t)$ has a minimum at $\theta_1(t)$. Therefore, both conditions are met and we can conclude that

$$|\theta_1(t)| \to \pm 1 \quad \text{as } t \to \infty$$

Also, having $\theta_1(t) \neq 0$, we can restate Eqn. D.10 as:

$$\theta_k(t) \to 0 \quad \text{as } t \to \infty \quad \text{for } 1 < k \leq m$$

Hence, we can formally state that

$$\mathbf{w}(t) \to \mathbf{q}_1, \quad \text{as } t \to \infty$$

Bibliography

[1] D. Willshaw and C. von der Malsburg, "How patterned neural connections can be set up by self-organization," *Proceedings of the Royal Society of London Series B*, vol. 194, pp. 431–445, 1976.

[2] "The nervous system." [Online]. Available: http://www.emc.maricopa.edu/faculty/farabee/biobk/BioBookNERV.html

[3] D. Willkomm, S. Machiraju, J. Bolot, and A. Wolisz, "Primary user behavior in cellular networks and implications for dynamic spectrum access," *IEEE Commun. Mag.*, vol. 47, no. 3, pp. 88–95, 2009.

[4] A. Ghasemi and E. S. Sousa, "Spectrum sensing in cognitive radio networks: requirements, challenges and design trade-offs," *IEEE Communications Magazine*, vol. 46, pp. 32–39, Apr. 2008.

[5] S. Haykin, "Cognitive radio: Brain-empowered wireless communications," *IEEE J. Select. Areas Commun.*, vol. 23, no. 2, pp. 201–220, Feb. 2005.

[6] M. A. McHenry, P. A. Tenhula, D. McCloskey, D. A. Roberson, and C. S. Hood, "Chicago spectrum occupancy measurements and anal-

ysis and a long-term studies proposa," in *Proc. Workshop on Technology and Policy for Accessing Spectrum (TAPAS)*, 2006, pp. 1–12, http://www.sharedspectrum.com/.

[7] FCC Spectrum Policy Task Force, "Report of the spectrum efficiency working group," http://www.fcc.gov/sptf/reports.html, Tech. Rep., 2002.

[8] M. A. McHenry, P. A. Tenhula, D. McCloskey, D. A. Roberson, and C. S. Hood, "Chicago spectrum occupancy measurements and analysis and a long- term studies proposal," in *Proc. Workshop on Technology and Policy for Accessing Spectrum (TAPAS)*, 2006, pp. 1–12.

[9] R. I. Chiang, G. B. Rowe, and K. W. Sowerby, "A quantitative analysis of spectral occupancy measurements for cognitive radio," *Proc. IEEE Vehicular Technology Conference*, pp. 3016–3020, 2007.

[10] M. H. Islam, C. L. Koh, S. W. Oh, X. Qing, Y. Y. Lai, C. Wang, Y. C. Liang, B. E. Toh, B. E. Toh, G. L. Tan, and W. Toh, "Spectrum survey in singapore: Occupancy measurements and analysis," in *Proc. 3rd International Conference of Cognitive Radio Oriented Wireless Network and Communications (CROWN- COM08)*, 2008, pp. 1–7.

[11] K. A. Qaraqe, H. Celebi, M. S. Alouini, A. El-Saigh, L. Abuhantash, M. Al-Mulla, O. Al-Mulla, A. Jolo, and A. Ahmed, "Measurement and analysis of wideband spectrum utilization in indoor and outdoor environments," in *Proc. IEEE 18th Signal Processing and Communications Applications Conference (SIU-2010)*, 2010, pp. 1–4.

[12] W. W. Lu, "Point-of-view article: Opening the u.s. mobile communications market," *Proceedings of IEEE*, vol. 96, no. 9, pp. 1450–1452, 2008.

[13] S. Haykin, "Point-of-view article: Cognitive dynamic systems," *Proceedings of IEEE*, vol. 94, no. 11, pp. 1910–1911, 2006.

[14] J. Mitola, "Cognitive radio: An integrated agent architecture for software defined radio," Ph.D. dissertation, Royal Inst. Technol. (KTH), Stockholm, Sweden, 2000.

[15] S. Haykin, *Cognitive Wireless Communication Networks.* Springer, 2007, ch. Fundamental issues in cognitive radio, pp. 1–43.

[16] M. Jamshidi, "System of systems engineering - new challenges for the 21st century," *IEEE Aerospace and Electronic Systems Magazine*, vol. 23, no. 5, pp. 4–19, 2008.

[17] J. Pearl, *Causality: Models, Reasoning and Inference*, 2nd ed. Cambridge University Press, 2009.

[18] Y. Chen, G. Yu, Z. Zhang, H. hwa Chen, and P. Qiu, "On cognitive radio networks with opportunistic power control strategies in fading channels," *IEEE Trans. Wireless Commun.*, vol. 7, pp. 2752–2761, July 2008.

[19] Y.-C. Liang, Y. Zeng, E. Peh, and A. T. Hoang, "Sensing-throughput tradeoff for cognitive radio networks," *IEEE Trans. Wireless Commun.*, vol. 7, pp. 1326–1337, Apr. 2008.

[20] S. Kim, J. Lee, H. Wang, and D. Hong, “Sensing performance of energy detector with correlated multiple antennas,” *IEEE Signal Processing Lett.*, vol. 16, no. 8, pp. 671–674, aug. 2009.

[21] S. Atapattu, C. Tellambura, and H. Jiang, “Energy detection based cooperative spectrum sensing in cognitive radio networks,” *IEEE Trans. Wireless Commun.*, vol. 10, no. 4, pp. 1232 –1241, Apr. 2011.

[22] S. Zhang, T. Wu, and V. Lau, “A low-overhead energy detection based cooperative sensing protocol for cognitive radio systems,” *IEEE Trans. Wireless Commun.*, vol. 8, no. 11, pp. 5575–5581, Nov. 2009.

[23] J. Lunden, V. Koivunen, A. Huttunen, and H. Poor, “Collaborative cyclostationary spectrum sensing for cognitive radio systems,” *IEEE Trans. Signal Processing*, vol. 57, no. 11, pp. 4182 –4195, Nov. 2009.

[24] K.-L. Du and W. H. Mow, “Affordable cyclostationarity-based spectrum sensing for cognitive radio with smart antennas,” *IEEE Trans. Veh. Technol.*, vol. 59, no. 4, pp. 1877–1886, May 2010.

[25] J. Lunden, S. Kassam, and V. Koivunen, “Robust nonparametric cyclic correlation-based spectrum sensing for cognitive radio,” *IEEE Trans. Signal Processing*, vol. 58, no. 1, pp. 38 –52, Jan. 2010.

[26] W. A. Gardner, “Exploitation of spectral redundancy in cyclostationary signals,” *IEEE Signal Processing Mag.*, vol. 8, pp. 14–36, 1991.

[27] W. A. Gardner, W. A. Brown, and C. K. Chen, "Spectral correlation of modulated signals: part ii-digital modulation," *Proc. IEEE*, vol. 35, no. 6, pp. 595–061, 1987.

[28] D. J. Thomson, "Spectrum estimation and harmonic analysis," *Proc. IEEE*, vol. 70, pp. 1055–1096, Sept. 1982.

[29] S. Haykin, *Cognitive Dynamic Systems.* Wiley, 2012.

[30] B. Farhang-Boroujeny, "Filter bank spectrum sensing for cognitive radios," *IEEE Trans. Signal Processing*, vol. 56, pp. 1801–1811, May 2008.

[31] Z. Quan, S. Cui, and A. H. Sayed, "Optimal linear cooperation for spectrum sensing in cognitive radio networks," *IEEE J. Select. Topics in Signal Processing*, vol. 2, pp. 28–40, Feb. 2008.

[32] G. Ganesan and Y. Li, "Cooperative spectrum sensing in cognitive radio, part I: Two user networks," *IEEE Trans. Wireless Commun.*, vol. 6, pp. 2204–2213, June 2007.

[33] ——, "Cooperative spectrum sensing in cognitive radio, part II: Multiuser networks," *IEEE Trans. Wireless Commun.*, vol. 6, pp. 2214–2222, June 2007.

[34] P. Setoodeh and S. Haykin, "Robust transmit power control for cognitive radio," *Proc. IEEE*, vol. 97, no. 5, pp. 915–939, 2009.

[35] P. Setoodeh, "Dynamic models of cognitive radio networks," Ph.D. dissertation, McMaster University, Aug. 2010.

[36] P. Kaligineedi, M. Khabbazian, and V. Bhargava, "Malicious user detection in a cognitive radio cooperative sensing system," *Wireless Communications, IEEE Transactions on*, vol. 9, no. 8, pp. 2488 –2497, august 2010.

[37] H. Li and Z. Han, "Catch me if you can: An abnormality detection approach for collaborative spectrum sensing in cognitive radio networks," *Wireless Communications, IEEE Transactions on*, vol. 9, no. 11, pp. 3554 –3565, november 2010.

[38] R. Qiu, Z. Hu, Z. Chen, N. Guo, R. Ranganathan, S. Hou, and G. Zheng, "Cognitive radio network for the smart grid: Experimental system architecture, control algorithms, security, and microgrid testbed," *Smart Grid, IEEE Transactions on*, vol. 2, no. 4, pp. 724 –740, dec. 2011.

[39] X. Zhang and C. Li, "The security in cognitive radio networks: a survey," in *Proceedings of the 2009 International Conference on Wireless Communications and Mobile Computing: Connecting the World Wirelessly*, ser. IWCMC '09. New York, NY, USA: ACM, 2009, pp. 309–313.

[40] F. Khozeimeh and S. Haykin, "Dynamic spectrum management for cognitive radio: an overview," *Wireless Communications and Mobile Computing*, vol. 9, no. 11, pp. 1447–1459, Nov. 2009.

[41] O. Holland, A. Attar, N. Olaziregi, N. Sattari, and A. H. Aghvami, "A universal resource awareness channel for cognitive radio," *Personal, Indoor and Mobile Radio Communications, 2006 IEEE 17th International Symposium on*, pp. 1–5, Sept. 2006.

[42] D. Hubel and T. Wiesel, “Functional architecture of macaque visual cortex,” *Proceedings of the Royal Society of London Series B*, vol. 198, pp. 1–59, 1977.

[43] ——, “Receptive fields, binocular interaction and functional architecture in the cat’s visual cortex,” *Journal of Physiology*, vol. 160, pp. 106–154.

[44] J. Kaas, M. Merzenich, and H. Killackey, “The reorganization of somatosensory cortex following peripheral nerve damage in adult and developing mammals,” *Annual review of Neurosciences*, vol. 6, pp. 325–356, 1983.

[45] N. Suga, *The extent to which bisonar information is represented in the bat auditory cortex*. New York: Wiley-Interscience, 1985, pp. 653–695.

[46] K. L. Du and M. N. S. Swamy, *Neural Networks in a softcomputing Framework*. Springer, 2006.

[47] C. von der Malsburg, *An Introduction to neural and electronic networks*. Academic Press, 1990, ch. Network self-organization.

[48] ——, “Self-organization of orientation sensitive cells in the striate cortex,” *kybernetik*, vol. 14, pp. 85–100, 1973.

[49] T. Kohonen, “Self-organized formation of topologically correct feature maps,” *Biological Cybernetics*, vol. 43, pp. 59–69, 1982.

[50] ——, “The self-organizing map,” *Proceedings of the IEEE*, vol. 78, no. 9, pp. 1464–1480, Sept. 1990.

[51] ——, *Self-Organizing Maps*, 2nd ed. Springer, 1997.

[52] S. Haykin, *Neural networks and learning machines*, 3rd ed. Upper Saddle River, New Jersey 07458: Prentice Hall, 2008.

[53] L. Wiskott and T. J. Sejnowski, *Constrained Optimization for Neural Map Formation: A Unifying Framework for Weight Growth and Normalization*, ser. Self-Organizing map formation: foundations of neural computation. The MIT Press, 2001, ch. 6, pp. 83–128.

[54] D. Polani, *Measures for the Organization of Self-Organizing Maps*, ser. Self-Organizing Neural Networks. New York: Physica-Verlag Heidelberg, 2002, ch. 2, pp. 13–44.

[55] D. Tsigankov and A. Koulakov, "A unifying model for activity-dependent and activity-independent mechanisms predicts complete structure of topographic maps in ephrin-a deficient mice," *Journal of Computational Neuroscience*, vol. 21, no. 1, pp. 101–114, 2006.

[56] J. Cang, L. Wang, M. Stryker, and D. A. Feldheim, "Roles of ephrin-as and structured activity in the development of functional maps in the superior colliculus." *The Journal of neuroscience*, vol. 28, no. 43, pp. 11 015–11 023, 2008.

[57] D. Hebb, *The organization of behavior: a neuropsychologocal theory.* Wiley, 1949.

[58] K. Hakim, S. Jayaweera, G. El-howayek, and C. Mosquera, "Efficient dynamic spectrum sharing in cognitive radio networks: Centralized dy-

namic spectrum leasing (c-dsl)," *IEEE Trans. Wireless Commun.*, vol. 9, no. 9, pp. 2956 –2967, Sept. 2010.

[59] S. Jayaweera, M. Bkassiny, and K. Avery, "Asymmetric cooperative communications based spectrum leasing via auctions in cognitive radio networks," *IEEE Trans. Wireless Commun.*, vol. 10, no. 8, pp. 2716 –2724, august 2011.

[60] S. Jayaweera, G. Vazquez-Vilar, and C. Mosquera, "Dynamic spectrum leasing: A new paradigm for spectrum sharing in cognitive radio networks," *IEEE Trans. Veh. Technol.*, vol. 59, no. 5, pp. 2328–2339, June 2010.

[61] G. El-Howayek and S. Jayaweera, "Distributed dynamic spectrum leasing (d-dsl) for spectrum sharing over multiple primary channels," *IEEE Trans. Wireless Commun.*, vol. 10, no. 1, pp. 55–60, Jan. 2011.

[62] H. Zheng and C. Peng, "Collaboration and fairness in opportunistic spectrum access," *Communications, 2005. ICC 2005. 2005 IEEE International Conference on*, vol. 5, pp. 3132–3136, May 2005.

[63] R. Zhang and Y.-C. Liang, "Exploiting multi-antenna for opportunistic spectrum sharing in cognitive radio networks," *IEEE J. Select. Topics in Signal Processing*, vol. 2, pp. 88–102, Feb. 2008.

[64] D. Niyato and E. Hossain, "Competitive spectrum sharing in cognitive radio networks: a dynamic game approach," *IEEE Trans. Wireless Commun.*, vol. 7, pp. 2651–2660, July 2008.

[65] R. Diestel, *Graph Theory*, 3rd ed. Verlag Berlin Heidelberg: Springer, 2005.

[66] R. Nelson and R. J. Wilson, *Graph colouring.* Harlow, Essex CM20 2JE, England: Longman Scientific & Technical, 1990.

[67] Q. Zhao, B. Krishnamachari, and K. Liu, “On myopic sensing for multi-channel opportunistic access: structure, optimality, and performance,” *IEEE Trans. Wireless Commun.*, vol. 7, no. 12, pp. 5431–5440, Dec. 2008.

[68] Q. Zhao, S. Geirhofer, L. Tong, and B. M. Sadler, “Opportunistic spectrum access via periodic channel sensing,” *IEEE Trans. Signal Processing*, vol. 56, no. 2, pp. 785–796, Feb. 2008.

[69] H. Su and X. Zhang, “Cross-layer based opportunistic mac protocols for qos provisionings over cognitive radio wireless networks,” *IEEE J. Select. Areas Commun.*, vol. 26, no. 1, pp. 118–129, Jan. 2008.

[70] S. Geirhofer, L. Tong, and B. M. Sadler, “Cognitive medium access: constraining interference based on experimental models,” *IEEE J. Select. Areas Commun.*, vol. 26, no. 1, pp. 95–105, Jan. 2008.

[71] A. Adas, “Traffic models in broadband networks,” *IEEE Commun. Mag.*, vol. 35, no. 7, pp. 82–89, 1997.

[72] D. Werra and A. Hertz, *Graph colouring and variations.* New York, NY, 10010, USA: Elsevier science publishers B.V, 1989.

[73] Z. Tuza, "Graph colorings with local constraints a survey," *Discussiones Mathematicae-Graph theory*, vol. 17, no. 2, pp. 161–228, 1997.

[74] D. Brélaz, "New methods to color the vertices of a graph," *Communications of the ACM*, vol. 22, no. 4, pp. 251–256, 1979.

[75] M. Caramia and P. Dell'Olmo, "Bounding vertex coloring by truncated multistage branch and bound," *Networks*, vol. 44, no. 4, pp. 231–242, 2004.

[76] I. Mendez Diaz and P. Zabala, "A branch-and-cut algorithm for graph coloring," *Proceedings of the Computational Symposium on Graph Coloring and its Generalizations*, pp. 55–62, 2002.

[77] C. Gomes and D. Shmoys, "Completing quasigroups or latin squares: A structured graph coloring problem," *Proceedings of the Computational Symposium on Graph Coloring and its Generalizations*, pp. 22–39, 2002.

[78] A. Mehrotra and M. A. Trick, "A column generation approach for graph coloring," *INFORMS Journal on Computing*, vol. 8, no. 4, pp. 344–354, 1996.

[79] M. Chiarandini, I. Dumitrescu, and T. Stützle, *Handbook on Approximation Algorithms and Metaheuristics, Computer & Information Science Series*. Boca Raton, FL, USA: Chapman and Hall/CRC, 2007, ch. Stochastic Local Search Algorithms for the Graph Colouring Problem, pp. 63–1–63–17.

[80] M. Chiarandini, "Stochastic local search methods for highly constrained combinatorial optimisation problems," Ph.D. dissertation, Computer Science Department, Darmstadt University of Technology, Darmstadt, Germany, 2005.

[81] A. H. Gebremedhin, "Parallel graph coloring," Ph.D. dissertation, University of Bergen, Norway, 1999.

[82] D. Welsh and M. Powell, "An upper bound for the chromatic num- ber of a graph and its application to timetabling problems," *Computer Journal*, vol. 10, pp. 85–86.

[83] T. H. Cormen, C. E. Leiserson, R. L. Rivest, and C. Stein, *Introduction to Algorithms*, 2nd ed. The MIT Press, 2001.

[84] N. Linial, "Locality in distributed graph algorithms," *SIAM Journal on Computing*, vol. 21, no. 1, pp. 46–48, 1992.

[85] G. D. Marco and A. Pelc, "Fast distributed graph coloring with $o(\delta)$ colors," in *In Proc. of 12th ACM-SIAM Symposium on Discrete Algorithms (SODA)*, 2001, pp. 630–635.

[86] C. S. K. Kothapalli, M. Onus and C. Schindelhauer, "Distributed coloring in $o(\sqrt{\log n})$ bit rounds," in *In Proc. of 20th IEEE Int. Parallel and Distributed Processing Symposium (IPDPS)*, 2006.

[87] M. Szegedy and S. Vishwanathan, "Locality based graph coloring," in *In Proc. of the 25th ACM Symposium on Theory of Computing (STOC)*, 1993, p. 201207.

[88] G. S. Stent, “A physiological mechanism for hebb’s postulate of learning,” *Proceeding of the National Academy of Sciences*, vol. 70, pp. 997–1001, 1973.

[89] J. P. Chageux and A. Danchin, “Selective stabilization of developing synapses as a mechanism for the specification of neural networks,” *Nature*, vol. 264, pp. 705–712, 1976.

[90] J. E. Z. Chen, S. Haykin and S. Becker, *Correlative Learning: A Basis for Brain and Adaptive Systems.* New York: Wiley-Interscience, 2007.

[91] R. Linsker, “From basic network principles to neural architecture,” *In Proceedings of National Academy of Science*, 1986.

[92] C. Fyfe, *Hebbian learning and negative feedback networks.* Springer, 2005.

[93] E. Oja, “A simplified neuron model as a principle component analyzer,” *Journal of Neural Biology*, vol. 15, pp. 267–273, 1982.

[94] S. Haykin, D. J. Thomson, and J. Reed, “Spectrum sensing for cognitive radio,” *Proc. IEEE, Special Issue on Cognitive Radio Networks*, vol. 97, no. 5, pp. 849–877, 2009.

[95] M. Frigo and S. G. Johnson, “The design and implementation of FFTW3,” *Proc. IEEE*, vol. 93, no. 2, pp. 216–231, 2005, special issue on “Program Generation, Optimization, and Platform Adaptation”.

[96] [Online]. Available: http://www.nvidia.com/object/tegra-2.html

[97] [Online]. Available: http://www.qualcomm.com/snapdragon/specs

[98] Http://www.bluetooth.com/.

[99] Http://ieee802.org/11/.

[100] T. Taleb, A. Jamalipour, Y. Nemoto, and N. Kato, "Demaps: A load-transition-based mobility management scheme for an efficient selection of map in mobile ipv6 networks," *IEEE Trans. Veh. Technol.*, vol. 58, no. 2, pp. 954–965, Feb. 2008.

[101] N. V. Lopes, M. J. Nicolau, and A. Santos, "Evaluating rate-estimation for a mobility and QoS-aware network architecture," *Software, Telecommunications & Computer Networks, 2009. SoftCOM 2009. 17th International Conference on*, no. 24, pp. 348–352, Sept. 2009.

[102] A.-C. Pang and H.-W. Tseng, "Dynamic backoff for wireless personal networks," *Global Telecommunications Conference, 2004. GLOBECOM '04. IEEE*, vol. 3, no. 29, pp. 1580–1584, Dec. 2004.

[103] Zhigang Wen, Tao Luo, Weidong Xiang, Sudhan Majhi, and Y. Ma, "Autoregressive spectrum hole prediction model for cognitive radio systems," *Communications Workshops, 2008. ICC Workshops '08. IEEE International Conference on*, no. 19, pp. 154–157, May 2008.

[104] K. W. Choi and E. Hossain, "Opportunistic access to spectrum holes between packet bursts: A learning-based approach," *IEEE Trans. Wireless Commun.*, vol. 10, no. 8, pp. 2497–2509, Aug. 2011.

[105] Https://www.sharcnet.ca/.

[106] A. T. Hoang and Y.-C. Liang, "A two-phase channel and power allocation scheme for cognitive radio networks," *The 17th Annual IEEE International Symposium on Personal, Indoor and Mobile Radio Communications (PIMRC'06)*, 2006.

[107] Y. Xing, C. N. Mathur, M. A. Haleem, R. Chandramouli, and K. P. Subbalakshmi, "Dynamic spectrum access with QoS and interference temperature contraints," *IEEE Trans. Mobile Comput.*, vol. 6, no. 4, pp. 423–433, Apr. 2007.

[108] S. Haykin, "Adaptive filters," *Proceedings of IEEE*, p. submitted paper, 2011.

[109] K. Zhou and J. C. Doyle, *Essentials of Robust Control*. Prentice Hall, 1997.

[110] B. A. Francis and P. P. Khargonekar, *Robust Control Theory*. Springer, 1995.

[111] S. Haykin, "New vision for the world of wireless communications enabled with cognition," in *Personal Indoor and Mobile Radio Communications (PIMRC), 2011 IEEE 22nd International Symposium on*, sept. 2011, pp. 2335 –2337.

[112] D. Challet and Y. Zhang, "Emergence of cooperation and organization in an evolutionary game," *Physica A: Statistical and Theoretical Physics*, vol. 246, no. 3-4, pp. 407–418, Dec. 1997.

[113] D. Challet, M. Marsili, and Y.-C. Zhang, *Minority Games: Interacting Agents in Financial Markets.* Oxford University Press, 2005.

[114] M. Petrova, M. Michalopoulou, and P. M. andho andnen, "Self-organizing multiple access with minimal information: Networking in el farol bar," in *GLOBECOM Workshops (GC Wkshps), 2010 IEEE*, Dec. 2010, pp. 1151–1156.

[115] I. Aoki, K. Yamamoto, K. Kimura, H. Murata, and S. Yoshida, "Experimental study of minority game-based interference management for spectrum sharing," in *Communication Systems (ICCS), 2010 IEEE International Conference on*, Nov. 2010, pp. 585–589.

[116] Y. Saito, K. Yamamoto, H. Murata, and S. Yoshida, "Robust interference management to satisfy allowable outage probability using minority game," in *Personal Indoor and Mobile Radio Communications (PIMRC), 2010 IEEE 21st International Symposium on*, Sept. 2010, pp. 2314–2319.

[117] P. Mähönen and M. Petrova, "Minority game for cognitive radios: Cooperating without cooperation," *Physical Communication*, vol. 1, no. 2, pp. 94–102, 2008.

[118] M. Fukushima, "Stochastic and robust approaches to optimization problems under uncertainty ," in *Proc. of International Conference on Informatics Research for Development of Knowledge Society Infrastructure (ICKS)*, 2007, pp. 87–94.

[119] P. Sharma, "Time-series model for wireless fading channels under isotropic and non-isotropic scattering environments," *IEEE Commun. Lett.*, vol. 9, pp. 46–48, 2005.